

Syracuse University

SURFACE at Syracuse University

Dissertations - ALL

SURFACE at Syracuse University

8-26-2022

Numerical Investigation of The Effect of Inlet Turbulence Intensity on a Bluff-Body Stabilized Flame at Near Blow-off Condition

Amir Ali Montakhab

Syracuse University, Amontakhab@live.com

Follow this and additional works at: <https://surface.syr.edu/etd>



Part of the [Mechanical Engineering Commons](#)

Recommended Citation

Montakhab, Amir Ali, "Numerical Investigation of The Effect of Inlet Turbulence Intensity on a Bluff-Body Stabilized Flame at Near Blow-off Condition" (2022). *Dissertations - ALL*. 1649.

<https://surface.syr.edu/etd/1649>

This Dissertation is brought to you for free and open access by the SURFACE at Syracuse University at SURFACE at Syracuse University. It has been accepted for inclusion in Dissertations - ALL by an authorized administrator of SURFACE at Syracuse University. For more information, please contact surface@syr.edu.

ABSTRACT

This thesis investigates the effect of a boundary condition on the dynamics of a bluff-body stabilized flame operating near blow-off condition. Special emphasis is given to the effect of inlet turbulence intensity. This work is motivated by the understanding that more stringent regulations on fossil fuels generated emissions necessitate the design of combustion systems that operate at very fuel-lean conditions. Combustion at very lean conditions, however, induces flame instability that can ultimately lead to flame fluttering and eventual extinction. The dynamics of the flame at lean conditions can therefore be very sensitive to its boundary conditions. To better understand this, a numerical investigation was needed as experimental research used for our model validation ceased to provide this information. The first stage of the numerical research is based on the experiment conducted in the Volvo Flygmotor AB program. The numerical models are validated by comparing the results with the available experimental data. The near blow-off equivalence ratio is then determined using the validated set of models. The effect of ITI on the flame dynamics is subsequently investigated for a lean flame that is near blow-off condition. For the computational analysis Large Eddy Simulation (LES) method was selected for its accuracy and efficiency. Combustion is accounted for through the transport of chemical species and the turbulence-combustion interaction through laminar finite-rate model. The sensitivity to inlet turbulence is assessed by carrying out simulations at near blow-off condition. The inlet turbulence intensity is varied in increments of 5%. It is observed that while the inlet intensity of 5% causes blow-off, further increase to 10% preserves a healthy flame on account of more heat release arising from greater entrainment of combustible mixtures into the flame zone just behind the bluff-body. This balance is again lost as the inlet turbulence intensity is further increased to 15%. These conclusions are first obtained using 2D LES and selected cases are verified through 3D LES. Further, the importance of chemical kinetics is addressed by comparative analysis using global and detailed chemical kinetics models. The results jointly highlight strategies that can be used to reduce the required computational costs without loss of critical flow features of near blow-off bluff body turbulent flame.

Numerical Investigation of
The Effect of Inlet Turbulence Intensity on a
Bluff-Body Stabilized Flame at Near Blow-off
Condition

Amir Ali Montakhab

B.Sc., Iran University of Science and Technology, 2002

M.Sc., California State University of Northridge, 2010

DISSERTATION

Submitted in partial fulfillment

of the requirements for the degree

Doctor of Philosophy in Mechanical and Aerospace Engineering

Syracuse University

August 2022

Copyright © Amir Ali Montakhab 2022

All Rights Reserved

ACKNOWLEDGMENTS

First and foremost I would like to express my humbleness and gratitude toward the Creator of the universes who with His infinite knowledge and unbounded compassion has created everything, seen and unseen, out of nothing while constantly has been nourishing them from the beginning till the Last Day. This is an acknowledgement of His mercy toward me for giving me the ability and means to pursue the advanced degree. He has allowed me to increase my understanding in physics of combustion, although minuscule compared to His infinite Knowledge. May completion of this stage increase my humbleness toward His vast and mighty Kingdom.

I would like to acknowledge the perseverance and continual support of my advisor Dr. Benjamin Akih Kumgeh to whom I am and will be indebted not only for teaching me physical sciences but also for teaching me the methodology of thinking and technical presenting. This, I will carry on for the rest of my life. I would also like to thank him for giving me the opportunity to continue my advanced education by accepting me as a part-time student and to work on an interesting research topic. His clear thoughts and constructive feedback have helped me in carrying out the thesis in a timely manner. His dedication, perseverance, patience, and depth of knowledge were encouraging and inspiring.

I would like to thank Dr. Ashok Sangani, Dr. Mehmet Sarimurat and Dr. Jeongmin Ahn, Dr. Yiyang Sun, and Dr. Thong Dang for generously offering their time and accepting to be part of my defense committee. I would also like to extend my appreciation to Dr. Mehmet Sarimurat and Dr. Jeongmin Ahn for their participation and constructive comments in my oral examination.

I have the privilege to have benefited from the teaching of Dr. Jacques Lewalle, Dr. Mellisa Green, Dr. Mark Glauser, Dr. Alan Levy, and Dr. Young Moon. I thank them for sharing their knowledge in

fluid mechanics, turbulence, advanced mathematics and statistics.

I wish to thank my colleagues in Thermodynamics and Combustion Lab. Dr. Chenwei Zheng, Dr. Apeng Zhou, Dr. Nathan Peters, Dr. Mazen Eldeeb, Dr. Deshawn Coombs, Dr. Shirin Jouzdani, and Ahmet Bahar for sharing their experiences and knowledge with me.

None of this work would have been possible without the support of the Syracuse University research computing department. I especially would appreciate the dedication of Matthew Hanley who supported the troubleshooting and resolving problems during the numerical research.

I am grateful for the unconditional love of my family. Their continued encouragement and blessings led me to where I am today. This work would not have been accomplished without the support of my parents, and my wife, Leyla Amjadi. They faithfully stood by me and were always willing to listen and offer their help and wisdom.

Syracuse, New York

May, 2022

Contents

Abstract	i
Acknowledgement	iv
List of Figures	viii
1 Introduction	1
1.1 Introduction	1
1.2 Motivation	4
1.3 Literature Review	7
1.3.1 Dynamics of bluff body flame	7
1.3.2 Dynamics of bluff body lean blow-off	18
1.3.3 Effect of ITI on lean blow-off	20
1.3.4 Mesh sensitivity on flame dynamics	26
1.4 Specific Objectives	26
2 Experimental and Computational Methods	29
2.1 Experimental Test Rig Set-up	29
2.2 Governing Equations And Theoretical Modeling	32
2.2.1 Conservation Equations For Reacting Flows	32
2.2.2 Turbulence Modeling Method	36
2.2.3 Premixed Turbulent Combustion Modeling	38
2.2.4 Turbulence-chemistry Interaction Modeling	41

2.2.5	Computational Domain And Set-up	44
2.2.6	Thermodynamics and Transport Properties	47
2.2.7	Numerical Method	47
2.3	Using Methods to Address Thesis Objectives	48
3	Validation of Volvo test case	51
3.1	The Experimental Setups	52
3.2	Model Validation - 2D and 3D LES	53
3.3	Mesh Sensitivity	60
4	Determination of Near Blow-off Equivalence Ratio	68
4.1	Approaching Blow-off Through 2D LES And Detailed Chemistry	69
4.2	Blow-off Through Reduction of Equivalence Ratio	74
4.3	Verifying 2D and 3D Behavior At Near Blow-off	77
5	Effect of Inlet Turbulence Intensity On The Flame At Near Blow-off Equivalence Ratio	83
5.1	The Effect of Inlet Turbulence Intensity On A Strong Flame	85
5.2	The Effect of ITI On Near Blow-off Flame	88
5.2.1	Effects of ITI On A Lean Flame Using 2D LES And 1-step chemistry vs. Detailed Chemistry	92
5.3	Implication of ITI Effect On Blow-off	97
6	Conclusion and outlook	102
	Vita	114

List of Figures

1.1	World energy consumption distribution in 2015. (Energy Information Administration, [1])	2
1.2	World energy consumption by energy source in quadrillion Btu. (World Energy Outlook 2018, Energy Information Administration, [1])	2
1.3	Illustration of the instability of the shear layer (circled red), the recirculation zone, between shear layers, and the asymmetric instability process or wake region, (boxed green). Picture adapted from Prasad and Williamson [23]. The schematic on the right is to illustrate the concept [14].	9
1.4	Profiles of U-rms. in five cross sections downstream the flame holder (a) 15 mm (b) 38 mm (c) 61 mm (d) 150 mm (e) 376 mm (open symbols-measurements, solid lines-LES, dotted lines $k - \epsilon$ RANS) [27]	10
1.5	Profiles of V-rms. in five cross sections downstream the flame holder (a) 15 mm (b) 38 mm (c) 61 mm (d) 150 mm (e) 376 mm (open symbols-measurements, solid lines-LES, dotted lines $k - \epsilon$ RANS) [27]	10
1.6	Instantaneous and time-averaged flow field obtained by LES for increasing reactant temperature, decreasing temperature ratio, from 3.5 to 1.0. Left column: Instantaneous vorticity and flame. Right column: Time-averaged flame location overlapped with mean vorticity(upper half) and mean temperature(lower half) [18].	13

1.7	Simulated temperatures profiles at $x = 0.15, 0.35$ and 0.55 m behind the bluff body for Sjunnesson test rig. The dotted line is experimental values and dashed line and solid line are the results from TFC and Dispersion models, respectively. The top row is the simulation results before calibration and the bottom row is the simulated results after calibration [34]	14
1.8	Instantaneous temperature profile for the reduced kinetic model; (a) & (c) $\Phi = 0.6$ & 0.45 with EDC model; (b) & (d) $\Phi = 0.6$ & 0.45 with Laminar Combustion model, research conducted by Kiel et al. [9]	20
1.9	(a) Experimental setup by Chowdhury and Cetegen. (b) Schematic of ITI level control method used in the experiment [3]	23
1.10	Instantaneous images of CH_2O and OH PLIF in addition to heat release region overlaid on the vorticity contours. (a) $ITI=24\%$ $\phi = 0.76$, (b) $ITI=30\%$ $\phi = 0.73$ showing the overlap of the reaction zone over the shear layer vortices, (c) shows the flame moving away from the high vorticity region at $ITI=30\%$ [3].	24
2.1	Experimental setup for the Volvo test cases depicting the method of controlling the inlet turbulence intensity by honeycomb screen. The flame holder is also shown in a magnified view.	30
2.2	Regime diagram of premixed turbulent combustion according to Borghi [71]	32
2.3	The left figure is depicting the normalized species mass fraction for premixed methane laminar flame and the right chart shows the chemical time scales of different reactions in comparison to mixing time scale [77].	41
2.4	The computational domain selected for this project.	45
2.5	Coarse mesh with 47,000 quadrilateral cells, min, max element size= 0.6, 3.6 mm, min orthogonal quality= 0.87, max aspect ratio= 3.42	45
2.6	Extra fine mesh with 550,000 quadrilateral cells, min, max element size= 0.4, 0.6 mm, min orthogonal quality= 0.87 and max aspect ratio= 2.24	46
2.7	Research Workflow	50

3.1	Comparison of simulated mean x-axis velocity in 2D and 3D with experimental results at two different locations, left: at 1.5cm behind the bluff body, right: at 15cm behind the bluff body	58
3.2	Comparison of simulated mean temperature in 2D and 3D with experimental results at two different locations, left: at 15cm behind the bluff body, right: at 35cm behind the bluff body	58
3.3	Comparison of transversal temperature profiles at two different locations for adiabatic wall versus constant wall temperatures, left: at 1.5cm behind the bluff body, right: at 6cm behind the bluff body	60
3.4	The flame development from the ignition with patching method implementing 3rd order numerical scheme, MUSCL.	61
3.5	Mesh qualities used in 3D model validation analysis.	62
3.6	Mesh sensitivity analysis. Screenshots of different mesh configurations around the upper tip of the bluff body. The green mark shows where the measurement between two nodes was taken for the table 3.5	62
3.7	Mesh sensitivity analysis. The comparison of temperature contours between fine unstructured (top) and extra fine structured mesh (bottom). Unstructured fine mesh shows richer dynamic structures due to cell alignment with flow especially in the recirculation zone.	64
3.8	Mesh sensitivity analysis. the figure shows the average transverse velocity profiles at four different locations. Wide variation may indicate averaging and transient effects.	65
3.9	Mesh sensitivity analysis. The results are shown based on transverse temperature profiles at three different locations	66
4.1	Instantaneous images of CH ₂ O PLIF, OH PLIF and heat release region overlaid on the vorticity contours and velocity field for flame near blow-off (a) flamelet merging, (b) occurrence of shear layer extinction, (c) pocket formation, (d) flame fragmentation and (e) asymmetric flame structure [3].	71

4.2	Numerical simulation captures all the stages of blow-off observed in experimental data	72
4.3	Instantaneous and simultaneous contours of hydroxyl (OH) and formaldehyde (CH_2O) superimposed on vorticity distribution in the computational domain when $\phi = 0.65$ and the flame is robust and stable.	73
4.4	Instantaneous and simultaneous contours of hydroxyl (OH) and formaldehyde (CH_2O) superimposed on vorticity distribution in the computational domain when $\phi = 0.32$. The flame is weak and is near blow-off.	74
4.5	The effect of equivalence ratio variation on the flame structure	75
4.6	Determination of blow-off equivalence ratio. Temperature contours are shown in a descending order from $\phi=0.55$ to $\phi=0.30$. Due to flame behavior at $\phi = 0.30$, this is taken as the blow-off equivalence ratio	76
4.7	The comparison of non-reacting (top) and reacting flow (bottom) in terms of vortex shedding effect. The absence of the shedding in the reacting case improves 2D approximation of the 3D flow.	78
4.8	Comparison of axial velocity between 2D, 3D, and experimental results. The x-positions are normalized by the length of the bluff body and the velocities are normalized by incoming flow velocity	79
4.9	The instantaneous temperature contour of the bluff-body stabilize flame operating near blow-off condition. This is based on 3D simulation using tetrahedron grids with LES and detailed chemistry models at $\phi = 0.30$.	81
4.10	Same contour as figure 4.9 showing the result in isometric view. The vortex shedding downstream of the flow is more visible.	81
4.11	Top view of the 3D domain showing the consistency of the flame near bluff-body stabilizer in span-wise direction while showing variation in the flame extinguished region further downstream.	82
5.1	Comparison of instantaneous inlet velocity profiles for ITI=1.7%, red line, and ITI=27.5%, broken line. In both cases the mean velocity is set at 17.6 m/s	84

5.2	Comparison of instantaneous velocity contours for ITI=1.7%, top, ITI=27.5%, bottom, for non reacting cases. The vortex shedding phenomena are produced in both cases while the turbulent behavior is more dominant in higher ITI case as shown by the more intense vortices especially behind the bluff-body region.	85
5.3	Effect of ITI on instantaneous temperature contour, top: ITI=0%, middle: ITI=5%, bottom: ITI=10%. The propane-air flame is at $\phi = 0.65$ and initial temperature of 288K operating at atmospheric pressure.	86
5.4	Effect of ITI on instantaneous velocity contour, top: ITI=0%, middle: ITI=5%, bottom: ITI=10%. The propane-air flame is at $\phi = 0.65$ and initial temperature of 288K operating at atmospheric pressure.	87
5.5	Effect of ITI on instantaneous vorticity contour at $\phi = 0.65$, top: ITI=0%, middle: ITI=5%, bottom: ITI=10%.The propane-air flame is at $\phi = 0.65$ and initial temperature of 288K operating at atmospheric pressure.	88
5.6	Effect of ITI on inlet sgs turbulent viscosity at different locations from the inlet. This is an instantaneous result, hence the variations in location of the peaks.	89
5.7	Effect of ITI on recirculation zone as seen in temperature contours. Increased ITI shortens the recirculation zone. This affects the heat release and strength of the flame.	90
5.8	Blow-off caused by varying the ITI - temperature contours. flame extinguishes for ITI of 5% but survives at 10%	91
5.9	Flame with detailed chemistry survives with ITI=10% even 80ms after the blow-off time with 5%. With global chemistry with 10% ITI the flame blew off 34ms later than the blow-off with 5% ITI.	93
5.10	Chemical kinetic impact analysis on flame blow-off prediction. Top:detailed chemistry at t=660ms of flow time, middle:no signs of blow-off at t=900ms of flow time with one-step chemistry, bottom:one-step chemistry at t=1.36s of flow time	94
5.11	At ITI=10% more heat release is evident behind the bluff-body by higher concentration of hydroxyl (OH) compared to ITI = 5% and 15%	96

5.12	Effect of ITI on sgs turbulence viscosity in the flow field. Shown is the field of turbulent viscosity at 0%, 5%, and 10% from top to bottom.	98
5.13	Effect of elevated ITI on the flame temperature. the profile is taken 1 cm behind the bluff body	99
5.14	Vorticity magnitude 1 cm behind the bluff body at three different ITI's	100

To my parents, wife, son, siblings, my extended family, and Muslim Community of Syracuse and Houston for their support, encouragement, and dedication.

O Allah! Indeed I ask You for beneficial knowledge, and a good Halal provision, and actions which are accepted.

- Prophet Mohammad (pbuh)

Chapter 1

Introduction

1.1 Introduction

This thesis seeks to increase our understanding of a bluff-body stabilized reacting flow near its blow-off combustion in order to control it in conditions deemed to favor lower harmful gas emissions. It is embedded in a broader concern about energy consumption patterns and clean air initiatives.

Combustion can be defined as a controlled process in which the energy content of fossil fuels is rapidly released as thermal energy. Main fossil fuels include coal, oil, and natural gas. The energy released is mainly used in transportation, heating, and electricity generation. A look at the current energy consumption patterns brings out the role of combustion.

Figure 1.1 shows the energy consumption distribution in 2015. It shows that 85% of total energy consumption in the world is provided by the combustion process. It is predicted that world energy consumption in 2040 will be twice that of 1990. The macroeconomic growth of two heavily populated continents, Asia and Africa, is the driving force for this energy consumption increase.

Figure 1.2 shows the energy consumption history and projections for the time period of 1990 to 2040. A few observations can be made: projected world energy consumption increase for bio and renewable energy is steady but is only 10% of the total consumption. Globally, the most dominant energy

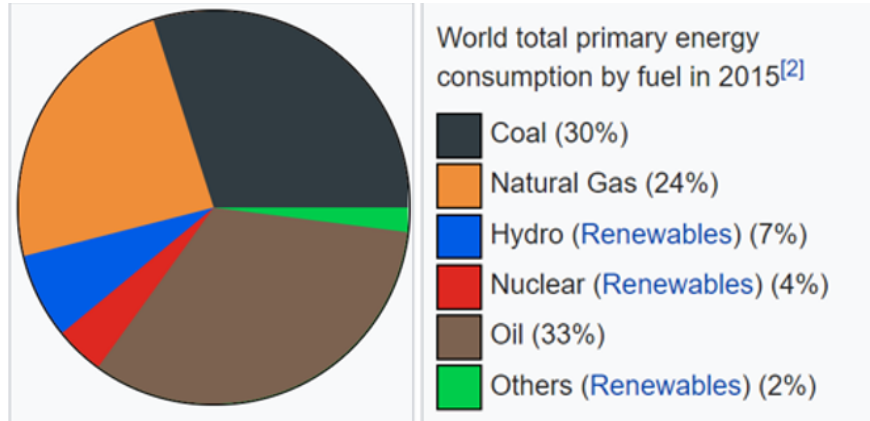


Figure 1.1: World energy consumption distribution in 2015. (Energy Information Administration, [1])

source will remain fossil fuels. Nuclear energy will remain steady. These projections therefore point to the continued importance of oil, natural gas, and other fossil fuels. It also points to the continued relevance of the combustion process that is used to harness the chemical energy of the fuels.

The downside of combustion process is pollutant generation. Resulting from the combustion process are unburned hydrocarbons (UHCs), particulate matters (PMs), carbon monoxide (CO), carbon dioxide (CO₂), and various oxides of nitrogen (NO_x). These can cause smog, acid rain, ozone depletion, climate change, and various public health issues such as asthma in kids and elderly

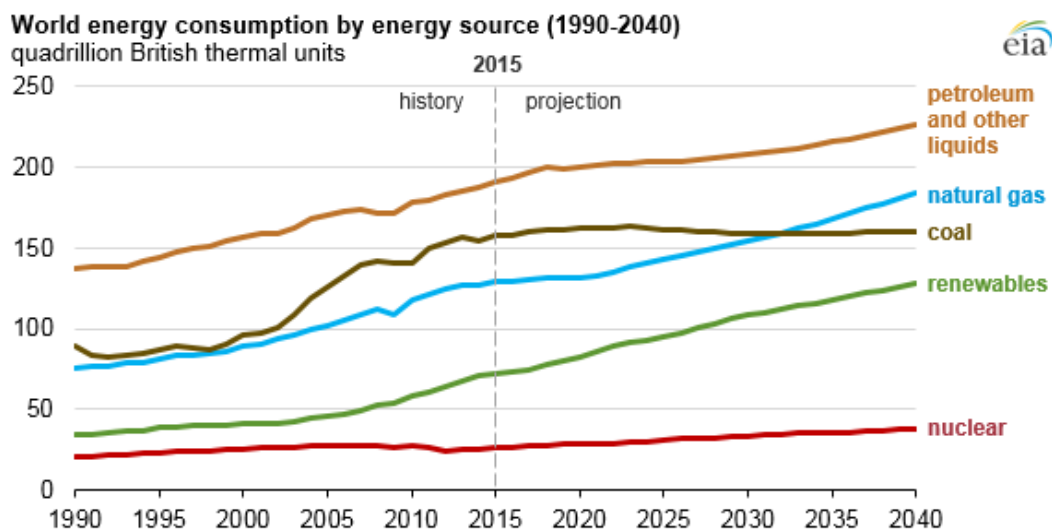


Figure 1.2: World energy consumption by energy source in quadrillion Btu. (World Energy Outlook 2018, Energy Information Administration, [1])

people.

Restrictions on pollutant emissions for in-land, marine, and air vehicles are getting tighter in many countries due to their increasing negative impacts. Regulations become more rigorous to the point that a complete re-design of combustors in many industries becomes inevitable. For instance, in order to meet the recent NO_x emission requirements imposed by some air quality management districts, a fully premixed combustors technology needed to be developed in furnaces used for homes and commercial buildings heating.

Conventional household or commercial furnaces are designed with partially premixed burners. These were used by all HVAC manufacturers in North America for many years. The recent regulations on NO_x emission causing a shift in burner designs for this equipment. Fully premixed burners are proven to be suitable design for these ultra-low NO_x furnaces when they operate with more excess air compared to conventional partially premixed burners. By increasing the excess air and enhancing the mixing process of the reactants, thermal NO_x concentration in high temperature zones of the conventional flame subsided to great extent causing an overall cleaner combustion process. This, however, imposes stability issue in the combustor when they are operating near the low flammability limit of the fuel. As a result, the flame becomes more sensitive to environmental and boundary conditions compared to conventional partially premixed flames. In order to fully understand the dynamics of these types of combustors more rigorous experimental and computational research are needed. Establishing the correlation between boundary condition and the flame dynamics is a key area of future bluff body flame research.

This thesis will first determine the physical models needed to validate a standard bluff body experiment known as the Volvo Flygmotor test case conducted by Sjunnesson et al. [2]. This requires a critical assessment of many variables in modeling the combustion processes including but not limited to dimensionality of the model, turbulence and chemistry models, chemical kinetics, mesh configuration and resolution, dependency of material properties on temperature, and the turbulence-chemistry interaction model. This research will examine all these variables to arrive at

the optimal model combination in terms of accuracy and computational cost.

To advance our understanding of science-based simulations of turbulent premixed bluff body stabilized flame we need to rationalize the models needed for prediction of these type of flames in the most efficient computational method without losing the key features of the flame dynamics needed for this prediction. Once accomplished then further investigation with established numerical methods becomes possible to analyze the sensitivity of lean flame dynamics to the variation of inlet turbulence intensity (ITI). These are the main goals of this work.

1.2 Motivation

Premixed flame stabilization in high speed flows has been an important topic in combustion research. Practical applications include flame stabilization in afterburners of military aircraft, gas turbines, and industrial furnaces. The bluff-body is one approach to flame stabilization. An alternative to bluff-body stabilization technique is the swirl stabilization method. Flames which are anchored to a bluff-body are intrinsically unsteady due to the vortex shedding phenomenon. These vortices are initiated at the tips of the bluff body which has triangular cross section in the experiment we are validating. This phenomenon is partially suppressed in strong or rich flames due to heat dilatation effect resulted from the chemical reaction as it will be discussed further in the following sections.

This research is concerned with the physics of bluff-body stabilized turbulent flame. The work is driven by the concern about increasing air pollution related to the burning of fossil fuels. This pollution has led to more stringent regulations on combustion emissions. In order to meet these regulations, fully premixed combustor systems operating close to lean flammability limits of the fuels are required. By premixing the air and fuel with higher percentage of excess air, the adiabatic flame temperature and the related thermally generated pollutants, specifically Nitric Oxides are reduced. As explained, operating at this condition which is close to fuel low flammability limit (LFL) introduces flame stability issue.

At leaner conditions, the effect of vortex shedding becomes more dominant and by further decreasing the equivalence ratio it can cause undesirable flame blow-out in the combustion system. In order to better understand the interaction between turbulence and chemical reactions at near blow-off condition, a computational analysis is needed. Since experimental results at near blow-off condition is scarce, the model used to investigate the flame dynamics at very lean condition can be validated against available experimental results at richer flame condition. This will provide us with a higher level of certainty about the models used to predict the interaction of turbulence and chemical reactions and ultimately the flame dynamics at near blow-off condition where there are no experimental results available pertaining to this geometry at this very lean condition.

The expectation from the numerical investigation is that at near blow-off condition the vortex shedding mechanism becomes stronger in the combustor domain increasing the instability and eventually causing blow-off. The bluff body anchors the flame by generating a low velocity region behind the bluff-body, which is called recirculation zone. This will prevent flashback and blow-out from a combustion domain. However, by making the flame leaner and close to flammability limit the generated sinusoidal vortices initiated at the tips of the bluff body outweigh the anchoring capability of the bluff body and at certain conditions cause flame blow-off or extinction. By further decreasing the fuel to air ratio the adiabatic flame temperature decreases and the heat release dilatation can no longer sustain a healthy flame. It is expected that at the very lean operating condition close to flammability limit every fluctuation in the boundary condition imposes flame stability problems. Understanding the trend and how these changes in boundary conditions impact the flame stability at near blow-off condition is the main goal of this research.

The boundary condition of interest in this research is inlet turbulence intensity or ITI. This parameter is in fact the indicator of level of reactants turbulence level entering the combustor calculated from the fluctuating velocity components. It is tied to the geometry and shape of the combustor inlet condition and can be controlled by different devices such as turbulators and dampers with variable opening proportion. In order to investigate the effect of ITI on the flame extinction, the blow-off

equivalence ratio is first determined given the numerical set-up used in model validation. The near blow-off equivalence ratio is then chosen such that for an inlet turbulence intensity of 0%, no blow-off is observed. The ITI is then varied in increments of 5% and the sensitivity of near blow-off flame to the increasing ITI is then investigated.

Since experimental data pertaining to this topic are rare, a model verification was performed against available experimental results. This achieved by carefully tuning the correct model combinations such that all flow dynamics are captured with a reasonable computational cost. Once models are established then they are employed to explore the less understood effect of ITI on flame instability.

This study is therefore intended to increase our understanding of the sensitivity of bluff-body flames to varying inlet turbulence intensity. The completion of this thesis will also advance our understanding about the predictability of 2D versus 3D LES models when the bluff body stabilized combustor is operating at different equivalence ratios. This will be the topic of chapter 3. In chapter 4, the process of finding the near blow-off equivalence ratio is discussed. In chapter 5, it will be shown that 3D effects of turbulence can be neglected to the extent of seeing the trends in flame dynamics even at near blow-off conditions. Also, the non-linear relationship between increasing the inlet turbulence intensity at near blow-off flame condition with respect to flame stability behind the bluff body will be demonstrated in that chapter.

One important implication of this research is although it focuses on the Volvo test rig in which the premixed flame is specifically stabilized by a prismatic bluff-body with isosceles triangle cross section the results obtained can be extended to any types of bluff body stabilized premixed flames with understanding that the values obtained for blow-off equivalence ratio can vary depending of type of test being validated. This view is supported by the fact that the non-linear correlation observed in this specific case was observed experimentally in different experimental setup conducted by Cetegen [3], with conceptual similarity to our numerical investigation.

1.3 Literature Review

Bluff-body stabilized flames have been the subject of investigations for many decades. The complexity of these types of flames has led to persisting challenges that need to be addressed. Further, from initial focus on experimental characterization of these flames, the advantage of complementary numerical modeling and simulation is now recognized. In order to situate this work within this active research field, a literature review is provided.

The literature review first considers the study of the dynamics of bluff-body flames. It then reviews the study of blow-off phenomena. This is further followed by a focus on lean blow-off and the effect of ITI on flame dynamics. With respect to numerical simulations of the flame problem, research on the necessary elements of accurate simulation is considered. After summarizing the outstanding challenges, the specific objectives of this thesis are then presented.

1.3.1 Dynamics of bluff body flame

Several experiments have been conducted to understand the dynamics of bluff body stabilized premixed flames [2, 4–11]. Sjunnesson et al. [2] performed an experiment using a prismatic bluff body. The tests include two non-reacting and two reacting cases. Transversal mean and root mean square axial velocities as well as mean temperature and CO concentration at different locations were measured. Blanchard et al. [11] set up a rig for V-gutter bluff body stabilized flame study. One operating condition for propane-air mixture at stoichiometric condition was tested with the goal of comparing the results with a numerical study. The simulations showed that changing the sidewalls to periodic boundaries and thickening the boundary layer near the flameholder reduces the effect of the symmetrical vortex shedding that had been seen in both simulation and experiment.

Experiments and flow analyses have established key features of the bluff-body stabilized flame. Generally, the flow around bluff body consists of boundary layer, separating shear layer, recirculation zone and wake [12, 13]. From observations by Lieuwen and Shanbhogue et al. [14], the

boundary layer does not significantly impact the flame dynamics when Reynolds number is less than 200,000 [15]. The Reynolds number for the Sjunnesson test rig is around 48,000, so that the impact of the boundary layer on the flame dynamics is negligible. The shear layer bounds the recirculation zone [16] and separates the unburnt mixture from the burnt mixture. The zone can envelope or overlap the kelvin-Helmholtz (KH) instability [17]. The instability is due to material acceleration as a result of gas expansion in the combustion zone [18]. This vorticity, unlike the Bernard-Von Karman vorticity street (BVK), will attach to the bluff body. It is continuously being generated giving the sense of not being shed as in the case of Bernard-Von Karman instability. The vortices due to KH instability are relatively symmetric compared to BVK instability, which is sinusoidal. The KH instability has much lower time scale compared to BVK and they convect continuously downstream with no detachment from the bluff body tips and rolls up into larger vortices [14]. The Kelvin-Helmholtz instability has been referred to as symmetric vortex shedding [19–21].

It has been understood that the bluff body stabilizes the flame by generating an attached low velocity recirculation zone down stream of the bluff body. The recirculation zone, which contains hot gases from chemical reaction, establishes a continuous flame by becoming a heat source for the ignition of fresh incoming fuel-air mixture [22]. The fresh mixtures are entrained either from the downstream of recirculation zone in a strong flame or via gaps in the shear layer in weak flame or both [3]. Chemical reactions occur within the entrained hot gases. The wake is the asymmetrical instability that occurs after the recirculation zone and contains vortices with large temporal and integral scales, see Fig. 1.3.

The sinuous wake or vortex shedding initiated from the bluff body in non-reacting flow is pushed downstream of the flow, after the re-circulation zone. This is due to the effects of heat release and volume dilatation in the reacting flow. A low velocity region is thus created for the aerodynamic anchoring of the flame.

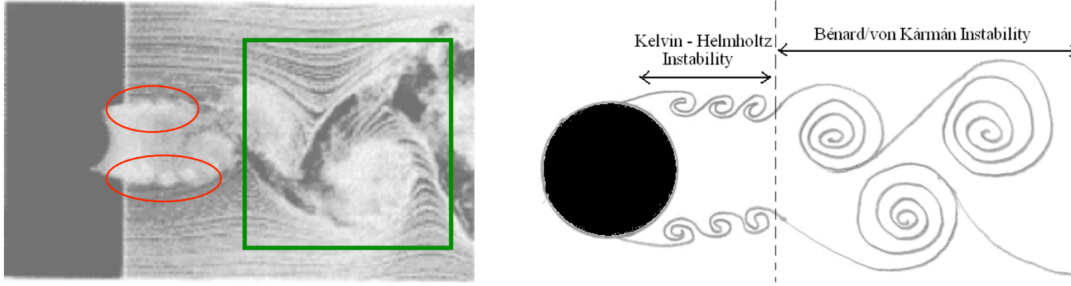


Figure 1.3: Illustration of the instability of the shear layer (circled red), the recirculation zone, between shear layers, and the asymmetric instability process or wake region, (boxed green). Picture adapted from Prasad and Williamson [23]. The schematic on the right is to illustrate the concept [14].

The presence of the bluff body and the fact of having two fluids moving in parallel with two different velocities cause instabilities in the flow dynamics. While the first phenomenon (asymmetrical vortex shedding) is largely suppressed due to dilatation effect of chemical heat release [14], the latter phenomenon (symmetrical or the so-called Kelvin-Helmholtz instability) is generated by the effect of velocity gradients in the vicinity of shear layer. This instability is characterized by small vortices with very small characteristic times. These vortices are being continuously generated from the tips of the bluff body, while never being detached. The relative location of the shear layer with respect to Kelvin-Helmholtz vorticity region has a determining factor on flame stability [17] and can be a function of incoming mixture velocity as well as the fuel to air ratio of the mixture [3].

The temperature ratio, T_b/T_u , or density ratio, ρ_u/ρ_b , between burnt and unburnt mixture can be a deterministic factor for the transition from symmetric shear layer to asymmetric vortex shedding. Cocks [24] and Emerson [25] showed that the transition from asymmetric to symmetric vortex shedding takes place for a density ratio of 1.7-3.4. It was numerically shown that by increasing the density ratio, sinusoidal shedding appears less frequently and eventually disappears from the entire domain at $\rho_u/\rho_b = 6.8$ [14].

Numerical simulations using Reynolds Averaged Navier Stokes (RANS) and unsteady RANS (URANS) coupled with various combustion models have been used to simulate time averaged prop-

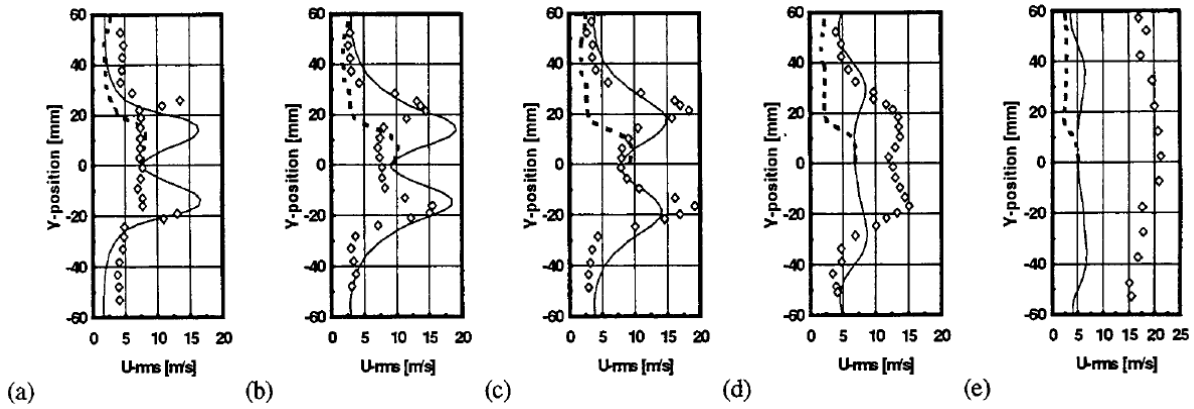


Figure 1.4: Profiles of U -rms. in five cross sections downstream the flame holder (a) 15 mm (b) 38 mm (c) 61 mm (d) 150 mm (e) 376 mm (open symbols-measurements, solid lines-LES, dotted lines $k - \epsilon$ RANS) [27]

erties of bluff-body stabilized flame such as temperature and species mass fractions [26]. However, the highly dynamic nature of bluff-body turbulent premixed flames cannot be fully captured by RANS approaches, especially near blow-off conditions. The use of Large Eddy Simulation (LES) therefore becomes attractive for this problem due to its ability to capture greater details of the flow field, besides the unsteady nature of the bluff-body turbulent premixed flame. Ryden [27] was one of the earliest researcher to attempt a validation of the Volvo test rig using the LES turbulence model. He demonstrated an overall improvement in the prediction capability of the flame dynamics using the LES model even on a coarse mesh in 2-dimensional computational domain.

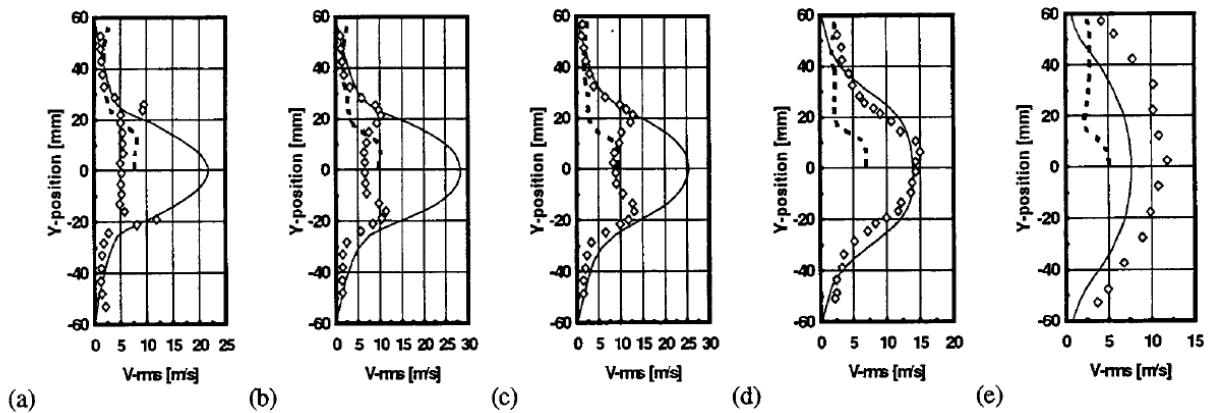


Figure 1.5: Profiles of V -rms. in five cross sections downstream the flame holder (a) 15 mm (b) 38 mm (c) 61 mm (d) 150 mm (e) 376 mm (open symbols-measurements, solid lines-LES, dotted lines $k - \epsilon$ RANS) [27]

He compared results obtained from LES with those from $k - \varepsilon$ RANS turbulence model. He demonstrated an advantage of LES over the $k - \varepsilon$ RANS model in prediction of velocity RMS in both directions. This comparison can be seen in figures 1.4 and 1.5. However, he observed that both turbulence models showed steeper gradients in the flame region and more constant velocity in the recirculation zone compared to measurements. In the case of the LES, he attributed this computational behavior to exaggerated vortex shedding prediction due to lack of proper grid resolution and high interaction between turbulence and combustion.

Attempts have also been made to distinguish between reacting and non-reacting flow features associated with bluff-bodies. Fureby and Moiled [28] presented a LES model to investigate both non-reacting and reacting flows around a triangular bluff body with different operating conditions. They captured some of the unsteadiness expected in the flow structures. With respect to reacting flows and associated flame models, Fureby [29] and Bai et al. [30] compared LES premixed combustion flamelet and finite rate chemistry models with respect to their prediction of experimental data. The simulated results were found to be comparable to experimental results with respect to the turbulent flame thickness and flame speed.

Wang and Bai [31] also conducted a LES study of turbulent premixed flames using the level-set G-equation method. They studied the interaction between the flame front and turbulent eddies as well as the effect of sub-grid scale (SGS) eddies of the flame surface wrinkling. They observed that time-averaged mean flow properties mainly depend on the resolved large scale eddies while the turbulent flame speed and spatially filtered intermediate species and reaction rates strongly depend on the small SGS eddies. They also concluded that fine grids and filter size may have to be used to capture the influence of the SGS eddies.

Li et al. [12] conducted an LES analysis of bluff body stabilized flame. They also used the level-set flamelet approach to analyze the unsteadiness observed in the Volvo rig. They used both reflecting and non-reflecting inlet boundary conditions. They relate the combustion instability to the close loop of acoustic wave, vortex shedding, flame oscillation, and heat release which is formed due to a

resonance between the vortex shedding in the separated shear layer and one of the acoustic modes of the chamber in the case with reflecting inlet boundary conditions.

In terms of the impact of temperature ratio on the flow field, Erickson [18] showed numerically that as the reactant temperature increases, and the flame temperature ratio decreases, the flame generated vorticity is reduced. Also the vortex shedding originated from the bluff body continues to dominate the fluid dynamics. He also showed that as a result of the temperature ratio decrease the flame brush thickness increases and this can be an indication of large scale asymmetric fluid dynamics domination in the fluid dynamics. He numerically showed that this domination occurs at $T_b/T_u \leq 1.5$. The effect of the temperature ratio is shown in fig. 1.6 from [18]. As it can be seen from this figure as T_b/T_u ratio is decreasing the impact of vortex shedding become more dominant. At $T_b/T_u = 1.25$ and less the reacting flow approaches the dynamics of a non-reacting flow by minimizing the normalized length of the recirculation zone to less than unity behind the bluff-body.

For model validation against experimental results obtained from premixed bluff-body stabilized flame, there are also other works by many researchers. Engdar et al. [32, 33] has used the Flamelet Library Approach (FLA) as implemented in a commercial code Star-CD to model a lean premixed flame that is stabilized by a triangular prism bluff body. He investigated the impact of using three different turbulent flame speed models with combination of four different turbulence model such as standard $k - \epsilon$, a cubic nonlinear $k - \epsilon$, standard $k - \omega$, and SST $k - \omega$ models on the mean flame position, which in turn yields the temperature and species distribution over the computational domain. He observed a good agreement between numerical and experimental results from all combination of flame speed and turbulence models. However, he reported the inability of RANS to capture the periodic fluctuations due to its broad averaging. The turbulence intensity downstream of the flow was therefore underpredicted in all of these models.

Ghirelli [34] formulated a dispersion model for turbulent premixed combustion and showed that with this model more accurate results can be obtained with less calibration effort compared to the previous model, the Flame Speed Closure (FSC) model which is based on work by Lipatnikov

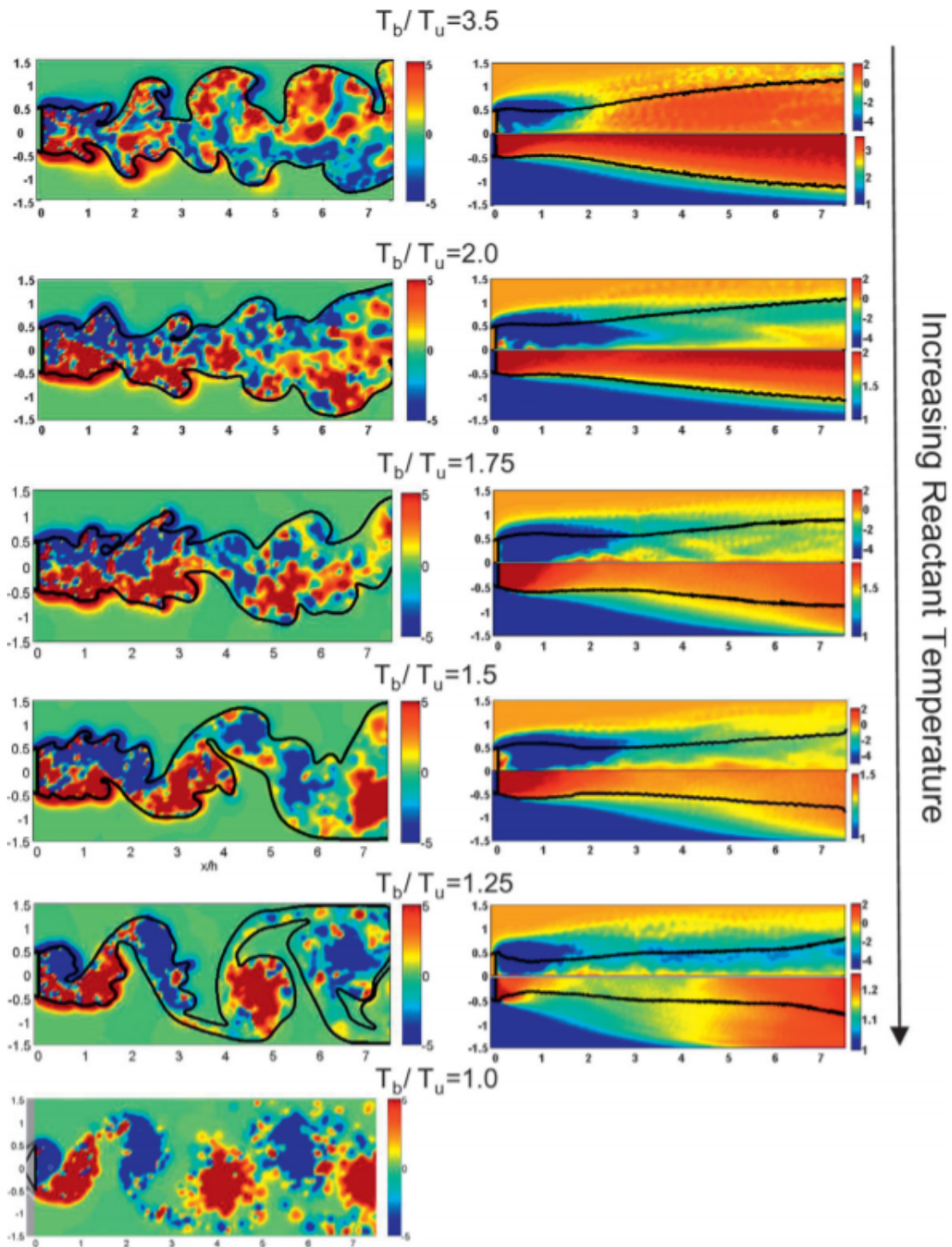


Figure 1.6: Instantaneous and time-averaged flow field obtained by LES for increasing reactant temperature, decreasing temperature ratio, from 3.5 to 1.0. Left column: Instantaneous vorticity and flame. Right column: Time-averaged flame location overlapped with mean vorticity(upper half) and mean temperature(lower half) [18].

and Chomiak [35–39]. The final result does not show much improvement unless it is manually calibrated to match closer with the experimental result. Figure 1.7 shows the temperature profiles at different locations using both TFC and Dispersion Models. The top row is the results from non-calibrated model while the bottom row shows the result from the calibrated model. It is obvious that a good agreement between experimental and simulation results are seen when the model is calibrated to match closer with experimental results. Also there is no indication of how this model performs at near blow-off condition as it is indicated that the laminar combustion rate is neglected in this model and this according to the author is needed for more accurate flame prediction in transient situation of ignition. The FSC model from which the dispersion model is developed, is based on the Turbulent Flame Closure model (TFC) [40]. The TFC model is only valid in the intermediate steady combustion with constant flame speed, which is not the case for an extinguishing flame.

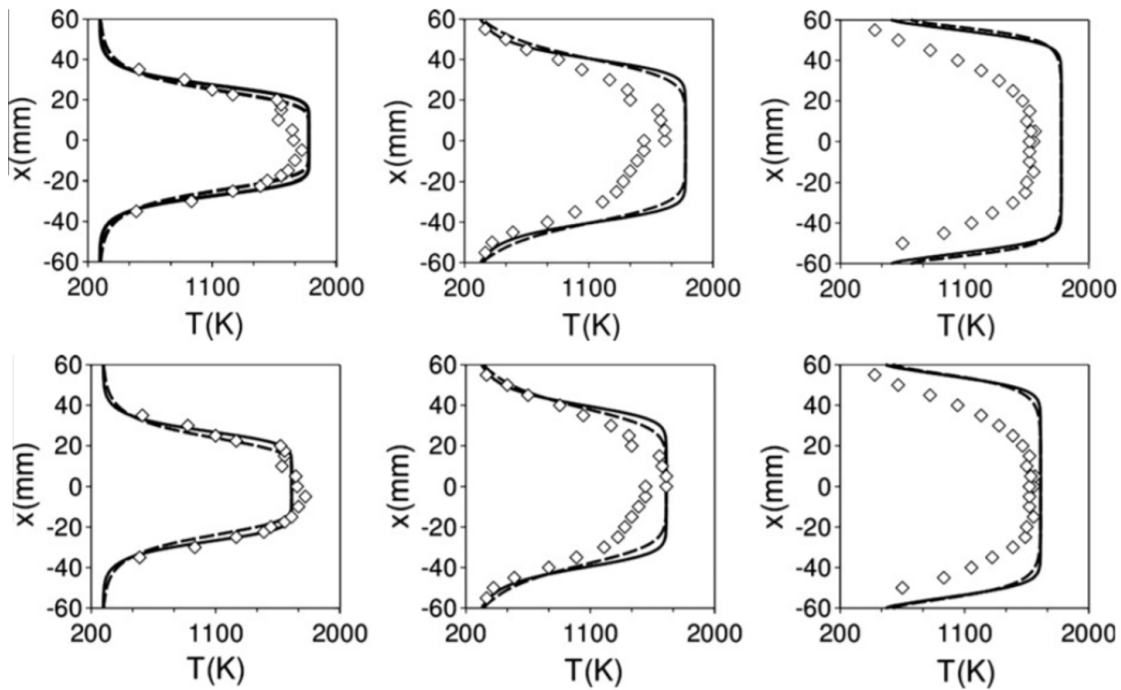


Figure 1.7: Simulated temperatures profiles at $x = 0.15, 0.35$ and 0.55 m behind the bluff body for Sjunnesson test rig. The dotted line is experimental values and dashed line and solid line are the results from TFC and Dispersion models, respectively. The top row is the simulation results before calibration and the bottom row is the simulated results after calibration [34]

Jones et al. [41] implemented the LES-pdf method with the Eulerian stochastic field solution method in conjunction with a mechanism of 4 reactions and 7 chemical species to validate a premixed propane-air triangle bluff-body experiment. His work showed an overall good agreement with the averaged experimental data but temperature and velocity RMS, and CO error were still around 10%.

Flame simulations also seek to capture acoustics properties. Lee [42] investigated the combustion-driven instability and the acoustic coupling due to duct enclosure in bluff-body stabilized premixed turbulent flame utilizing an URANS (Unsteady Reynolds Averaged Navier Stokes) turbulence model combined with the BML (Bray-Moss-Libby) combustion model and modified reaction rate closure in order to capture the changes in the flame surface density. He observed self-sustained hydrodynamic instability induced by large scale vortices under lean condition. He also reported the appearance of wrinkling of the flame due to Kelvin-Helmholtz instability when the flame is stronger and the convection of large scale instability downstream of the flame. He discovered that the acoustic excitation in lean flame condition due to heat release modulation and its correlation with pressure fluctuation in the combustion domain. This research was mainly focused on validating this set of models against the experimental results. It did not provide any further insight on how the model will work with detailed chemistry near flame blow-off condition. It was sought to justify using URANS as a valid turbulent model against LES when the flame is richer and stronger with an equivalence ratio above 0.65.

The choice of a turbulent flame model continues to be a challenge because of inadequate performance of most. New models are also being introduced. Moreau [43] devised a relatively new chemically reacting model referred to as Self-Similar Turbulent Flame (SSTF) and compared his numerical result with the data obtained from well-established Turbulent Flame Closure (TFC) model using the commercial code Star-CD. The SSTF model was based on the turbulent flame brush thickness founded on the Kolmogorov theory of turbulence and the concept of self-similarity. He claimed better agreement with experiments for of the results obtained from the new model compared to the older model. He argued that the newer model had an advantage over the TFC model due to its larger

margin for future improvement.

Park [44] also devised a new sub-grid scale model for the validation of turbulent premixed bluff-body flame using Large Eddy Simulation. He and his co-worker developed a dynamic sub-grid scale model, with scale fluctuation, and integrated this model with the G-equation in order to capture the flame front propagation. They also introduced a new turbulent flame speed model based on sub-grid turbulent diffusivity and the flame thickness. They compared their results with conventional sub-grid scale Smagorinsky model and experimental data. They observed overall agreement between results obtained from both sub-grid scale models in terms of measured mean temperature and velocity profiles. In particular, they established that the simulation results using the dynamic SGS model are in better agreement with experimental data than the data based on the static Smagorinsky model. This judgement was based on the predictions of temperature, velocity and its fluctuation components in the downstream transient region behind wake. Both combustion models were successful in capturing the global flame propagation behaviors.

Other studies have focused on the combination of turbulence and flame models. Salvador [45] simulated a combustion experiment conducted by Sanquer in 1998 [8]. He implemented the LES turbulence model and the Xi turbulent-combustion model. The Xi model was developed by Tabor et al. [46] and is integrated into the OpenFOAM software. Salvador modelled the flame propagation speed utilizing the flame surface density and the surface wrinkling function developed by Weller [47]. He found good agreement between the numerical solution and experimental data but pointed out that the one-equation Smagorinsky sub-grid scale model yields similar results albeit with more complicated and computationally more expensive dynamic Xi turbulent model unless the coefficients in the latter model are tailored for improvement.

Some combustion models depend on higher moments of model variables. Zhou [48] proposed second-order moment combustion model. He compared the results with eddy-break-up and probability density function combustion models based on Large Eddy Simulation of an experimental premixed bluff body flame. He reported good agreement between his results and the experimen-

tal data for time-averaged and root mean square of the temperatures profile. He generalized his finding to both non-premixed and premixed combustion. He claimed that second-order moment combustion model is capable of yielding acceptable statistical results in LES at any conditions while eddy-break-up and probability density function combustion models cannot always predict a flame that agrees closely with close-to experiment results. By using the second-order moment combustion model, he observed organized large vortex and thin flame surface structures in bluff-body stabilized premixed combustion for instantaneous results. Due to incorporation of higher moments of combustion variables in this model, a higher computational cost is expected. It was reported that simulating the bluff-body stabilized flame needed in order of months to be completed compared to the order of weeks which is expected when second-order moment combustion model is not implemented. Although some improvement in the predicted results are reported but still there are some discrepancy between the simulated and experimental statistical results despite the significant additional computational cost.

The main focus of all these studies were to validate various sets of numerical model against the available experiment results by examining different parameters of computational modeling such as turbulence, chemical kinetics, and turbulence-chemistry interaction models. Although all these works contribute to better understanding of how numerical models can be adjusted in order to get acceptable results from numerical simulation, they do not consider the near blow-off flow dynamics. They also fail to consider how changing the boundary conditions at the lean near blow-off equivalence ratio can potentially impact the flame dynamics. This research is intended to fill this gap by establishing a reliable set of numerical models that benefits from previous experience and explores regions where fewer or no numerical investigations have been conducted. This helps to understand the sensitivity of lean flame to inlet turbulence intensity boundary condition and it helps to identify the most cost effective approaches to simulate bluff body flames.

1.3.2 Dynamics of bluff body lean blow-off

Blow-off phenomena and the impact of different boundary conditions have been studied by few researchers. They explained the phenomenological mechanism that leads to flame extinction. They also address how changing some flow parameters upstream of the flame can change the blow-off equivalence ratio. Chaparro et al. [10] experimentally studied the blow-off characteristics of bluff-body stabilized premixed flames under upstream velocity modulation. They found that the blow-off equivalence ratio exhibits a dependence on the flow modulation frequency.

The effect of spatial equivalence ratio gradients on blow-off characteristics of bluff-body stabilized premixed flame was experimented by Chaudhuri et al. [49, 50]. They observed that varying this parameter changes the overall flame structure, but it did not affect the flame holding characteristics. This is due to the inability of the outer richer mixture to influence the flame stabilization zone.

There is a need for understanding the blow-off mechanism. The flame blow-off mechanism for bluff-body stabilized flames has been explored by Lieuwen et al. [14]. He analyzed a series of experimental and computational results on the dynamics of bluff body stabilized flames. He proposed a phenomenological explanation of the blow-off process. Nair et al. [51, 52] characterized two stages of near blow-off events. They observed that the first stage of flame blow-off is the localized extinction along the flame sheet. They noted that this stage acts as a marker for potential flame blow-off but they also observed that the flame can survive indefinitely at this condition. A more violent flapping of the flame front and an asymmetric mode of flame oscillations is considered as the last stage before flame extinction [49]. Sajjad et al. [15] also gathered various data regarding flame blow-off from about fifty sources. By utilizing chemical kinetics and transport calculations they developed correlations between extinction time scales and stretch rates. There are other studies that propose a flamelet based description of local extinction and relate this phenomenon to excessive flame stretch [53, 54]. Further Chaudhuri et al. [55] studied the behavior of turbulent conical premixed flames anchored at their apex by a bluff body flame holder experimentally. They studied

the flame blow off characteristics under upstream flow oscillations and spatial equivalence ratio gradients. They also studied the flame blow-off behavior under transfer function characteristics and examined the effects of lateral flame confinement.

Mehta et al. [56] showed both experimentally and also computationally that alternating vortex shedding can occur near flame blow-off or in flames burning at low dilatation ratios. Shanbhogue [15] numerically studied the combustion dynamics leading to blow-off in bluff body stabilized flames and described the phenomenology of the blow-off process. The study focused on the processes responsible for flame stabilization and the development of physics-based correlations for flame stability limits. It is reported that close to blow-off, temporal localized extinction occurs intermittently on the flame shear layer. They also observed that these localized extinction events are not enough to cause a complete flame blow-off and under certain conditions the flame can persist indefinitely at this condition. They reported an increase in the frequency of local flame extinction as blow-off is approached. This eventually leads to large scale alteration of the wake zone as a final step before blow-off.

Kiel et al. [57] used Large Eddy Simulations (LES) to investigate the effect of turbulence-chemistry interaction on flame stability. He implemented two different chemical mechanisms, namely, one semi-global chemical mechanism with 14 species and 44 reactions and a skeletal mechanism with 30 species and 114 reactions extracted from a detailed kinetics mechanism developed by Konnov [58]. He reported his observation in terms of dependency of blow-off condition on the turbulence-chemistry interactions and how choosing the correct models in combination with fine mesh in areas with high gradient can predict the flame vortex shedding interaction and flame blow-off more accurately and closer to experimental results. They confirmed that flame instability leading to complete extinction is a result of asymmetrical Von-Karman vortex shedding phenomenon. They understood the initiation and strengthening of vortex shedding phenomenon to be the result of weakening of the dilatation effects in flames with lower equivalence ratio and close to the blow-out condition. The main issue with using higher fidelity combustion models is the additional

computational cost and the extreme fine tuning of the model and numerical parameters that is needed to achieve convergence. Also the process of fine tuning of the numerical set-up is highly problem dependent. The performance of using high fidelity turbulence-chemistry interaction TCI modeling can be seen in figure 1.8 from the study conducted by Kiel et al. [9].

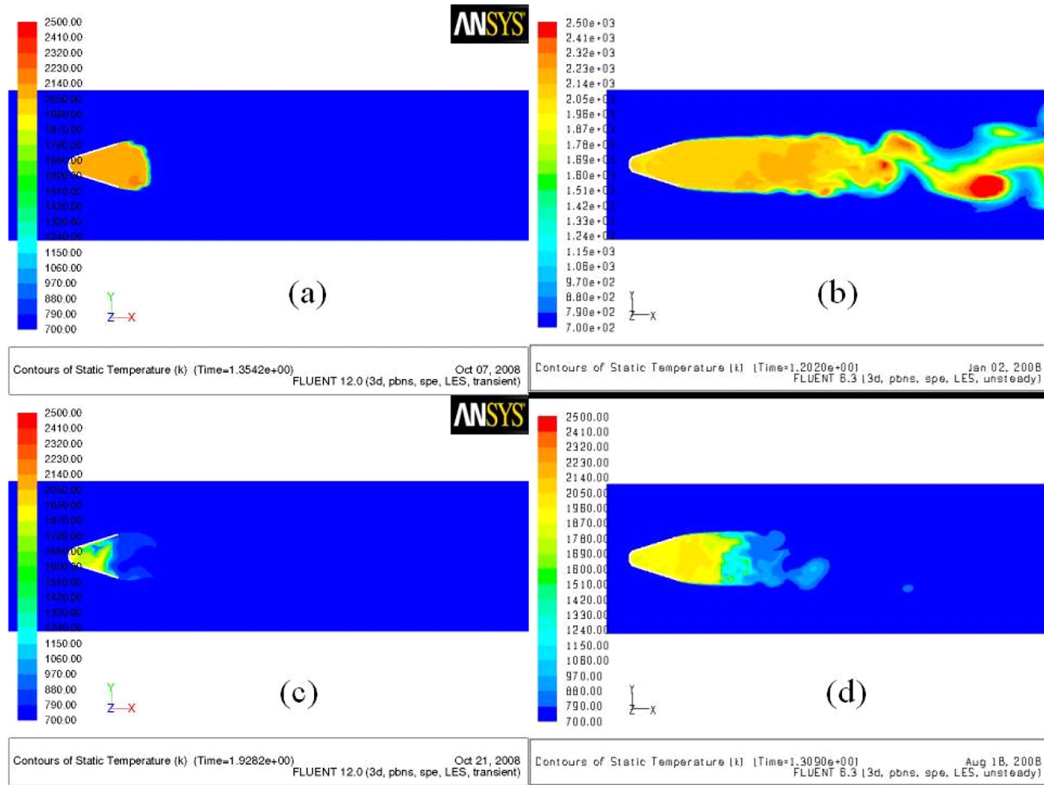


Figure 1.8: Instantaneous temperature profile for the reduced kinetic model; (a) & (c) $\Phi = 0.6$ & 0.45 with EDC model; (b) & (d) $\Phi = 0.6$ & 0.45 with Laminar Combustion model, research conducted by Kiel et al. [9]

This figure shows the improvement of prediction of blow-off equivalence ratio by taking the TCI in the combustion modeling.

1.3.3 Effect of ITI on lean blow-off

The previous research has focused on investigation of blow-off mechanism in bluff-body stabilized flames, however, a complete physical understanding of the final blow-off mechanism and the

effect of boundary conditions on this mechanism also requires further research to develop our understanding about this phenomenon. The details of the blow-off mechanism, especially, the effect of inlet turbulence intensity on the flame dynamics just prior to blow-off is still not thoroughly understood. This work is expected to fill this gap by investigating the inlet turbulence intensity as a parameter which can potentially affect the flame structure and at lean condition even cause blow-out. It will be demonstrated how varying this boundary condition can lead to the unexpected blow-out although the normal operating conditions with prescribed boundary condition may not lead to this extinction. Determining the conditions under which turbulence causes the blow-out is of importance so methods to stabilize the flame at these sensitive conditions can be developed. The effect of this parameter on the flame dynamics at near blow-off condition were addressed by some researchers.

Chaparro and Cetegen [10] studied the blow-off of premixed bluff-body stabilized flame under upstream velocity modulation. They oscillated the upstream velocity around different mean inlet velocities and found that the blow-off equivalence ratio varies based on the flow modulation frequency. They also carried out detailed analysis of the flow field in the flame stabilization zone obtained by particle image velocimetry. They used three different types of flame holders and experimented with three different incoming velocity of 5, 10, and 15 m/s. The flow speed was modulated sinusoidally at frequencies up to 400 Hz with a constant-velocity modulation amplitude of $u_{rms}/U_m = 0.08$ upstream of the flame holder. More importantly, they find the non-linearity of the effect of increasing the modulation frequency on the blow-off equivalence ratio at inlet velocity of 5m/s inline. This experimental study will be important to this work. At this particular velocity, the impact of increasing the incoming velocity modulation frequency was to make the flame more stable, contrary to their observation at 10 and 15 m/s inlet velocity cases. They also reported the dependency of this non-linearity on the shape of the flame holder.

Chowdhury [3] has confirmed the correlation between extinction behavior of a flame at lean conditions and the inlet turbulence boundary condition. The relevant experimental set-up is shown in figure 1.9. He and Cetegen set up an experiment in which they allow the variation of inlet

turbulence intensity (ITI) and the mean velocity and examined the flame response to these variations when it operates close to the blow-off condition. They used simultaneous imaging of hydroxyl (OH) and formaldehyde (CH₂O) fluorescence and particle image velocimetry (PIV) to visualize the flame and its interaction with the flow field. They observed the strong dependency of lean blow-off limits to the ITI at different incoming velocities. They found that precursor of the blow-off was the penetration of reactants into the recirculation zone from local flame disappearance in the reaction zone. They reported higher flame strain that arises from increasing ITI and reduced flame strain limit as blow-off equivalence is approached. A similar experimental observation was reported by Lieuwen [14]. Figure 1.9 shows the schematic of the Chowdhury and Cetegen test setup.

What is unique to the outcomes of the Cetegen testing was the non-linear correlation between increasing inlet turbulence intensity and blow-off limits. They observed that at certain incoming velocity, increasing ITI from 24% to 30% level will actually increase the burning rate and cause flame stabilization instead of the expected flame extinction [17]. This is an interesting result and will be further discussed in this work. They attribute this behaviour to the balance between mixing or pre-heating of reactants and the dynamic vortex shedding phenomena which become more dominant as the flame approaches blow-off. They visualized the overlapping of the OH and CH₂O contours with the vorticity contour. This can reveal the location of the reaction zone and its relative position to high vorticity regions of shear layer. This relative location can actually determine the strain rate of the flame front which eventually cause flame stretch and extinction in lower equivalence ratios, Fig. 1.10.

They also related the burning fraction to the strain rate of the flame. This in turn relates to the relative location of the reaction zone to the high vorticity region of shear layer. Figure 1.10 shows complex flame structure based on CH₂O and OH contours as well as their overlaid structure. At ITI=30% the flame moves away from the high vorticity region and this causes the flame to become more stable, with a higher burning fraction.

It has also been observed numerically that the dynamics of the flame stabilized by a bluff body at

lean conditions is very sensitive to upstream boundary conditions [59, 60]. Afarin and Tabejamaat investigated the effect of the inlet turbulence intensity (ITI) on the $H_2 - CH_4$ flame structure. They used Large Eddy Simulations and considered three different levels of ITI: 4%, 7% and 10%. For modelling the sub-grid turbulence-chemistry interaction of the numerically unresolved, they used the modified version of the Eddy Dissipation Concept (EDC) called Partially Stirred Reactor (PaSR). They also used a full chemical kinetics mechanism of GRI-2.11 to account for the combustion. They

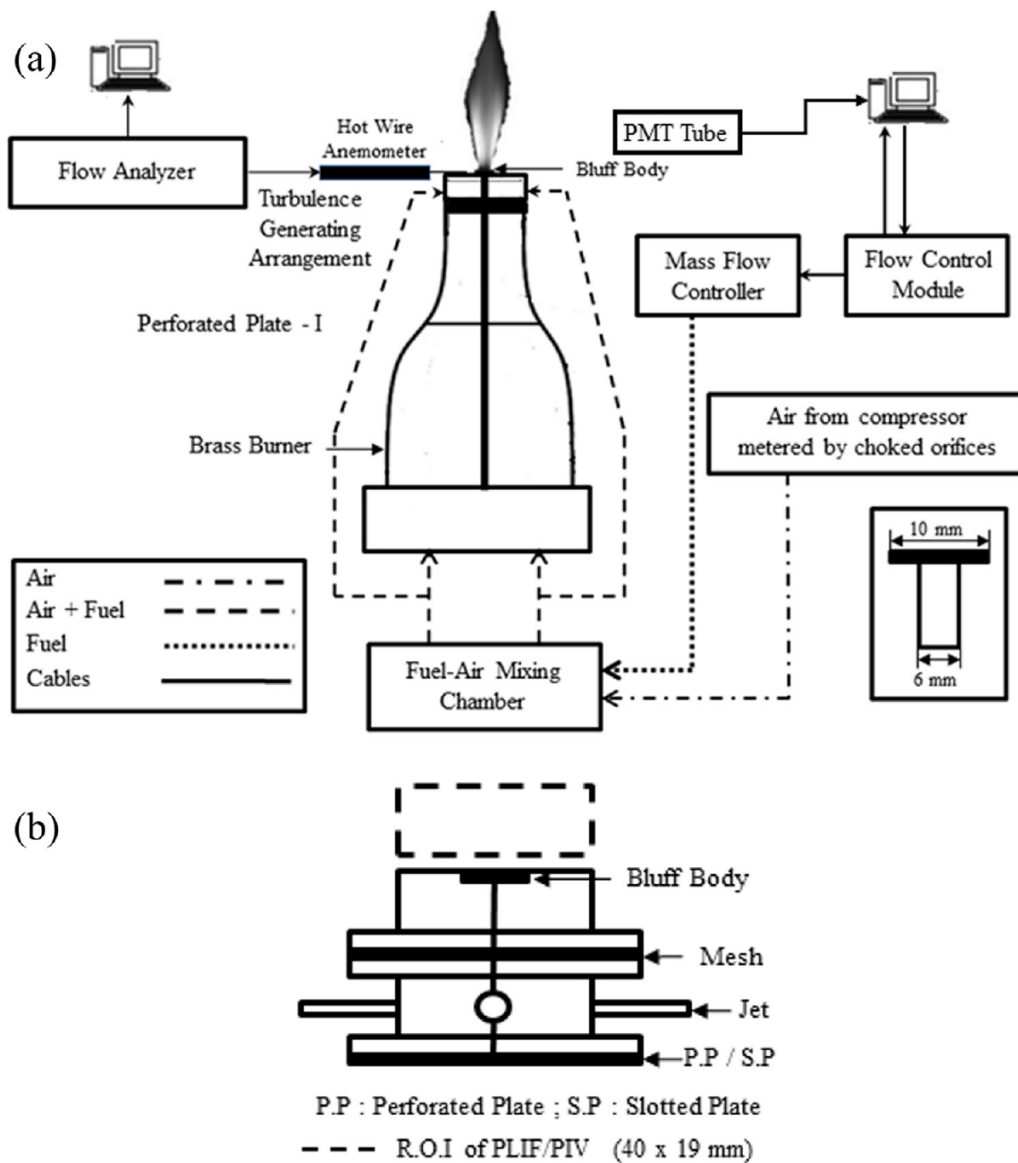


Figure 1.9: (a) Experimental setup by Chowdhury and Cetegen. (b) Schematic of ITI level control method used in the experiment [3]

monitored the temperature, CO and OH mass fractions profiles in addition to the contours of OH, CH₂O, and HCO radicals. These represent the flame front, the premixed zone, and the heat release rate, respectively.

They found that increasing the fuel inlet turbulence intensity has a profound effect on the flame structure, particularly at low oxygen mass fraction. They described this as arising from the fact that increasing the fuel turbulence intensity increases the diffusion of the unburnt fuel which reduces the peak temperature and weakens the reaction zone. This behavior weakens the combustion zone and results in a decrease in the peak values of the flame temperature and OH and CO mass fractions. They argued that increasing the inlet turbulence intensity decreases the flame thickness, and increases flame instability. They also found that these adverse effects of increasing ITI can be reduced by increasing the reactant temperature which reinforces the reaction zone by damping the OH, CH₄

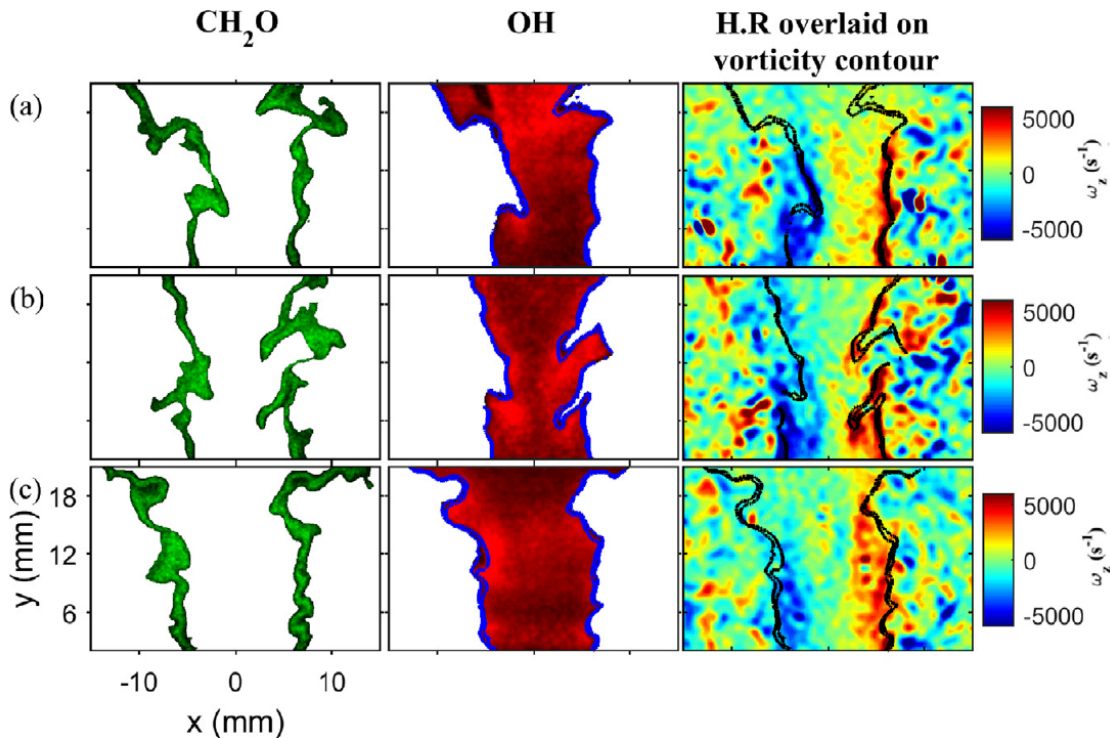


Figure 1.10: Instantaneous images of CH₂O and OH PLIF in addition to heat release region overlaid on the vorticity contours. (a) ITI=24% $\phi = 0.76$, (b) ITI=30% $\phi = 0.73$ showing the overlap of the reaction zone over the shear layer vortices, (c) shows the flame moving away from the high vorticity region at ITI=30% [3].

and temperature oscillations and reduces the convection of reactants into the recirculation zone via reaction zone. They used the data obtained from Dally test rig [61] to validate their results.

Tabor and Baba-Ahmadi [60] explored two mathematical models for turbulence generation at inlet. They used Synthetic inlets and precursor simulation techniques to generate different profiles for inlet turbulence intensity. They found that the synthetic method can generate random field at inlet close to turbulence conditions and the length scales and turbulence energy levels can be specified and controlled. However, this model is inaccurate in terms of random fluctuation development into more probabilistic turbulence. For the precursor simulation method, a more accurate turbulence field can be generated at the inlet. They opted for the use of the precursor model in combination with LES to model the inlet turbulence intensity in OpenFOAM.

The orientation of the bluff body is also of interest. Lin [62] et al. conducted a numerical study to investigate the effects of inlet turbulent intensity and the angle of attack on the flame and flow fields in a channel with an inclined bluff body V-gutter flame holder. He varied the inlet turbulence intensity from 2% to 100%, with different bluff body angles of attack. He implemented the $k - \epsilon$ model for turbulence and eddy-dissipation model for chemistry-turbulence model. His Numerical results indicate that increasing the inlet turbulence intensity and V-gutter angle of attack has a direct impact on the increase of the magnitude of the downstream high turbulence areas with shedding vortices. These vortices in turn caused an increase in both velocity and temperature in the reacting turbulent flow.

Although these experimental and numerical studies are valuable by emphasizing on the importance of inlet turbulence intensity in the dynamics of near blow-off flame they do not establish a solid numerical methodology on how to investigate this correlation. Also they lack a numerical results pertaining to investigation of these effects on a practical bluff-body stabilized flame. Therefore this research is intending to fill this gap by developing a numerical methodology for parametric analysis of the effect of changing inlet turbulent intensity (ITI) on the flame structure, especially when it is lean and close to blow-off condition.

1.3.4 Mesh sensitivity on flame dynamics

It is well understood that the numerical study of the flame dynamics is sensitive to the mesh quality. Manickam et al. [63] studied the implementation of LES and validation against the experimental results obtained from Volvo test rig using algebraic flame surface wrinkling (AFSW) reaction. They also analyzed and compared the results obtained from three different mesh resolutions using the AFSW model. They showed that the non-reacting case with a coarse grid of 300,000 nodes over-predicts the turbulence quantities due to low dissipation at the early stages of the flow development. The medium mesh with 1.2 million cells and fine mesh with 2.4 million cells yield results that were closer to the experimental data. For the reacting case, the predicted results of mean, rms velocities, and reaction progress variable were shown to be in good agreement with the experimental data. However, they observed that the coarse mesh showed a shorter recirculation region due to a higher turbulent burning rate. He conducted an error assessment using two-grid estimator by Celik [64, 65], and the model and grid variation by Klein [66]. He showed that with medium mesh on non-reacting flows the flow field is well resolved while for the reacting flows with the fine mesh the resolution is not sufficient in the flame region. He concluded that the total error mainly depends on the numerical error and the influence of model error is relatively low in his configuration. This investigation points to the importance of assessing mesh effects on reacting and non-reacting flows.

1.4 Specific Objectives

From the above motivation and literature review, we observe a number of gaps and open questions. Firstly, the impact of inlet turbulence intensity on the flame when it is close to blow-off condition is not given due attention by previous researchers. The inlet turbulence intensity, as it will be shown later, has a significant impact on the flame dynamics in both rich and lean conditions, to the extent that the equivalence ratio for a specific gas cannot be taken as the sole determining factor in flame extinction. Also, the correlation between inlet turbulence intensity and blow-off has not been established in the previous computational studies. Experiments suggest that this relation between

turbulent intensity and blow-off is non-linear. Therefore, this research will include investigation of the effects of the inlet turbulence intensity (ITI) on the dynamics of a bluff-body stabilized flame operating very close to its blow-off condition.

This work is concerned with a critical assessment of models needed to simulate a bluff-body flame near lean blow-off conditions. It first focuses on the validation of the Volvo test case to identify the key models needed for good replication of the experiments. The turbulence modeling approach best suited for the complexity is the Large Eddy Simulation (LES) method.

Given the cost of LES, if a problem can be shown to be dominated by 2D flow behavior, then the possibility of using 2D LES needs to be explored. This 2D approach can be adopted if the 2D results are a reasonable representation of 3D flow results. This direction is explored in this work.

Also important is the examination of global chemistry models and more detailed reaction schemes with respect to predicting extinction phenomena. Further, the sensitivity of the predicted flow features to mesh resolution needs to be considered. These questions form part of the thesis, whose major attention is devoted to the effect of inlet turbulence intensity on blow-off.

To summarize, this research seeks:

- To determine combination of physical models and solution techniques needed to validate a bluff body flame using 3D LES.
- To establish whether 2D LES can predict bluff body flame behavior at healthy flame conditions, such as $\phi = 0.65$. If proved, then we can utilize 2D LES to determine lean blow-off limits and further investigate the effect of inlet turbulence on blow-off using a suitable combustion model. Further, it seeks to test the suitability of a one-step chemistry model for blow-off simulation.
- To determine whether the 2D LES of the near blow off flame is similar to 3D LES in terms of flow dynamics. Further, the 3D LES is used to test the sensitivity of the flow to mesh

resolutions.

These questions are explored using the LES method after first validating the set of physical models and simulation techniques against the experimental results from the Volvo program. These preliminary validation studies are done in 3D and 2D.

The 2D LES approach is then used to determine the blow-off limits. From the established blow-off limits, the effect of ITI on a near blow-off flame is then investigated and the results obtained with a detailed chemistry model are then contrasted with those of a one-step chemistry model. It needed to be emphasized that although this research is motivated by technological attempts to reduce NO_x emission, the models and simulations do not focus on predicting NO_x. Rather, the work recognizes that lean flames reduce NO_x through the associated lower flame temperatures. Since these lean flames are plagued by problems, such as flame blowoff, we are interested in understanding the dynamics of lean flames, especially near the lean blowoff limit. Thus, the work is about flame dynamics at low NO_x conditions, rather than NO_x prediction.

The work is driven by the hypothesis that turbulence, chemical kinetics, and flame stabilization mechanism interact in a manner that the flame behavior near criticality cannot be established a priori. Careful parametric studies are needed to establish sensitivity of the flames such as near lean blow-off.

Chapter 2

Experimental and Computational Methods

The research objectives are addressed using simulations. The set of models are first validated against a standard experiment. We therefore need to look at the computational methods and also understand the experiment used as a validation target.

2.1 Experimental Test Rig Set-up

The experimental set up used to obtain the validation target is first described, followed by the computational methods used in the simulations.

A schematic of the Volvo test rig is shown in Figure 2.1. The configuration consists of a 1.5-meter long rectangular duct, 0.24 m wide and 0.12 m in height. The apparatus is divided into the inlet and combustor segments. The inlet segment consist of combustion air flow, fuel inlet, flow conditioning, and seeding. A multi-orifice manifold is utilized for the injection of gaseous propane upstream of the inlet section for the reacting cases. A honeycomb panel, located in the inlet section between manifold and seeding sections, is used to control the turbulence level and mixture homogeneity. An equilateral triangle of side 0.04m is mounted at about 0.32m downstream of combustor segment inlet spanning the width of the duct and functions as the bluff body flame holder. The flow exits the combustor segment through a circular outlet. Experimental measurements available from the Volvo test rig include mean axial velocity and velocity fluctuation data from Laser Doppler Anemometer (LDA);

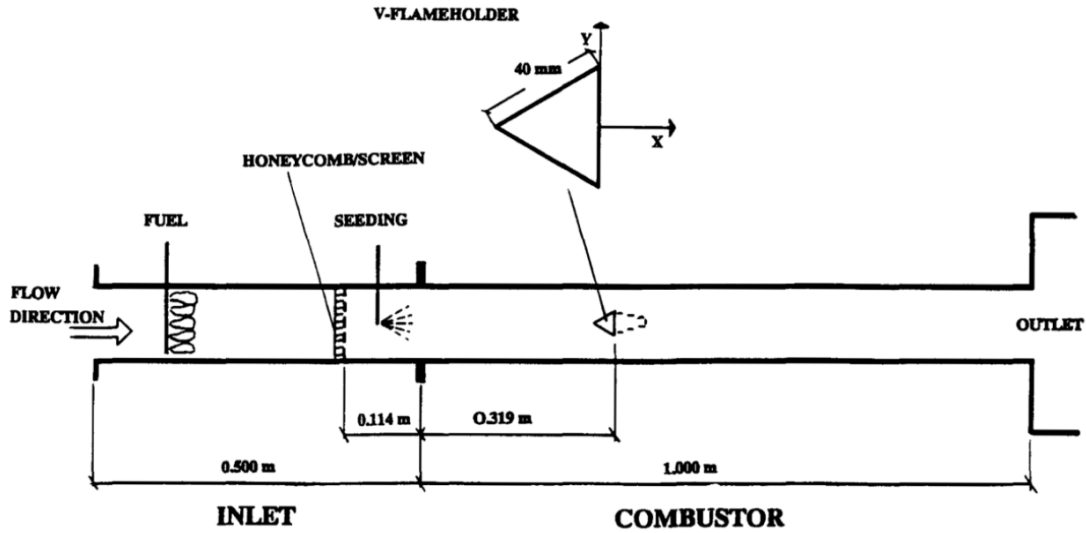


Figure 2.1: Experimental setup for the Volvo test cases depicting the method of controlling the inlet turbulence intensity by honeycomb screen. The flame holder is also shown in a magnified view.

and time averaged temperature and species data from Coherent Anti-Stokes Raman Scattering (CARS) methods. The data are provided as profiles of the mentioned quantities along a transverse line passing through the mid-plane of the domain at specific horizontal locations.

The combustor segment which includes the bluff body is water-cooled on the top and bottom walls, while it is air cooled on the side walls. The combustor segment is connected to a large circular duct to minimize the effect of outlet back pressure on the flame.

There are four cases investigated [2, 67], but here we focus on one case that is characterized by the inflow velocity and temperature of 17.3 m/s and 288 K, respectively, with an equivalence ratio of $\phi = 0.65$. The air mass flow rate is 0.6 kg/s. The Reynolds number of 48,000 is defined using the characteristic length of the equilateral triangular bluff body ($D = 0.04\text{m}$), the bulk inlet velocity of 17.3 m/s and the viscosity at the temperature of 288 K. For the reacting case with an equivalence ratio of 0.65, the mean adiabatic flame temperature is about 1800 K. The nominal pressure is 1 atm. The inlet turbulence intensity and mixture homogeneity are controlled by a honeycomb panel at the inlet segment. The inlet turbulence intensity is not well known but is estimated to be 3% [68]. The corresponding Kolmogorov length and time scales (at $T = 288\text{ K}$) are also estimated to be $7\mu\text{m}$ and

3.6 μ s, respectively [69]. The flame speed at the operating condition of the test is estimated to be between 30 to 40 cm/s [70].

The operating conditions under consideration are summarized in Table 3.1:

Case	Re	U_{bulk} [m/s]	ϕ	T_{in} [K]	T_{ad} [K]
Non-reacting	48,000	16.6	0.0	288	-
Reacting	48,000	17.3	0.65	288	1784

Table 2.1: Selected experimental operating conditions for simulation

Turbulent premixed combustion involves a wide range of length and time scales associated with flow motions and chemical reactions. The turbulent Reynolds number, Re_t , and the Karlovitz number, Ka , are often used to characterize turbulence-chemistry interactions.

$$Re_t = v' \times l / (S_L \times l_F) \quad (2.1)$$

$$Ka = t_F / t_\eta \approx l_F^2 / \eta^2 \quad (2.2)$$

where v' is the turbulent velocity fluctuation, l the turbulent integral length scale, S_L and l_F the flame speed and thickness, respectively. t_F and t_η are flame and the Kolmogorov time scales, respectively. η is the Kolmogorov length scale.

Fig. 2.2 shows the Borghi premixed combustion regime diagram. It classifies the premixed flame based on Karlovitz (Ka) and turbulent Reynolds (Re_t) numbers. For the experiment used in this research for model validation the flame is categorized into corrugated flamelet and thin reaction zone based on the calculation of the aforementioned turbulence and flame variables in equations (2.1) and (2.2). This classification is useful for explanation of discrepancies we will see between numerical and experimental results.

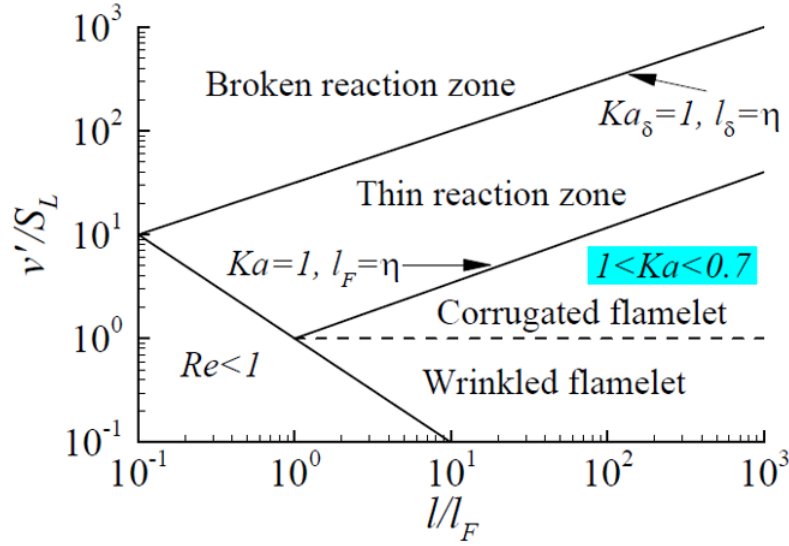


Figure 2.2: Regime diagram of premixed turbulent combustion according to Borghi [71]

2.2 Governing Equations And Theoretical Modeling

The governing equations consist of conservation equations for mass, momentum, and energy. For the gas mixture, we need to solve the species transport equations. Due to combustion, chemical reaction rates need to be accounted for as source terms in the species transport equations. Also, the equation of state for the gas mixture is needed to complete the system of equations.

2.2.1 Conservation Equations For Reacting Flows

The reacting flow modeled with LES is solved at two main scales: the resolved scales, which are normally of the order of the grid size, and subgrid scales (SGS), which model the dynamics truncated by the low-pass filtering process. The resolved scale is solved directly by conservation equations in addition to species transport equations and an appropriate equation of state. The formulation is based on the Favre-filtered (density averaged) conservation equations for mass, momentum, and energy. These equations are applied to the resolved scales by filtering out the subgrid scale dynamics over a well-defined set of spatial and temporal intervals. They can be expressed in the following Cartesian tensor form:

- Conservation of mass

$$\frac{\partial \bar{\rho}}{\partial t} + \frac{\partial \bar{\rho} \tilde{u}_i}{\partial x_i} = 0 \quad (2.3)$$

where u_i is the velocity component in spacial direction x_i .

- Conservation of momentum

$$\frac{\partial \bar{\rho} \tilde{u}_i}{\partial t} + \frac{\partial \bar{\rho} \tilde{u}_i \tilde{u}_j}{\partial x_j} = -\frac{\partial \bar{p} \delta_{ij}}{\partial x_j} + \frac{(\partial \tilde{\tau}_{ij} - \tau_{ij}^{SGS})}{\partial x_j} \quad (2.4)$$

In the above equation p and δ_{ij} are the pressure and the Kronecker delta, respectively, where overbars and tildes denote resolved-scale and Favre-averaged resolved-scale variables, respectively. $\tilde{\tau}_{ij}$ is the viscous tensor and it is modeled by

$$\tilde{\tau}_{ij} = \mu \left(\frac{\partial \tilde{u}_i}{\partial x_j} + \frac{\partial \tilde{u}_j}{\partial x_i} \right) - \frac{2}{3} \mu \frac{\partial \tilde{u}_k}{\partial x_k} \delta_{ij} \quad (2.5)$$

In the above equation μ is the kinematic viscosity. The effects of non-resolved scales that appear through the subgrid-scale (SGS) terms can be modeled by:

$$\tau_{ij}^{SGS} = \overline{\rho u_i u_j} - \bar{\rho} \tilde{u}_i \tilde{u}_j \quad (2.6)$$

Most sub-grid scale models are based on the eddy viscosity, ν_t , that is related to other field variables by

$$\tau_{ij}^{SGS} - \frac{\delta_{ij}}{3} \tau_{kk}^{SGS} = -2\nu_t \tilde{S}_{ij} \quad (2.7)$$

where \tilde{S}_{ij} is the symmetric part of the velocity gradient tensor, $\tilde{S}_{ij} = \frac{1}{2} \left(\frac{\partial \tilde{u}_i}{\partial x_j} + \frac{\partial \tilde{u}_j}{\partial x_i} \right)$.

- Conservation of energy

A multicomponent diffusion of gas phase mixture is not considered in this work. It is assumed that body forces and the energy flux due to composition gradients or chemical potential can be neglected. The transport equation for the energy can therefore be written as:

$$\frac{\partial \bar{\rho} \tilde{h}}{\partial t} + \frac{\partial \bar{\rho} \tilde{u}_i \tilde{h}}{\partial x_i} = \frac{D\bar{p}}{Dt} - \frac{\partial \tilde{q}_i}{\partial x_i} + \tilde{\tau}_{ij} \frac{\partial \tilde{u}_i}{\partial x_j} + \dot{Q} \quad (2.8)$$

where h is the enthalpy of the mixture, $D\bar{p}/Dt$ is the pressure material derivative, \tilde{q}_i is the energy flux and \dot{Q} is the heat source term due to radiative flux and it will be neglected due to the low emissivity of the gases involved.

The enthalpy of the mixture h is,

$$h = \sum_{k=1}^N Y_k h_k \quad \text{with} \quad h_k = h_{f,k}^0 + \int_{T_0}^T C_{p,k} dT \quad (2.9)$$

where $h_{f,k}^0$ is the enthalpy of formation of species k at a reference temperature T_0 and $C_{p,k}$ is the heat capacity of species k . Similarly the heat capacity c_p of the mixture is given by

$$c_p = \sum_{k=1}^N c_{p,k} Y_k \quad (2.10)$$

The energy/heat flux in direction x_i is modeled using Fourier's law and the transport of enthalpy due to species diffusion (mixing flows), as

$$q_i = -\rho \alpha \frac{\partial h}{\partial x_j} + \rho \alpha \sum_{k=1}^N \left(1 - \frac{1}{Le_k}\right) h_k \frac{\partial Y_k}{\partial x_j} \quad (2.11)$$

where α is the thermal diffusion coefficient ($\alpha = \lambda / \rho C_p$), and λ is the thermal conductivity. The Lewis number of species k , Le_k , is defined as:

$$Le_k \equiv \frac{\alpha}{D_k} = \frac{\lambda}{\rho C_p D_k} \quad (2.12)$$

It represents the ratio of thermal diffusivity to mass diffusivity. It is related to flame stretch and for Lewis number less than unity the effect of flame stretch on burning velocity is weak [70]. In this equation λ is the thermal conductivity of the unburnt reactants, ρ is the density of the reactant mixture, and C_p is the heat capacity of the unburnt mixture. D_k is the the binary mass diffusion of the reactants.

To close the conservation equations at the resolved scales, we also need to have the equation of state. For ideal gas which composes of a mixture of gases this can be written as:

$$P = \rho R_u T \sum_{k=1}^N \frac{Y_k}{W_k} \quad (2.13)$$

where R_u is the universal gas constant and W_k is the molecular mass of the k -th species.

Finally, the species transport is modeled by the following equations:

$$\frac{\partial \bar{\rho} \tilde{Y}_k}{\partial t} + \frac{\partial \bar{\rho} \tilde{u}_i \tilde{Y}_k}{\partial x_i} = - \frac{\partial \tilde{V}_{k,i} \tilde{Y}_k}{\partial x_i} + \tilde{\omega}_k \quad k = 1, \dots, N \quad (2.14)$$

where Y_k is the mass fraction of the k -th species, $V_{k,i}$ is the diffusion velocity in x_i direction, $\tilde{\omega}_k$ is the reaction rate of the k -th species, and N is the number of species. The chemical source term of the k -th species, $\tilde{\omega}_k$, is usually expressed in terms of forward and backward rate coefficients, which in turn are expressed as functions of the temperature using the Arrhenius equation. This will be discussed later.

Using Fick's law, the diffusion velocity $V_{k,i}$, can be modeled as:

$$V_{k,i}Y_k = -D_k \frac{\partial Y_k}{\partial x_i} \quad (2.15)$$

D_k is the diffusion coefficient of species k , which is related to the thermal diffusivity, α , and the Lewis number of species k , Le_k , as $Le_k D_k = \alpha$.

After combining the the convection and diffusive transport by diffusion model, the species transport equations become:

$$\frac{\partial \bar{\rho} \tilde{Y}_k}{\partial t} + \frac{\partial \bar{\rho} \tilde{u}_i \tilde{Y}_k}{\partial x_i} = \frac{\partial}{\partial x_i} \left(\bar{\rho} D_k \frac{\partial \tilde{Y}_k}{\partial x_i} \right) + \tilde{\omega}_k \quad k = 1, \dots, N \quad (2.16)$$

2.2.2 Turbulence Modeling Method

Numerical simulations of turbulent flows can be achieved via three major numerical models: Reynolds-Averaged Navier-Stokes Equation (RANS), Large-Eddy Simulation (LES), and Direct Numerical Simulation (DNS) [72]. DNS method is the most expensive modeling method because it seeks to capture all the details and scales of the flow field. RANS is the cheapest modeling method since it neglects the transient effects in the flow by averaging the data over larger time and spatial steps. LES, on the other hand, is an optimized modeling method in terms of the computational cost and accuracy of the result [73].

For this work the LES method is adopted because of its ability to capture the essential temporal behavior of a complex flow field. This method is capable of fully resolve the flow field at the integral scale and obtaining the main features of the transient effects at the sub-grid scale. We would like to know the instantaneous species concentration, flame structure, and the blow-off mechanism, hence the need for more accurate turbulence modeling. LES is the optimal choice between accuracy and cost since a DNS study would be too costly. A low-pass filtering operation is performed explicitly or

implicitly in LES to separate the large-scale motions from the small-scale ones. The filter is defined as:

$$\tilde{f}(x) = \int_{-\infty}^{\infty} f(x') G_f(x-x') dx' \quad (2.17)$$

where G_f is the filter function and satisfies the normalization condition $\int G_f(x') dx' = 1$. The size and structures of the small scale motions are determined by the filter function. According to the Favre filter [74], any instantaneous variable (f) can be expressed as the sum of a Favre-averaged filtered scale (\tilde{f}) and a sub-filter scale (f''):

$$f = \tilde{f} + f'' \quad (2.18)$$

where

$$\tilde{f} = \frac{\overline{\rho f}}{\bar{\rho}} \quad (2.19)$$

The advantage of this model is that it takes advantage of the fact that the vortex structure at small scale is almost universal so that we can rightfully expect that resolving the subgrid scale with Direct Numerical Simulation or modeling it by LES will not have a significant difference in terms of the final results.

The Wall-Adapting Local Eddy-Viscosity (WALE) sub-grid scale model has been widely used because it improves the prediction of the wall stress rate as well as turbulence intensities [75]. For reasons connected with the wall behavior of the sub-grid scale model, Poinso et al. [76] defined a new operator based on the traceless symmetric part of the square of the gradient velocity tensor

$$\tilde{g}_{ij} = \frac{\partial u_i}{\partial x_j}:$$

$$S_{ij}^d = \frac{1}{2}(\tilde{g}_{ij}^2 + \tilde{g}_{ji}^2) - \frac{1}{3}\delta_{ij}\tilde{g}_{kk}^2 \quad (2.20)$$

Following the velocity gradient assumption, the WALE model is written as,

$$v_t = (C_w \bar{\Delta})^2 \frac{(S_{ij}^d S_{ij}^d)^{3/2}}{(\tilde{S}_{ij} \tilde{S}_{ij})^{5/2} + (S_{ij}^d S_{ij}^d)^{5/4}} \quad (2.21)$$

$$\bar{\Delta} = \sqrt[3]{\Delta_1 \Delta_2 \Delta_3} \quad (2.22)$$

where C_w is the WALE constant and its published value is in the range $0.55 \leq C_w \leq 0.60$ [75]. However, intensive validation during a European Union research project involving the original model developers has shown consistently superior results in ANSYS Fluent with $C_w = 0.325$ [77]. Therefore, this default setting is used for this simulation. The filter width $\bar{\Delta}$ is usually proportional to the grid size.

It is known that by using the WALE method for near wall flow treatment the concern for having the right grid resolution in order to meet stringent boundary layer resolution can be neglected [78]. Also, it is observed that this problem is not effected by shear stresses from the no-slip boundary condition since the length scale of the dominant flow is determined by the vortex shedding and flame front dynamics [12].

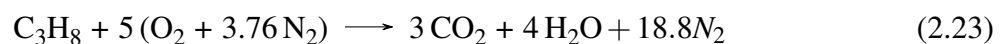
2.2.3 Premixed Turbulent Combustion Modeling

In premixed combustion, the fuel and oxidizer are mixed before they enter the combustion chamber. Combustion then takes place in the chamber, transforming unburnt reactants to burnt combustion products. In this type of combustion, fuel and oxidizer are mixed at the molecular level prior to ignition. Combustion occurs as a flame front propagating into the unburnt reactants. Premixed

combustion is much more difficult to model than non-premixed combustion. The reason for this is that premixed combustion usually occurs as a thin, propagating flame front that is stretched and contorted by turbulence. For subsonic flows, the overall rate of propagation of the flame is determined by both the laminar flame speed and the turbulent eddies. The laminar flame speed is determined by the rate of species and heat diffusion upstream into the reactants. The essence of premixed combustion modeling lies in capturing the turbulent flame speed, which is influenced by both the laminar flame speed and the turbulence. To capture the laminar flame speed, the internal flame structure would need to be resolved, as well as the detailed chemical kinetics and molecular diffusion processes. Because practical laminar flame thicknesses are of the order of millimeters or smaller, resolution requirements are not usually affordable.

Premixed flames can be modeled using Species Transport model or Composition PDF Transport model. These models can be implemented if modeling of finite-rate chemical kinetic effects are important. With Species Transport, two options are available to account for finite rate chemistry; Laminar Finite-Rate model and Eddy-Dissipation-Concept (EDC) model. If the flame is perfectly premixed, only one stream at one equivalence ratio enters the combustor, it is possible to use the premixed combustion model. However, the effect of transient combustion phenomena, such as ignition and extinction, cannot be captured by this model since it does not incorporate enough chemical kinetic behavior.

Combustion is a globally exothermic process and therefore releases heat when it occurs. The balanced reaction for the global reaction (combustion) of a fuel such as propane with air can be written as follows,



In its current formulation, only major species of the initial system prior to the reaction (left hand side reactants) and of the final system (right hand side products) are considered. In reality, the combustion process cannot occur in a single step; it involves a complex kinetic mechanism with numerous intermediate reactions.

Each elementary reaction is associated with a reaction rate. For the bi-molecular reaction in which the reactants A and B form the products C and D, we have:



The rate of depletion of A can be obtained from:

$$\frac{d[A]}{dt} = -k(T)[A][B] \quad (2.25)$$

where [A] refers to species concentration and $k(T)$ is the rate coefficient that depends on temperature. Typically the rate constant is given by an empirical Arrhenius expression:

$$k(T) = A_p T^n \exp\left(\frac{-E_a}{R_u T}\right) \quad (2.26)$$

where A_p , E_a , and R_u are respectively the pre-exponential factor, the activation energy and the universal gas constant. A_p , E_a , and n are the three constants determined experimentally or theoretically.

There are two chemical kinetic models used in this work; a global one-step reaction with 5 species and a skeletal mechanism for propane developed by Peters et al. [79] with 43 species and 188 reactions. This mechanism was deduced from a detailed mechanism developed by UC San Diego combustion group [80] which is based on Gri Mech 3.0 [81].

The detailed chemistry model is highly stiff because the time scales of various reactions have a very wide spectrum as it can be seen in Figure 2.3. Some chemical reactions are very fast while others, such as pollutant formations, are slow.

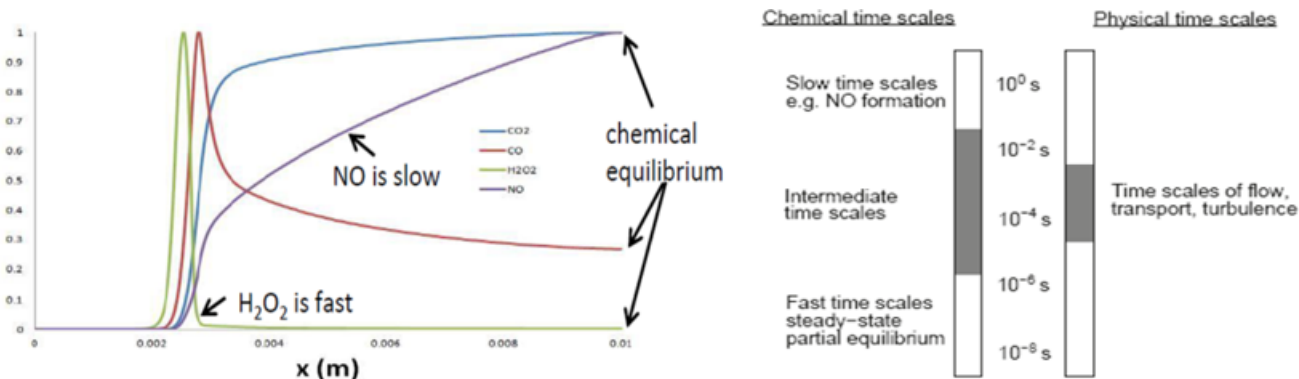


Figure 2.3: The left figure is depicting the normalized species mass fraction for premixed methane laminar flame and the right chart shows the chemical time scales of different reactions in comparison to mixing time scale [77].

Modeling chemical kinetics is costly but is required for capturing the transient behavior of combustion process such as ignition and extinction. In order to reduce the cost, some techniques have been developed to accelerate the simulation time. These include using the In Situ Adaptive Tabulation (ISAT) instead of direct integration of species transport equations, Dynamic Mechanism Reduction by suppressing negligible species and reactions at each cell and time step, and Chemistry Agglomeration by averaging cells that have similar temperature and mass fractions while mapping the reaction back to original cells. Although these tools accelerate the solution, they can compromise the accuracy of the predicted properties if used without care.

2.2.4 Turbulence-chemistry Interaction Modeling

There are two models to account for Turbulence-Chemistry Interaction (TCI) Modeling. They are the laminar flame with finite rate chemistry and the EDC modeling approach. Although both models allow for the integration of detailed chemical kinetic models, the major difference is that the laminar flame finite rate model takes temperature and species mass fraction to be constant for each cell at each time step while the EDC accounts for the fluctuation of these parameters during each time step

calculation. The EDC model is an extension of the eddy-dissipation model where the overall rate of reaction is assumed to be controlled by turbulent mixing. In the EDC model, however, the mixing and reaction time scale can be comparable and that calls for the inclusion of detailed chemical mechanisms in turbulent flows. The EDC model assumes that reactions occur within small turbulent structures, called the fine scales. The length of the fine scales is modeled as

$$\xi^* = C_\xi \left(\frac{\nu \varepsilon}{k^2} \right)^{1/4} \quad (2.27)$$

where * denotes fine scale quantities, C_ξ is volume fraction constant, and ν is the kinematic viscosity.

The volume fraction of the fine scales is calculated as $(\xi^*)^3$. Species are assumed to react in the fine structures over a time scale determined as:

$$\tau^* = C_\tau \left(\frac{\nu}{\varepsilon} \right)^{1/2} \quad (2.28)$$

where C_τ is a time scale constant that can be taken as 0.4082. When the LES turbulence model is used, k and ε represent the sub-grid scale turbulent kinetic energy and its dissipation, respectively. Combustion at the fine scales is modeled as a constant pressure reactor, with initial conditions taken as the current species concentrations and temperature in the cell. Reactions proceed over the time scale τ^* , governed by the reaction rates of the Arrhenius equation, and are integrated numerically using the ISAT algorithm [77].

The numerical simulation of transient combustion is of interest in this work due to intrinsically unsteady behavior of extinction processes. Also, due to the high Reynolds number, the turbulence-chemistry interactions cannot be simply assumed to be negligible [26]. More realistic turbulent combustion flows can thus be captured with models which account for temperature and reaction rate

fluctuations in each cell and at each time step. Ravi claimed that a combination of the LES model with EDC can predict the flame blowoff process more realistically [57]. Numerically, the LES describes the unsteady turbulent flow and the EDC incorporates temperature and species fluctuations in reaction rate calculations. In this work the laminar flame with finite rate chemistry is chosen for turbulence-combustion interaction modeling. The advantage of choosing laminar flame finite rate model is that this model takes temperature and species mass fraction to be constant for each cell at each time step. This will significantly reduce the computational cost while accounting for detailed chemical kinetics at each time step.

Combustion processes can be steady or unsteady. In steady combustion a propagating flame or an anchored flame shows a quasi-steady behavior on average. on the other hand unsteady combustion shows transient effect that develops over each time step. Examples of unsteady or transient combustion are ignition and extinction processes by which the flame initiation and annihilation are localized and temperature and species mass fraction are changing over time. It can also be a combustion process that is embedded in a highly turbulent and transient flow field with the same order of mixing and chemistry time scales. This type of regime is associated with high flame strain rate. The large turbulent eddies tend to wrinkle and corrugate the flame sheet, while the small turbulent eddies, if they are smaller than the laminar flame thickness, may penetrate the flame sheet and modify the laminar flame structure.

The numerical simulation of transient combustion is of interest in this research due to intrinsically unsteady behavior of extinction process. At the extinction process the chain terminating reactions becomes dominant and the interaction between the chemical kinetics of these intermediate reactions with the dynamics of mixing and turbulence and how they play roles in the final process of blow-off needs to be understood.

In the next section the computational domain as well as initial and boundary condition set-up implemented in the simulation are elaborated.

2.2.5 Computational Domain And Set-up

Figure 2.4 shows the computational domain selected for the premixed combustion. It consists of a flame stabilized by an equilateral triangular bluff-body with sides (h) 4 cm placed in a channel with height of 12 cm and span-wise dimension of 8 cm. The side walls are considered as periodic boundary conditions. The Mach number is low enough that the compressibility effects can be neglected. The Reynolds number based on the mean inlet velocity of the flow and characteristic length of the bluff body is high enough for the flow to be considered as turbulent. The reacting gases are assumed to be ideal gases.

The current experiment can be analyzed in 2D and 3D. The computational domains for 2D and 3D configurations only consist of the combustor segment which extends $4h$ upstream of the flame holder tip and $17h$ downstream of the flame holder trailing edges, with two walls on the sides being periodic boundaries that are $2h$ apart (see Fig. 2.4). Also, for the 3D configuration, the span wise extent is selected to be $2h$. The span wise distance is selected so as to assure that all span wise instabilities can be captured while making the domain size as small as possible. The inlet segment and circular duct that connects to the outlet of the combustor segment are absent from the computational domain. It is shown that the absence of circular outlet duct affects the flame structure, that can be alleviated by using coarser mesh in the outlet of the combustor segment. A steady uniform inlet velocity of 17.3m/s is assumed with no fluctuation for the 0% inlet turbulence intensity case while the spectral synthesizer method is used to generate ITI in other cases. In this synthesizer method, a divergence-free fluctuating velocity vector field is generated around the specified mean velocity by adding the Fourier harmonics. The inlet velocity generated by this method is random and transient. In all these cases, the inlet temperature of 288K is steady and uniform. The outlet boundary condition is pressure-based with a backflow of constant atmospheric pressure and temperature of 288K.

Three structurally similar grids with different resolutions will be used to examine the sensitivity

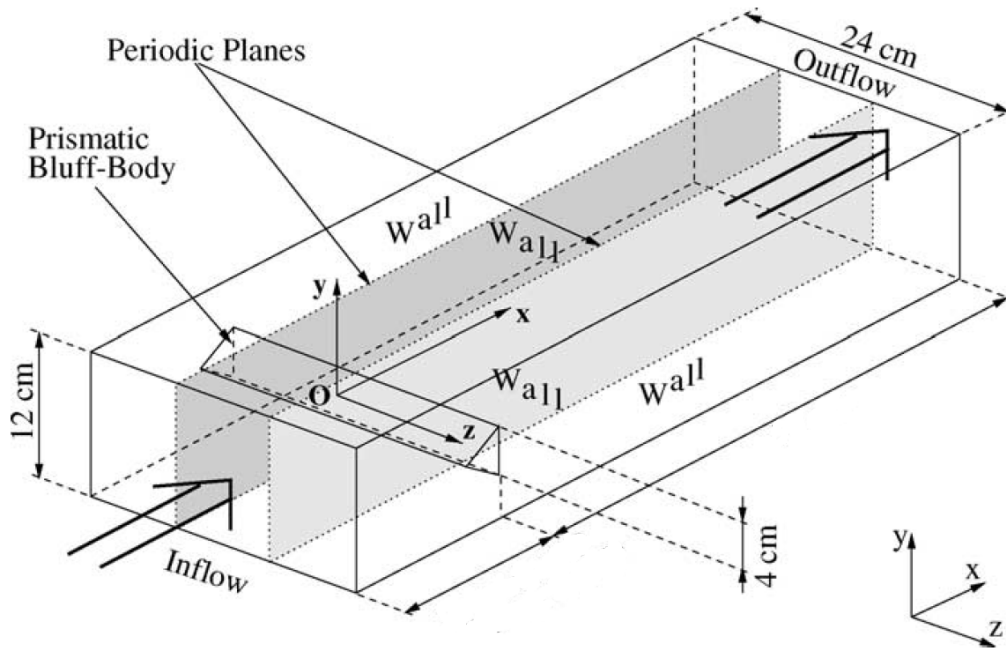


Figure 2.4: The computational domain selected for this project.

of the flame structure to mesh refinement. They are identified as coarse mesh shown in Fig. 2.5, fine mesh, and extra fine mesh shown in Fig. 2.6. In the experimental set-up, the lower and upper walls are water cooled. In the computational model, no-slip adiabatic wall boundary conditions are imposed. These conditions are employed to enable comparisons with other computational studies e.g. [68, 82]. The bluff body boundary conditions are initially considered as no-slip and adiabatic. It is hypothesized that the adiabatic wall condition have limited effect on the flame temperature while the bluff body with this condition has negligible affect on the flame structure and blow-off prediction.

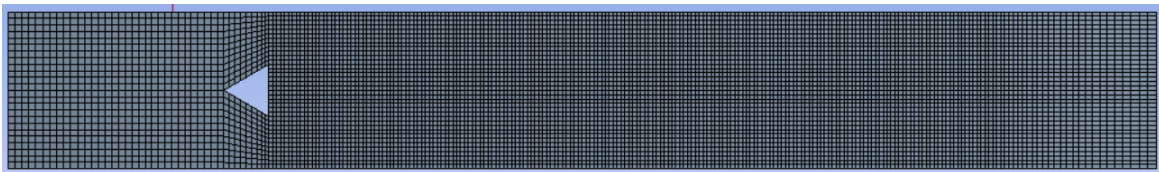


Figure 2.5: Coarse mesh with 47,000 quadrilateral cells, min, max element size= 0.6, 3.6 mm, min orthogonal quality= 0.87, max aspect ratio= 3.42

In order to investigate the effect of the boundary condition on the flame extinction, the near blow-off



Figure 2.6: Extra fine mesh with 550,000 quadrilateral cells, min, max element size= 0.4, 0.6 mm, min orthogonal quality= 0.87 and max aspect ratio= 2.24

equivalence ratio needs to be identified. The equivalence ratio, ϕ , is defined as the ratio of the actual fuel air ratio to the fuel to air ratio at stoichiometric conditions:

$$\phi = \frac{\left[\frac{\dot{m}_{fuel}}{\dot{m}_{air}} \right]_{actual}}{\left[\frac{\dot{m}_{fuel}}{\dot{m}_{air}} \right]_{stoichiometric}} \quad (2.29)$$

The fuel-air mixture is gradually diluted from the initial equivalence ratio of $\phi = 0.65$. The reason for choosing this ratio is that experimental results are available for model validation. The equivalence ratio of 0.5 is known to be the lower flammability limit (LFL) of propane at room temperature and pressure. It is thought that the prediction of complete blow-off highly depends on the turbulence-combustion interaction (TCI) model, and, hypothetically on the mesh resolution. The extinction process is expected to start at $\phi = 0.60$ and the complete blow-out should occur around $\phi = 0.55$ when the EDC model is used [57]. This range may be affected by model selection and mesh resolution.

The interaction between turbulence and combustion in this research is accomplished by Laminar Flame model. While utilization of this model might become justifiable for stronger flame based on the flame classification at richer condition, the implementation of this model can become questionable at near blow-off condition. This can be attributed to the fact that in a strong flame the penetration of small scale turbulence structure in the flame shear layer can become negligible, depending the Karlovitz and turbulent Reynolds numbers of the flow. In other word, for a strong flame the reaction rate can be taken as turbulent or mixing controlled phenomenon while in a lean

flame operating at low flammability limit the turbulent and chemistry time scales are comparable. Since the main goal of this research is a parametric study of flame response to varying inlet turbulence intensity the interest is not the determination of exact equivalence ratio at which the blow-off occurs. Rather the interest is to show the trend of this correlation and as it will be shown later this relation is correctly captured when the numerical results are put into context with experimental data pertaining to this type of investigation. The goal of this work therefore is to develop a numerical methodology for approaching this kind of problems in a most efficient manner while maintaining an acceptable level of accuracy for obtaining important combustion values such as near blow-off equivalence ratio or ϕ_{NBR} .

2.2.6 Thermodynamics and Transport Properties

All chemical species are assumed to be ideal gases. Their thermodynamic properties are temperature dependent, and are provided in the form of polynomial coefficients. Transport properties such as thermal conductivity, viscosity, and diffusivity are also temperature dependent. Transport properties for various species are provided as parameters of the intermolecular forces.

2.2.7 Numerical Method

The Semi-Implicit Method for Pressure Linked Equations (SIMPLE) algorithm is chosen to solve for the coupling of pressure and velocity in the momentum conservation equation. SIMPLE is one of the most stable schemes. For transient combustion problems that tend to be highly unstable, the SIMPLE approach has proven to work very well [83]. Here, the second order upwind scheme is mainly used for spatial discretization and the bounded second order implicit for temporal discretization. The second order upwind scheme has demonstrated an acceptable accuracy at computationally affordable cost. The bounded Second Order Implicit scheme is used for this transient simulation. To control the convergence process, all under-relaxation factors were selected such that reasonable convergence could be achieved with minimal iteration effort at each time step.

For the iteration process of the transport equations the convergence absolute criteria for the residuals of the transport equations are first chosen to be the default value of 10^{-3} . This is to help with the convergence issue observed at the early stages of LES iteration process which is due to strong unsteadiness at ignition. The initialization of the flame is conducted by introducing a patch behind the bluff body containing hot flue gases and this adds to unsteadiness of the early stages of iteration. Because of this, careful tuning is needed by controlling the under-relaxation convergence criteria for transport equations at the initialization of the numerical simulation. After gaining some traction in the iteration process, the convergence absolute criteria values for the residual of transport equation is gradually decreased by order of 10^{-1} until the number of iteration per time step does not go beyond 30 to 40. It was shown that 10^{-6} as convergence criteria will yield acceptable accuracy of results. Thus, this was used as the final value for which an accurate quasi steady state condition is established in the flame.

2.3 Using Methods to Address Thesis Objectives

The methodology used to reach the thesis objective is to validate the computational model against available experimental results. This is accomplished in 3D computational domain using the ANSYS Fluent. The physical and computational models as well as numerical parameters are selected and finely tuned for convergence and accuracy.

After validating the computational set-up, the investigation for near blow-off equivalence ratio begins. This is accomplished by gradually decreasing the equivalence ratio from the initial value of 0.65 which is taken from the experiment operating condition. The gradual decrease continues until the flame extinguishes. Once the blow-off equivalence ratio is established, then 0.02 is added to the blow-off equivalence ratio and set as the near blow-off equivalence ratio or NBE.

At the near blow-off condition the inlet turbulence intensity is increased from the primary value of 0% by increments of 5%. It is expected that by increasing the turbulence level in the upstream flow, the flame becomes more unstable and eventually blows off. In this research, the ITI value at

which the flame blows off is called the blow-off ITI. This phenomenon has been observed in some experiments including the one conducted by Cetegen et al. It would be interesting to see if these experimental observations can be replicated by computational analysis.

Also, in the experiment conducted by Cetegen et al. [17] a non-linearity behavior was observed between increasing inlet turbulence intensity and flame stability at certain conditions. To investigate this phenomenon, we increased the ITI after the blow-off ITI on the same lean flame to see if the non-linearity can be captured by computational modeling.

We also seek to establish a computationally cost effective methodology since the research is heavily involved with computational modeling of blow-off phenomena. First we needed to establish a reliable model to investigate the near blow-off equivalence ratio by running multiple cases with different mesh configurations and modeling parameters. Then we explored the impact of ITI on the flame at the near blow-off condition. In addition we needed to investigate the blow-off phenomenon in 3D domain in order to understand the similarities between 2D and 3D results.

The true impact of turbulence level and how it impacts the flame can only be understood by using high fidelity turbulence model such as LES. We seek to demonstrate that capturing the blow-off effectively requires detailed chemistry rather than global chemistry kinetics. The combination of high fidelity turbulence model with detailed chemical kinetics model that is needed to be incorporated into numerous cases guides the search for the most optimal computational methodology for this research.

The summary of the research workflow is presented in figure 2.7.

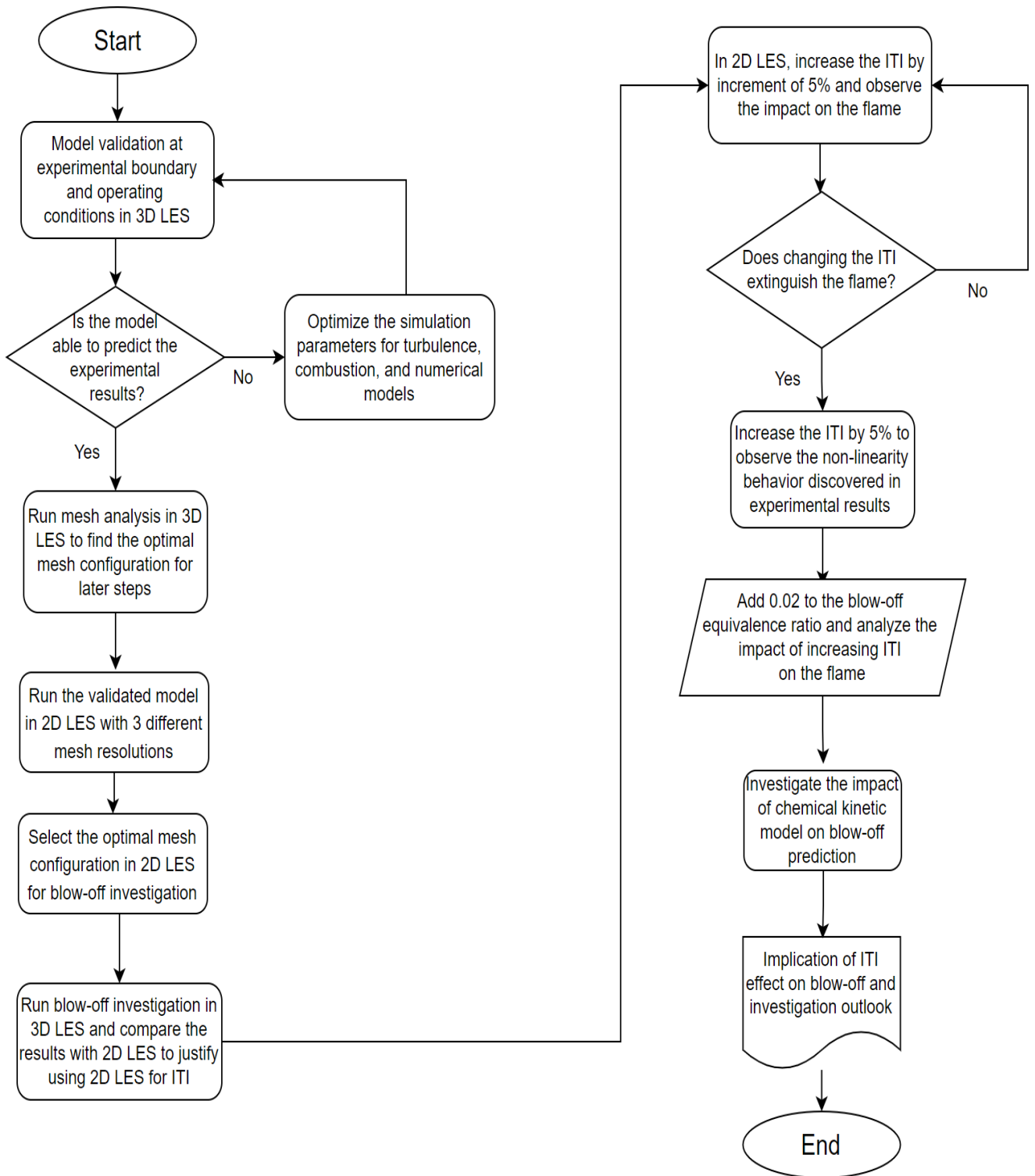


Figure 2.7: Research Workflow

Chapter 3

Validation of Volvo test case

In this chapter the data from Volvo Flygmotor experiment will be used to validate the numerical set-up and sub-grid scale (SGS) models implemented in this research. The experiment was conducted to characterize the behavior of afterburners of jet engine; it did not include the operating condition at much leaner condition pertaining to new emission requirements. First of all, the experiment was conducted at only one equivalence ratio, $\phi=0.65$, with propane-air mixture. Also, there are no experimental results relating the effect of inlet boundary condition on near blow-off flame. In fact, the blow-off dynamics and mechanism leading to this phenomenon is completely absent in that experiment. Therefore, the experimental test rig set-up is useful as validation targets to assess the reliability of the selected models. This is accomplished by comparing available experimental results with our obtained numerical results at those very specific experimental conditions. By validating the numerical models against the available data, we can reasonably extend the models to the numerical investigation of flames at near blow-off equivalence ratio. To establish the near blow-off equivalence ratio, we will investigate the effect of varying inlet turbulence intensity on the persistence of the flame at various equivalence ratio.

The near blow-off equivalence ratio is obtained by gradually decreasing the equivalence ratio to the point of complete flame extinction. Subsequently, the near blow-off equivalence ratio is established by introducing a bit more fuel into the mixture stream just to increase the equivalence ratio by 0.02

above the blow-off equivalence ratio [17]. Finally, at the near blow-off condition the impact of inlet boundary condition, specifically the inlet turbulence intensity, on this lean turbulent premixed bluff body flame will be investigated using the validated models and numerical.

The above description is the overview of the research structure. This research is conducted to develop our understanding about the relationship between varying the inlet turbulence intensity level and a lean turbulent premixed bluff-body stabilized flame dynamics and its response to the upstream turbulence variation. By showing this correlation we hope to establish the importance of this parameter in the new burner design process. This is necessary if they are to operate much closer to blow-off condition and meet the more stringent emission regulations.

3.1 The Experimental Setups

As described, the first step of this research is to validate the numerical models against the available experimental results. The experimental setup was explained in details in section 2.1. The experiment was conducted with a relatively strong flame of propane/air mixture with equivalence ratio of 0.65. The estimated frequency of the equipment for sampling is 100 Hz, that is, about 0.01s between sampling times. This time can be used to establish the averaging time span for the numerical results. The time step for the simulation is 10^{-6} s, therefore, the averaging shall be done over 10^4 time steps or the equivalent of 0.01s of the actual flow time. This will make the averaging time period comparable to the experimental time interval between sampling. In order to reach steady state conditions, the simulation is continued for about 6 flow throughputs. Each throughput is calculated based on the length of the computational domain and the mean incoming flow velocity [12]. After defining the averaging time interval and steady state criteria, the next step is to find the optimal numerical model combination which can describe the dynamics of the flame more accurately. These results and the comparison are presented as transverse velocity and temperature profiles at certain distances from the bluff body where the experimental data were taken. As part of validation process, a mesh sensitivity analysis was also conducted to understand how the mesh configuration and

resolution impact the flow structure with respect to computational time.

In the following sections, the results from model validation using large eddy simulation turbulence model in 3D and 2D will be explained and presented. The data obtained from 3D and 2D simulations are then compared with Volvo experimental results to assess the justification for using 2D simulations to capture the structure of the combustion flow.

We estimate that 2D LES is sufficient to capture the combustion flow. This has to be confirmed by comparing 3D LES with 2D LES results. We therefore first consider the 3D LES.

3.2 Model Validation - 2D and 3D LES

The numerical investigation was conducted using LES for its optimal balance between accuracy and computational cost. The main reason for selecting LES over RANS and URANS for turbulence modeling is the suitability of LES for prediction of unsteadiness such as in the bluff-body stabilized flame. RANS is applicable to steady flows. It enables simulation of time averaged flow properties. URANS uses the same approach as RANS but also solves the time-dependent Navier-Stokes equations to capture some flow transient effects on an unresolved grid. Without any explicit filtering or averaging, the only key difference between formulations of URANS and LES is the formula of the turbulence model and the output variables. URANS computes transient properties but it cannot predict unsteadiness as accurately and as detailed as LES [84]. Since the focus of this research is to observe the effect of inlet turbulence intensity on blow-off when the flame is lean and highly unstable, URANS cannot be the appropriate approach. On the other hand, it is observed that LES produces more accurate and reliable results compared to URANS in terms of predictability of unsteadiness, because LES resolves the inherent fluctuations over the grid resolutions while it models the sub-grid scale turbulence, thus capturing the turbulent mixing process in the flow field more accurately. It is important to know that mixing of reactants and burned and unburned gases are the key factors in this bluff-body premixed turbulent flame.

The rate of chemical reactions is described by Arrhenius equations. The chemical kinetics of the species is described using a reduced chemical kinetic model for propane by Peters et al. [79]. Table 3.1 is a summary of the numerical set-up.

Model	Type
Turbulence	LES
Turbulence SGS	WALE
Chemistry	Species Transport
Chemical Kinetics	Global (1-step) or detailed (43 species/188 reactions)
Chemistry Solver	Stiff Chemistry
Inlet Diffusion	Off
Diffusion Energy Source	Off
Full Multi-component Diffusion	Off
Thermal Diffusion	Off
Thickened Flame Model	Off
Pressure Outlet	Standard air for backflow
Turbulence-Chemistry Interaction	Laminar Finite Rate
Walls	No-slip-Adiabatic
Ignition Source	Patching
Pressure-Velocity Coupling	SIMPLE
Spatial Discretization - Gradient	Least Square Cell Based
Spatial Discretization - Pressure	Second Order
Momentum	Second Order
All Species	Second Order
Energy	Second Order
Density	Incompressible Ideal Gas
Heat Capacity	Mixing law
Thermal Conductivity	Ideal gas mixing law
Viscosity	Ideal gas mixing law
Mass Diffusivity	Kinetic Theory

Table 3.1: Numerical model set-up selection in ANSYS Fluent for simulation

For this research WALE was selected for the sgs turbulence modeling. The WALE constant C_w is found to yield more satisfactory results for a wide range of flows comparing to Smagorinsky constant C_s which is demonstrated not to be universal and it is more problem-dependant. The Smagorinsky constant needs to be fine-tuned for each specific problem. In addition WALE accounts for turbulence intensities with more emphasis than the Smagorinsky sgs model.

For chemistry modeling the species transport is chosen as this will solve the chemical kinetic mechanism directly. We assume that the detailed chemistry is needed for simulating the extinction phenomena. This assumption will be later verified by comparing with a global reaction model. More details will be provided in chapter 5 in this regard.

In order to solve for numerous intermediate chemical reactions (188 in this case), the Stiff Chemistry numerical solver is selected as the chemistry solver because of the wide range of time scale found among several reactions.

Diffusion terms were ignored since the problem is convection dominant and the species and other parameters are transported mainly by large eddies and through bulk flow by convection mechanism. A simple mixing model was used for material properties of the gas mixtures instead of the more complex multi-component mixture model.

The reacting flow is directly resolved from the grid resolution. However, since the flame thickness is in order of 400 to 600 micrometer the flame cannot be directly resolved in LES. One proposed solution was to artificially thicken the flame such that it can be resolved on the grid resolution. This method does not prove to be appropriate for the intend of this investigation since flame extinction is later explored at near blow-off condition with varying the inlet turbulent intensity and artificially thickened flames tend to resist the local flame extinction process along the flame shear layer which triggers the flame blow-off event.

For the turbulence-chemistry interaction, the laminar finite rate model is used. With combination of species transport and finite rate model Arrhenius equations can be incorporated to solve for the evolution of chemical species. According to the Borghi diagram classifying flame types [71], this reacting flow is in corrugated flamelet region. In this region, the turbulence time scale is the limiting factor and the chemical reaction can be safely assumed to be occurring very fast compared to the turbulence time scale within each grid at the given time step. Hence, the effect of turbulence on chemical reaction in the regime of this flame is negligible. The finite rate model also shows more

stability in the numerical solution and converges rapidly.

In order to account for pressure-velocity coupling the SIMPLE algorithm is used. SIMPLE is a segregated solver which computes the mass and momentum equations in a sequential manner [85]. For non-linear equations, the algorithm solve them iteratively for pressure and then for the velocities terms. The algorithm couples the pressure and velocity field by constraining the velocity field through mass conservation. Therefore, the corrected pressure equation is constructed from the continuity and momentum equations such that the velocity field satisfies the continuity equations. The segregated solver can be used for incompressible flows with low Mach number, such as the case here. This algorithm is more stable and provides control of the iteration process through under-relaxation factors for the transport equations. This is an imperative feature since simulating combustion, including phenomena such as ignition requires fine tuning of the numerical iteration processes. This fine-tuning feature provides the essential tools to control the convergence at the early stages of the flame development which, otherwise, will be difficult to obtain.

In terms of discretization, all the transport equations are discretized using a second order upwind numerical scheme. This scheme is selected due to its ability to balance between stability and accuracy of the numerical results. This scheme is designed to solve hyperbolic partial differential equations. It also utilizes the upstream variables to calculate the derivative in the flow field. The upstream turbulence intensity is transported downstream in a more effective numerical manner.

For closing the set of models the gas law is needed. Since the pressure is low and temperature is high enough, the ideal gas model is used.

For heat capacity, thermal conductivity, and viscosity of the gas mixture, the ideal gas mixing law is selected so that mixture properties are estimated from properties of the species. The heat capacity for each species is calculated using piece-wise temperature-dependent polynomials. The polynomial constants were based on the values obtained from NASA database and the chemical kinetic model [86].

The results of the validation for the 3D case are now presented. In figure 3.1, the comparison between measured and simulated mean x-velocity is shown at two different horizontal locations. We observe relatively good agreement between 3D results with experiment and some deviation for the results obtained from 2D LES. In figure 3.2, the mean temperature is depicted at two different horizontal locations. We observe a discrepancy between the simulated and measured values for the temperature, where the simulated profiles feature a maximum temperature that is about 150K higher than measured. This can be attributed to four things. First, the thermal boundary conditions in the simulation is adiabatic while in the test set up the walls are water and air cooled. Second, the mesh resolution around the flame shear layer in both 2D and 3D cases is not fine enough to resolve the flame. Third, the global chemical kinetic model that neglects some of the endothermic intermediate chemical reactions can potentially cause over-prediction of the flame temperature [68]. It is reported that the choice of reaction mechanism is crucial for the performance of a finite rate LES [87]. This can be attributed to the absence of endothermic intermediate reactions in global chemistry which can absorb some of the energy released during other exothermic reactions. Lastly, the flame and turbulence interaction at sub-grid scale level has important role in temperature prediction as under-prediction of this phenomenon can cause elevated temperature profile for the simulation. The simulated averaged temperature profiles suggest limited diffusion and flame brush causing steeper gradient around the flame shear layer compared to experiment.

From the profiles of mean temperature and mean x-velocity at three different locations it can be concluded that the results from 3D simulations have better agreement with the experimental results than 2D simulations. The difference is only pronounced where the flame is most unsteady. The better agreement of the 3D results can be attributed to the effect of vortex stretching that cannot be fully captured using 2D simulations. As it can be seen from the graphs, the 2D is still capable of capturing the main features of the flame, such as the effect of the recirculation zone. This recirculation plays an important role by generating a low velocity zone and by entraining the unburnt mixture into the hot flue gas zone to sustain the flame.

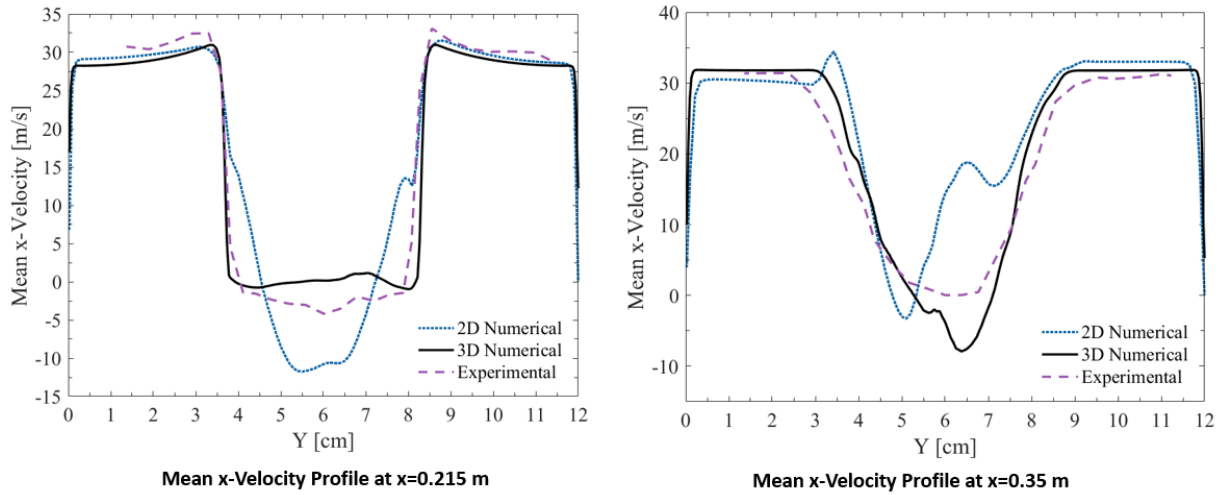


Figure 3.1: Comparison of simulated mean x-axis velocity in 2D and 3D with experimental results at two different locations, left: at 1.5cm behind the bluff body, right: at 15cm behind the bluff body

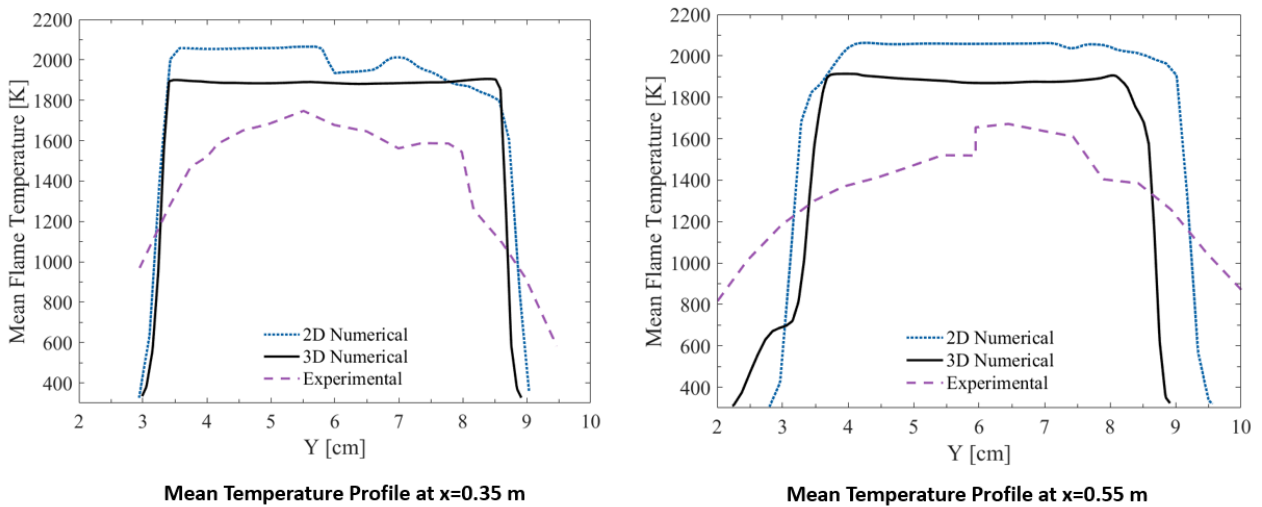


Figure 3.2: Comparison of simulated mean temperature in 2D and 3D with experimental results at two different locations, left: at 15cm behind the bluff body, right: at 35cm behind the bluff body

An important consideration is the amount of computational resources needed to complete the 3D simulation. The extra effort will not justify the use of 3D for investigating this type of flame since the improvement over 2D simulation is not significant. This argument will be further confirmed once the comparison between lean flame blow-off using both 2D and 3D domains is discussed in chapter 4. To state the key results briefly, it is observed that a complete flame blow-off occurs about 600 ms after the initialization of the problem. Given the time step of $1 \mu\text{s}$ and each step

taking roughly 30 iterations to converge, it will take months to have the blow-off simulated given that each iteration roughly takes about 4 seconds with resources used. Since blow-off is found by incremental decrease of equivalence ratio from the initial value of 0.65 numerous cases need to be conducted. This makes the utilization of 3D impractical for investigation of these types of problem. In addition in order to capture the extinction event, one considers the detailed chemical mechanism to be necessary, due to the unsteady nature of the flame and the competition of heat release and heat loss in unsteady reaction zones. The need to compute the chemical evolution of many species explains the exponential growth of computational resources in 3D LES compared to 2D LES. For this reason, it is of importance to find the optimal mesh structure and resolution that can combine the physical models and numerical schemes in 2D and yield results close to 3D simulation. Figures 3.1 and 3.2 shows the success of this approach and the limits at the center of the channel.

It is equally of interest to see if the 2D LES approach can capture the effect of inlet turbulence as observed in some experiments [3, 17]. We will see that the dynamics induced by changes in inlet turbulence intensity can be qualitatively captured in numerical investigation using the validated model in 2D LES formulation.

In order to understand the impact of wall temperature over the flame dynamics a case with constant wall temperature was simulated. It was observed that the wall boundary condition in terms of temperature being adiabatic or having a constant temperature does not have a significant impact on the flame dynamics or the steepness of the temperature profile near the flame shear layers as it is shown in fig. 3.3. The figure shows temperature profiles at 2 different locations behind the bluff body. These results obtained from 2D coarse mesh with global chemistry with $\phi=0.65$. The reason for this is that heat conduction by molecular diffusive transport is far less than the turbulent convection and mixing. Outside the shear layer the flow is not much affected by turbulent convection by vortices.

We further examined the third order MUSCL numerical scheme for the expectation of more accurate result in 2D simulation. The MUSCL is a third order numerical scheme based on the finite volume

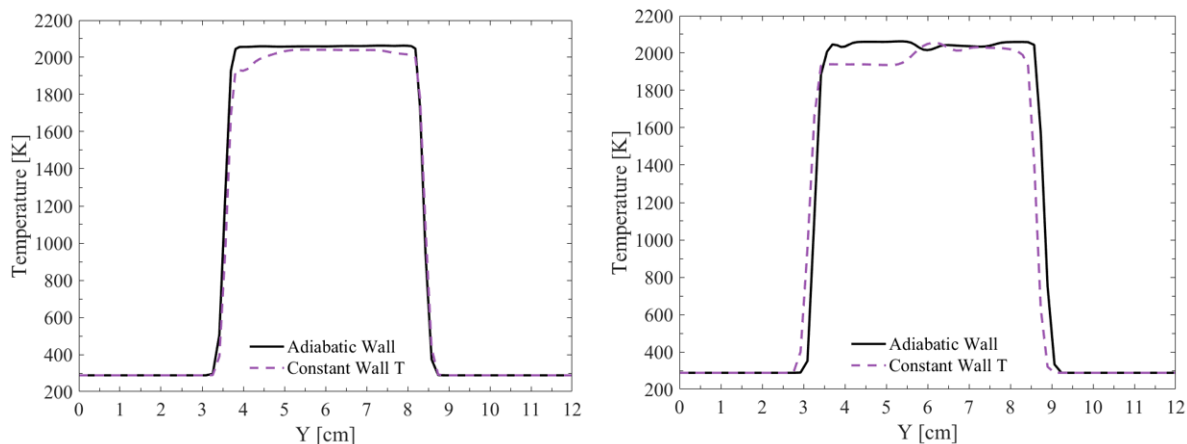


Figure 3.3: Comparison of transversal temperature profiles at two different locations for adiabatic wall versus constant wall temperatures, left: at 1.5cm behind the bluff body, right: at 6cm behind the bluff body

method and it is expected to yield more accurate results. However, when this scheme is used to solve for momentum, energy, and all 43 species transport equation, it caused more unrealistic flame thickening or excessive numerical diffusion at the beginning of simulation, following the ignition point. Eventually, the flame could not be established because the diffusion-induced with flashback phenomena evolved to cover the entire computational domain as shown in figure 3.4. This observation excludes the use of the MUSCL scheme in the flame development stage.

Returning to figure 3.1 and figure 3.2, we can conclude that the main features of the Volvo test case can be captured using 2D and 3D LES. The temperature is more difficult to fully capture but the 2D LES captures the main features of the flame in a manner that supports the further use of 2D LES in this work.

3.3 Mesh Sensitivity

The mesh sensitivity analysis was conducted with 2D and 3D configurations using three structured mesh resolutions for each; coarse mesh, fine mesh, and extra fine mesh with approximately 47,000, 186,000, and 550,000 quadrilateral cells, respectively in 2D and 440,000, 1,500,000, and 2,550,000 hexahedral cells, respectively in 3D. In addition, two 3D unstructured mesh using tetrahedral

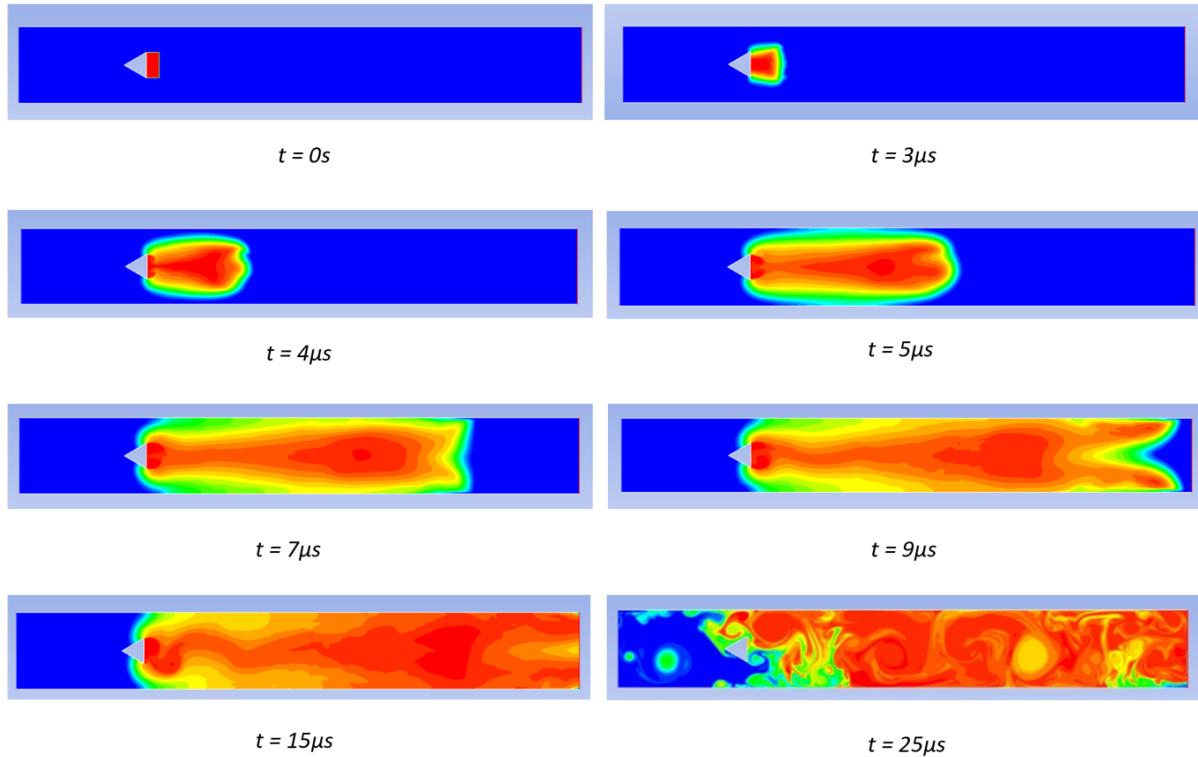


Figure 3.4: The flame development from the ignition with patching method implementing 3rd order numerical scheme, MUSCL.

structure were also designed to understand the impact of using this type of mesh on flame dynamics and temperature prediction. The equivalence ratio used for mesh study is 0.65 with 0% inlet turbulence intensity in all these configurations. Table 3.5 shows different parameters of mesh qualities for these configurations.

As it can be seen from the table the extra fine mesh with structured mesh along with fine mesh with unstructured mesh yield the best results in terms of temperature profile. Also their mesh qualities such as aspect ratio, skewness, and orthogonality are within the acceptable range.

Doing an appropriate mesh depends on the physical parameter of any numerical analysis and it is the core concept of any CFD simulations. Although there is no specific rule for meshing there are some parameters like skewness, aspect ratio, and orthogonality which are important characteristics of meshing. Here are the definition of these three important parameters and their acceptable ranges that must follow to generate a suitable mesh according to general understanding of numerical researchers

Summary of Mesh Sensitivity Analysis	Mesh Resolution	Total number of cells (M)	Min Aspect Ratio	Max Aspect Ratio	Avg Aspect Ratio	Min Orthogonality	Avg Orthogonality
3D-Structured	Coarse	0.46	1.01	5.62	2.15	0.82	0.99
	Fine	1.50	1.00	5.95	2.10	0.83	0.99
	Extra Fine -1	2.55	1.05	19.43	3.86	0.86	0.99
	Extra Fine -2	2.42	2.10	31.40	11.81	0.83	0.99
3D-Unstructured	Coarse	0.57	1.17	12.07	1.87	0.20	0.85
	Fine	1.06	1.16	10.26	1.90	0.22	0.85

Summary of Mesh Sensitivity Analysis	Mesh Resolution	Total number of cells (M)	Min Skewness	Max Skewness	Avg Skewness	Estimated Cell Length Around Flame (mm)	Max Temperature (°F)
3D-Structured	Coarse	0.46	5.27E-10	0.33	0.04	0.92	2230
	Fine	1.50	7.65E-10	0.33	0.03	0.63	2240
	Extra Fine -1	2.55	5.85E-10	0.33	0.01	0.28	1960
	Extra Fine -2	2.42	1.30E-10	0.33	7.50E-03	0.13	2180
3D-Unstructured	Coarse	0.57	4.40E-04	0.89	0.25	3.60	2290
	Fine	1.06	1.88E-04	0.86	0.25	2.14	1940

Figure 3.5: Mesh qualities used in 3D model validation analysis.

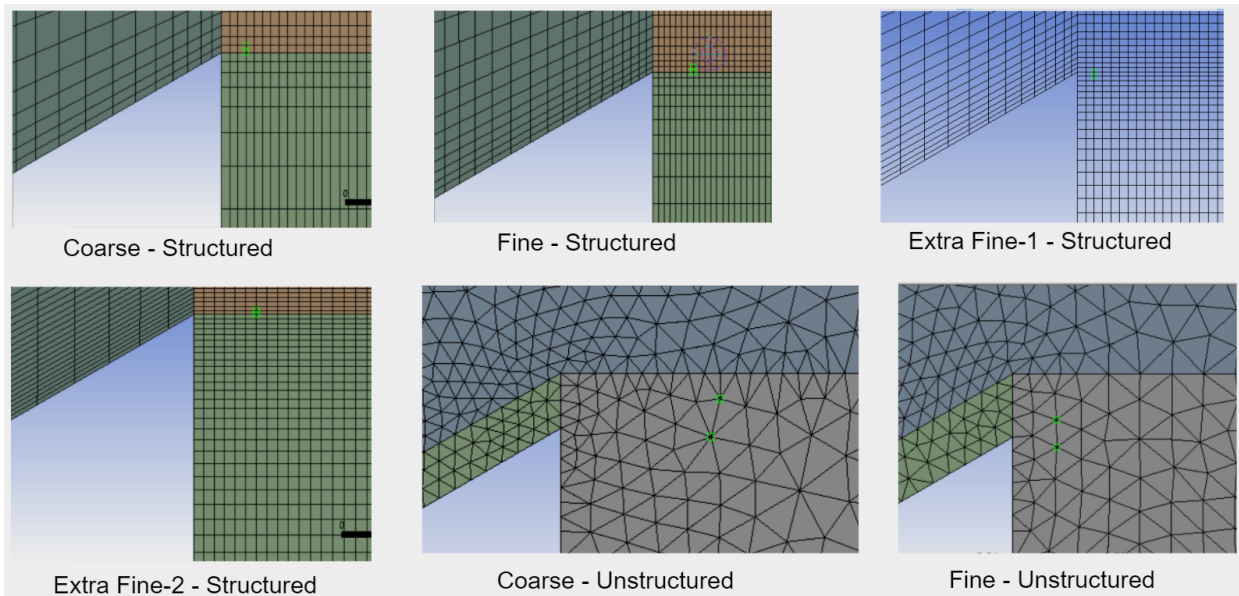


Figure 3.6: Mesh sensitivity analysis. Screenshots of different mesh configurations around the upper tip of the bluff body. The green mark shows where the measurement between two nodes was taken for the table 3.5

for CFD modeling:

- Cell aspect ratio: The aspect ratio is the ratio of longest edge length to shortest edge length. It should be equal to 1 for an ideal mesh. From our observation the max cell aspect ratio should

not exceed 15.

- **Skewness:** It is one of the primary quality measures for a mesh. According to the definition of skewness, a value of 0 indicates an equilateral cell (best) and a value of 1 indicates a completely degenerate cell (worst). Highly skewed faces and cells are unacceptable because the equations being solved assume that the cells are relatively equilateral/equiangular. It has been defined for the different type of mesh as follow:

Hexahedron and quad cells - skewness should not exceed 0.85;

Triangle cells - skewness should not exceed 0.85;

Tetrahedron cells - skewness should not exceed 0.9;

- **Orthogonality** It involves the angle between the vector that joins two mesh (or control volume) nodes and the normal vector for each integration point surface associated with that edge. The optimal average value for orthogonality shall be more than 0.85.

The boundary conditions and model used are similar in all these simulations; so, it is logical to pick a mesh configuration which is the most economical with regards to computational cost while yielding the closest results to experimental information. With these criteria, therefore, the fine mesh with unstructured mesh seems to be the best candidate for the further analysis. Thus, it is used to find the near blow-off equivalence ratio for comparison with the results with 2D computational domain. A comparison of structured-unstructured mesh effects is shown in figure 3.7.

The thought process here is that since the computational cost is high when using 3D model, accompanied by high fidelity turbulence model along with detailed chemistry in order to capture the near blow-off equivalence ratio, we compare the results obtained from 3D model with the results from 2D model used to see if the results are close enough for us to justify the much cheaper 2D model used to find the near blow-off equivalence ratio. This 2D mesh also used to investigate the impact of inlet turbulence intensity boundary condition on the flame at near blow-off condition. If

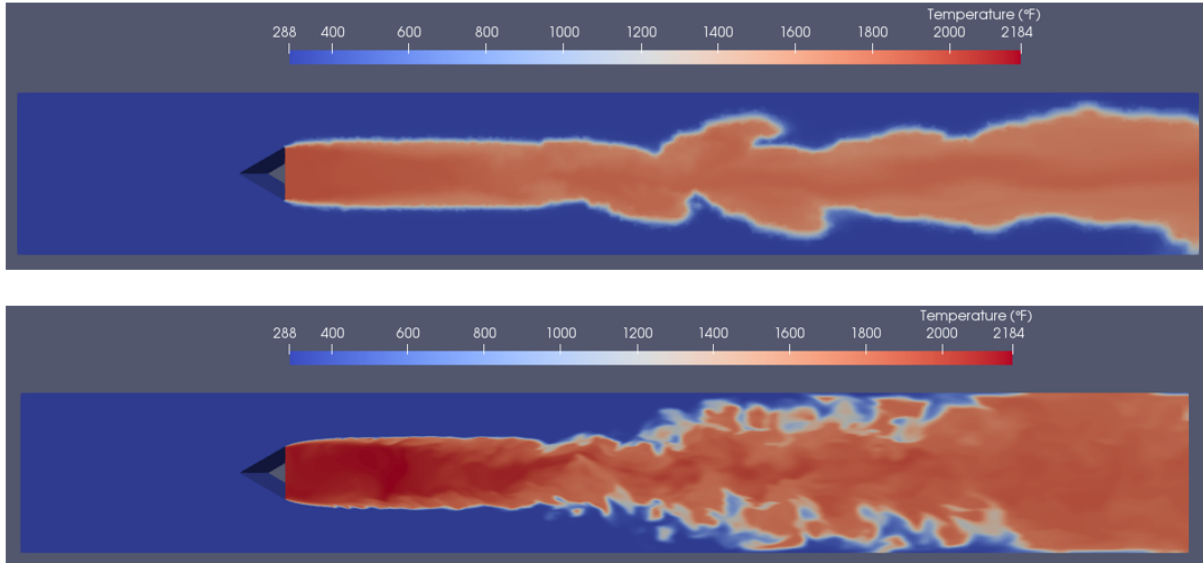


Figure 3.7: Mesh sensitivity analysis. The comparison of temperature contours between fine unstructured (top) and extra fine structured mesh (bottom). Unstructured fine mesh shows richer dynamic structures due to cell alignment with flow especially in the recirculation zone.

we find that the results between 3-dimensional and 2-dimensional are similar, then this significantly reduces the computational cost in other analyses by using the 2-dimensional model.

Comparison cannot only be based on contour plots. The profile comparison for x-axis mean velocity is shown in figure 3.8. Although the results does not show any mesh convergence, the experimental velocity profile is closer to the results from the extra fine mesh at two locations while it deviates more from experimental results at the other two locations when compered to results from coarse mesh. It should be noted that the averaging process may effect the profiles.

In Fig. 3.8 the max mean temperature predicted by the two grid resolutions are close, however, the flame brush is wider for the coarse mesh. Also, the mean temperature obtained from numerical results is higher than the mean temperature observed in experiment by about 250K.

It is observed from the analysis that when transient phenomena such as ignition and extinction become of interest, it is necessary to use species transport with detailed chemistry and LES for capturing the turbulence effects. We will discuss more about this in the chapter 5. Also the effect of mesh structure and resolution while using the above models has a significant impact on the

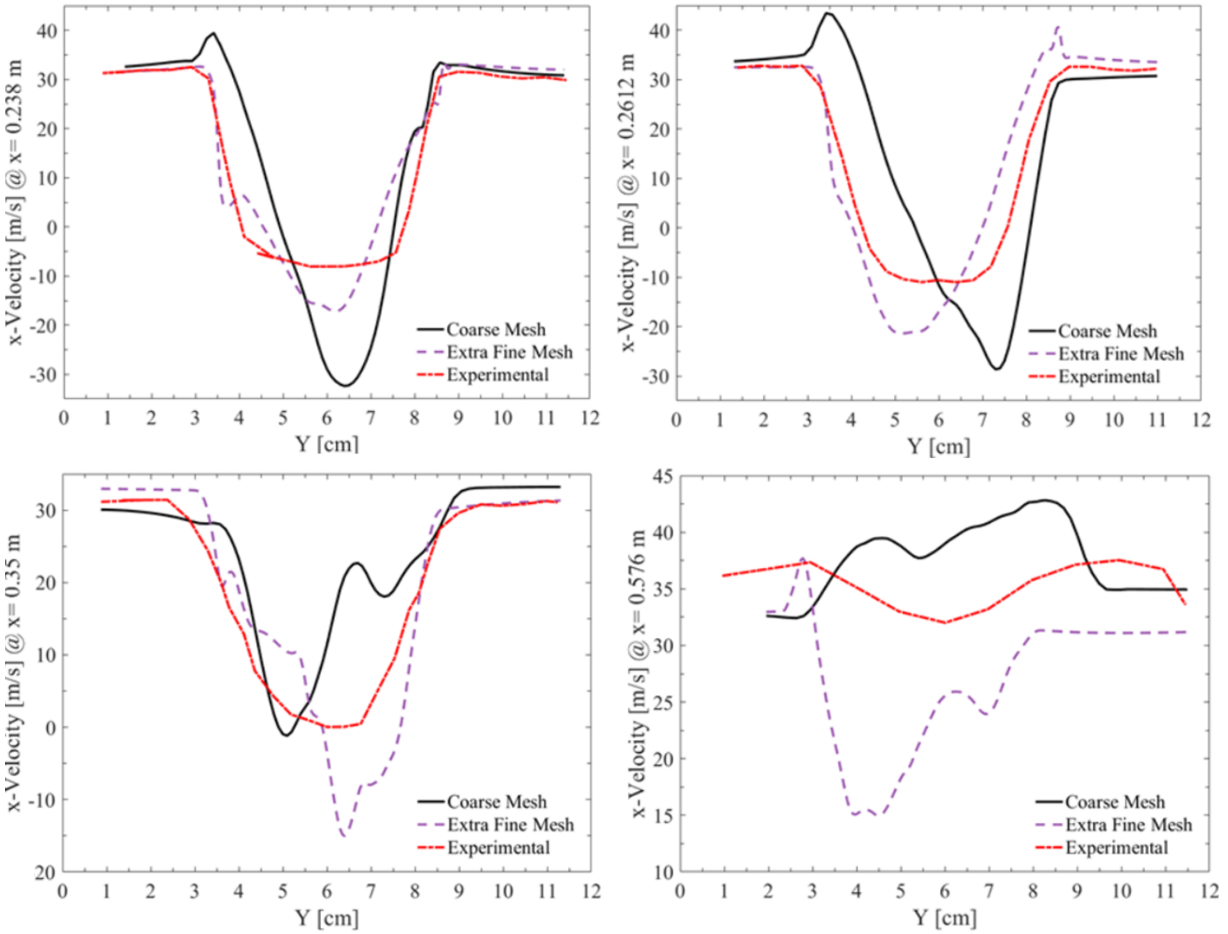


Figure 3.8: Mesh sensitivity analysis. the figure shows the average transverse velocity profiles at four different locations. Wide variation may indicate averaging and transient effects.

flame dynamics as it was shown in this study. The mesh resolution or refinement especially in high gradient areas also play an important role in the accuracy of the results. It is well understood from the investigation that resolution of grids or its concentration around flame shear layer as well as its aspect ratio throughout the computational domain and mesh configuration being structured or unstructured are crucial in terms of better prediction of flame profiles and contours. The study provided evidences of this while keeping the models and operating conditions the same. This allowed for identification of the impact of mesh sensitivity on the results. It should be noted that unlike in RANS, strict mesh convergence cannot be the target of LES filtered properties.

Another important finding is the flow alignment with mesh orientation is important in obtaining

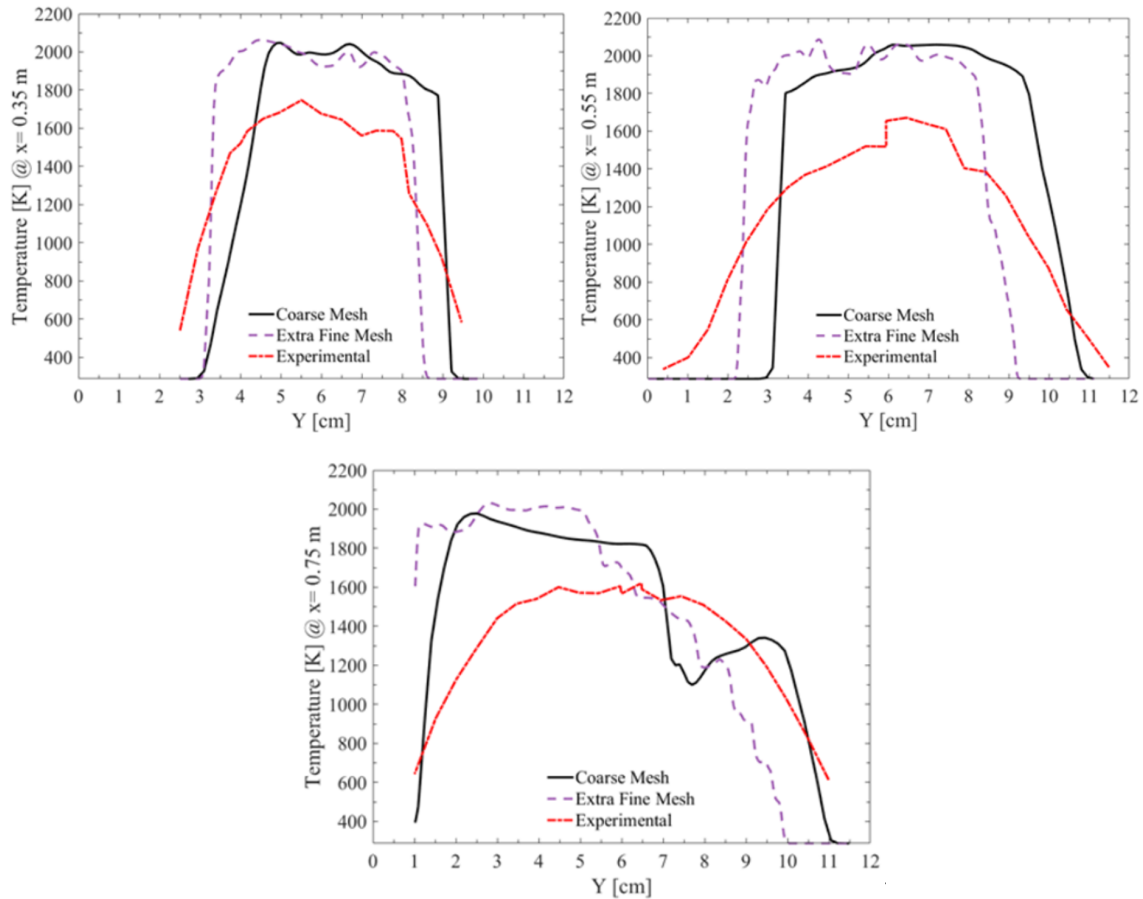


Figure 3.9: Mesh sensitivity analysis. The results are shown based on transverse temperature profiles at three different locations

better numerical results. This argument is validated since the results from the unstructured mesh provided more accurate results compared to structured mesh even though the mesh resolution in the latter case was much finer than the prior mesh. The temperature profile in the fine unstructured mesh matches better with experimental results when compared to the results from extra-fine structured mesh. In other word, with the mesh better aligned with flow streamlines the number of mesh nodes needed to provide the same accuracy can be reduced. This is because the unstructured mesh provide a better alignment especially in the flame region where there are high shear stresses. These stresses cause strong vortices around the recirculation zone boundaries or at the end of recirculation zone when the mixture of fuel and air is entrained into the hot gas products region. The entrainment of fresh mixture into the recirculation zone causes a better mixing process while keeping a healthy

flame attached to the bluff body. Since the subgrid scale turbulence models are affected by mesh quality and this turbulence is influenced by regions of high gradients, any alignment that improves prediction of stresses, influences the flow quality in that region.

In the next chapter the process of finding the near blow-off is explored. Also the comparison of the results between 2D and 3D simulations will be discussed. Further, the similarities observed in lean flame condition will be highlighted.

Determination of Near Blow-off Equivalence Ratio

This chapter deals with the determination of blow-off equivalence ratio using simulations. This phenomenon is explored by using the validated computational models in the first part of this research. The validated models will also be utilized to show that changing the inlet turbulence intensity has significant impact on the flame structure. The impact of inlet turbulence on flame dynamics is expected to be more pronounced near the blow-off equivalence ratio. This ratio therefore needs to be determined. The reason for this is at this condition the flame is weaker and more sensitive to boundary condition changes. As the flame becomes leaner, the maximum temperature is lowered. Heat transfer to unburnt mixture gets slower and flame propagation is endangered. Establishing the near blow-off equivalence ratio is therefore necessary. There are many parameters which impact the result of predicting the flame blow-off. Some of them are listed below:

- Turbulence and combustion models
- Method of approaching flame extinction condition
- Dimensions of the flow simulation at near blow-off equivalence ratio

This means that the ϕ_{NBR} is sensitive to these parameters and care must be taken in its determination. The process of finding the near blow-off equivalence ratio and the fluid dynamics leading to blow-off will be explored and analyzed in this chapter. This numerical analysis differs from experimental determination because of model and model sensitivities. However, the experimental blow-off dynamics can be considered captured in terms of response to changes.

4.1 Approaching Blow-off Through 2D LES And Detailed Chemistry

For the investigation of the near blow-off flame the 2D computational is selected. It will be shown later in details that the planar computational domain is capable of capturing the important features of flame dynamics such as the symmetrical and asymmetrical behavior in strong and weak flames, respectively, as well as the length of the recirculation zone with acceptable accuracy comparable to 3-dimensional analysis. It is generally agreed that turbulence is a 3-dimensional phenomenon mostly due to its vortex stretching effect. This vortex stretching, however, is less present in the reacting turbulent flow due to heat dilatation effect resulting from the energy release of the chemical reactions.

The comparison of the 2D and 3D results in this research is in fact the confirmation of previous research works conducted by Cetegen [55] and Soteriou [56]. Cetegen argued that even though the helical mode of instability dominates the dynamics of non-reacting flow with sinusoidal vortex shedding, this feature is lost in reacting flow and is replaced by more symmetrical instability at the shear layers especially in a more robust flames. This is due to the damping effect of heat dilatation over the vortex stretching phenomenon. The dissipation of vortex shedding in the reacting flow is to the extent that it makes the dynamics of turbulence to be practically two dimensional, with a negligible loss of accuracy. This is a crucial finding as it will simplify the computational work in a significant way, especially when detailed chemical kinetic models are combined with LES to capture the transient features of the flame such as extinction. It is also interesting to know that when the vortex stretching is viewed in planar projection it appears as the sinusoidal vortex shedding

phenomenon [88].

It was suggested that blow-off occurs when the balance between the rate of entrainment of reactants into the recirculation zone and the rate of burning vanishes [89]. This can be viewed as when the ignition time of the combustible mixture exceeds the residence time of the combustible mixture in the flame shear layers [90]. In a robust and stable flame the ignition of the mixture of reactants occurs in the shear layer where it is exposed to hot gases in the recirculation zone behind the bluff body.

Lieuwen et al. characterized the near blow-off event by two events or stages which are happening in a consecutive order [51, 52]. The first stage of flame blow-off is when flame shear layer extinguishes locally and intermittently, forming flame holes along the shear layer. They demonstrated that the flame can survive in this stage indefinitely, however, this phenomenon is acknowledged to be a major cause and initiator of blow-off process. The excessive stretch rates by the shear layer vortices coupling with the flame shear layer cause the local extinction of flame front. The second stage is characterized by a more sinusoidal movement of the flame shear layers and this was considered the final cause of blow-off.

Cetegen et al. [3] suggested 5 stages of blow-off process; (a) flamelet merging (b) localized extinction (c) pocket formation (d) fragmentation of the flame segments (e) asymmetric flame structure which is a significant wrinkling and distortion on the flame fronts were observed. Figure 4.1 demonstrates these terms graphically. The flamelet merging is defined as when narrow bands of wrinkled flame surfaces are created due to penetration of preheated reactants into combustion products. This can cause a extinction of flame surface and reduction of local burning rate. The localized extinction occurs by the effect of large-scale eddies interacting with the flame front. This imposes higher strain rate on the flame shear layer. Pocket formation is the consequence of flamelet merging and the localized extinction phenomena. These are islands of CH_2O in the regions filled with OH. The fragmentation of the flame segments is defined as when the significant localized extinction occurs causing the penetration of reactants into recirculation zone. The most obvious

characteristic of flame near blow-off is the intermittent change-over from symmetric to asymmetric mode. This is a well-observed phenomenon observed and reported by previous researchers, [14, 15, 55, 56, 91].

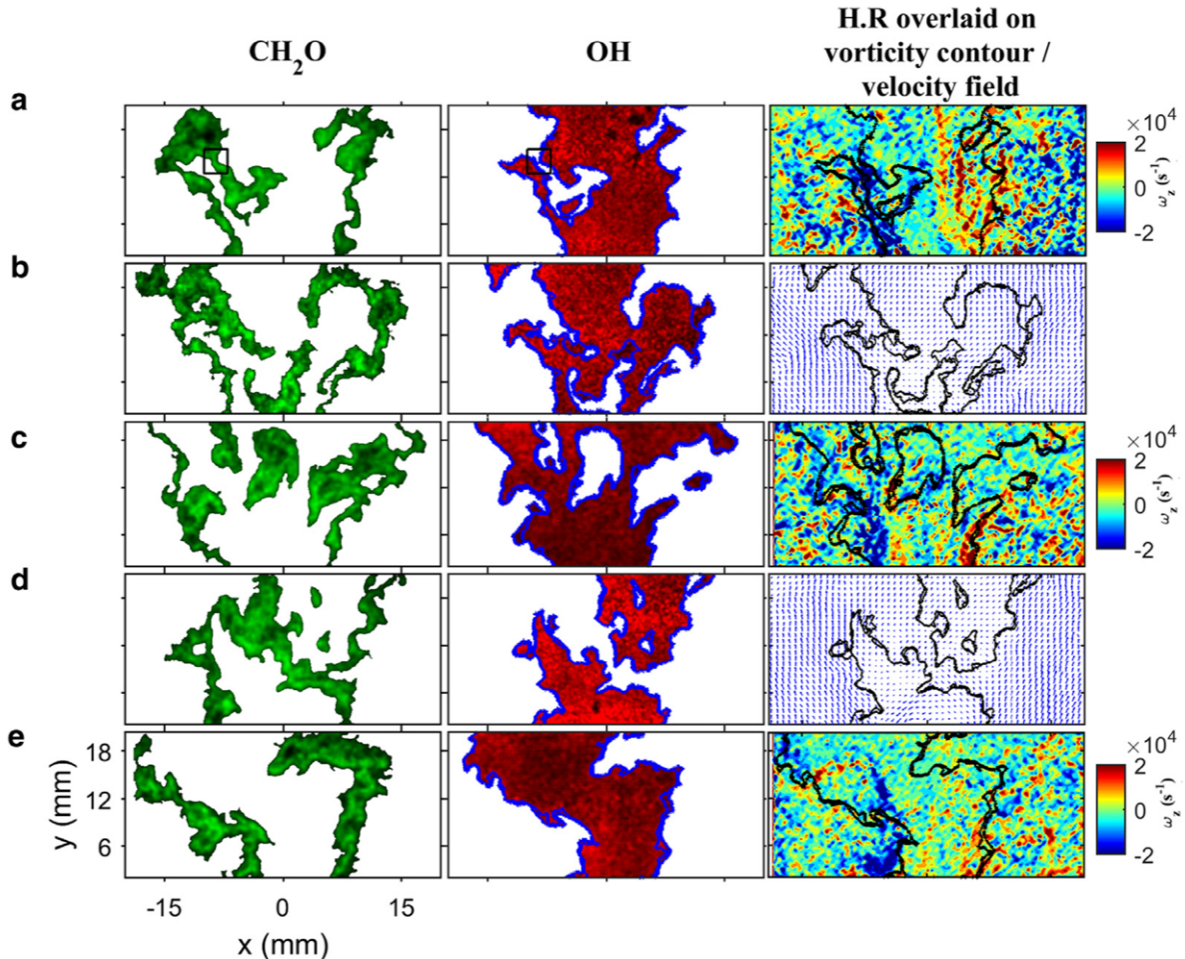


Figure 4.1: Instantaneous images of CH_2O PLIF, OH PLIF and heat release region overlaid on the vorticity contours and velocity field for flame near blow-off (a) flamelet merging, (b) occurrence of shear layer extinction, (c) pocket formation, (d) flame fragmentation and (e) asymmetric flame structure [3].

Similar stages of blow-off is observed with numerical result. Fig. 4.2 demonstrate these stages of blow-off as blow-off develops over flow time. Some studies sought to understand the transition between the symmetric instability and the asymmetric flame behavior. Some suggested that the transition occurs when the global temperature ratio is near unity. However, as it was explained in the previous chapters, wide variation exists in the reported values of threshold temperature or density

ratios. It was experimentally shown that the extinction of the flame along the shear layers causes the entrance and ignition of reactants into the recirculation zone.

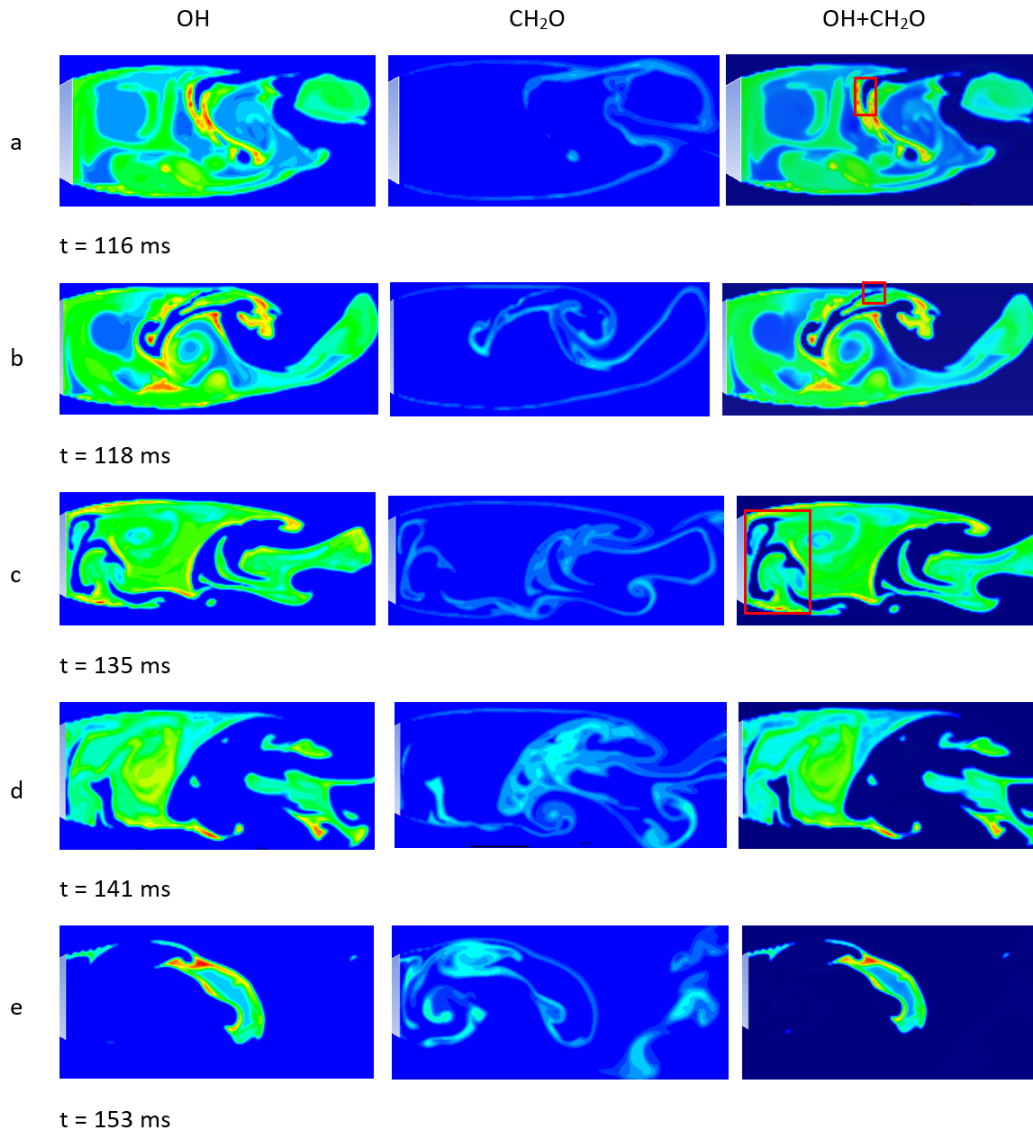


Figure 4.2: Numerical simulation captures all the stages of blow-off observed in experimental data

In contrast, for a robust and stable flame with higher heat-release ratio across the shear layers, the vorticities generated by the apexes of the bluff body are dissipated by the effect of heat dilatation. This dissipation effect is augmented by the increase in the viscosity of hot gases generated from chemical reactions. These two physical phenomena lead to damping of the vortices formed at the apexes of the bluff body. These vortices initiate the vortex shedding that we observe in the dynamics

of non-reacting 2-dimensional bluff body flow. In an exothermic reacting flow, however, the sinusoidal vortex shedding is replaced by symmetrical shear layers in robust bluff body stabilized flames. In these flame, the dominant instability is the so-called convective Kelvin-Helmholtz instability. The instabilities or vortices reside inside the recirculation zone and very close to shear layers for the stable flame as it is illustrated in figure 4.3.

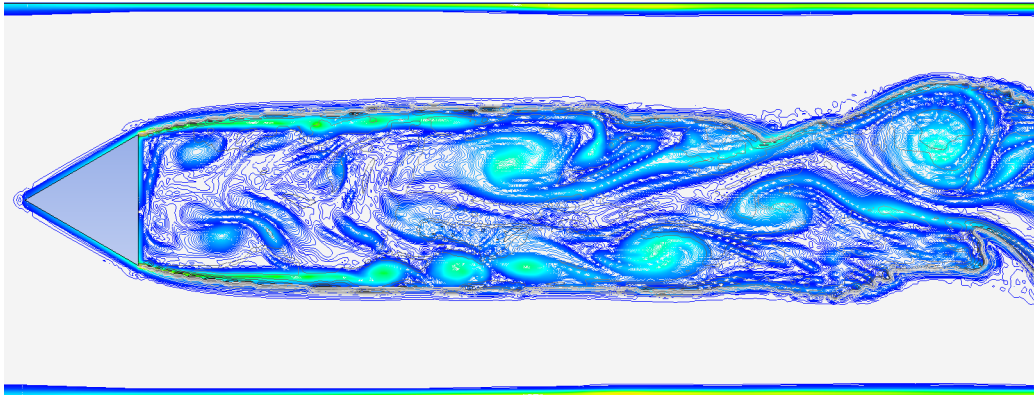


Figure 4.3: Instantaneous and simultaneous contours of hydroxyl (OH) and formaldehyde (CH_2O) superimposed on vorticity distribution in the computational domain when $\phi = 0.65$ and the flame is robust and stable.

This figure shows the instantaneous and simultaneous contours of hydroxyl (OH) and formaldehyde (CH_2O) superimposed on vorticity contour in the computational domain. The black line, which is an overlap of hydroxyl and formaldehyde contours represent the heat release region [3]. As it can be seen in this figure the heat release region encompasses the region of strong vortices in a stable and robust flame. This means that the stretching rate on the flame shear layer is low and the presence of vortices in the recirculation zone will not cause local flame extinction. This result is consistent with the experimental result conducted by Cetegen et al. [3]. They observed that in stable reacting flow the flame shear layer envelops the high vorticity regions in the recirculation zone behind the bluff body. The flame shear layers in this case is positioned in the low vorticity region and therefore the flame is less wrinkled and more symmetric.

Figure 4.4 shows the instantaneous contours of hydroxyl (OH) and formaldehyde CH_2O superimposed on vorticity distribution for the weak flame.

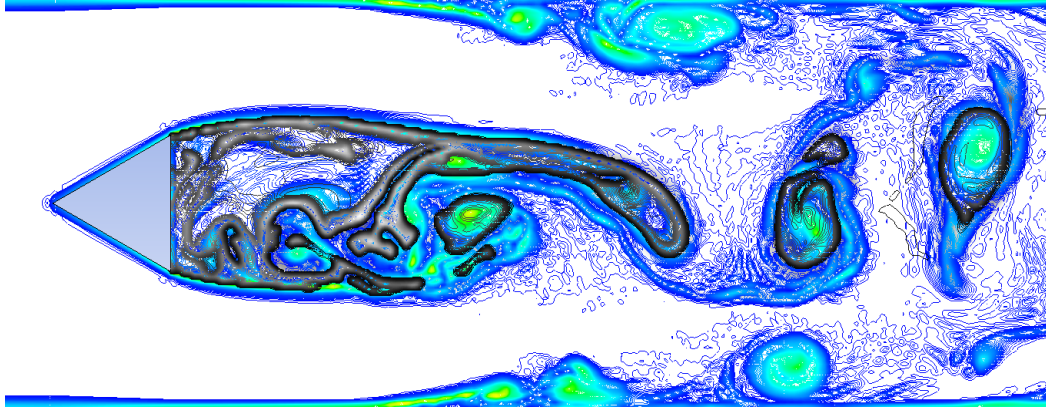


Figure 4.4: Instantaneous and simultaneous contours of hydroxyl (OH) and formaldehyde (CH₂O) superimposed on vorticity distribution in the computational domain when $\phi = 0.32$. The flame is weak and is near blow-off.

In contrast to the healthy flame shown in the previous figure where strong vortices lie inside the recirculation zone between two symmetrical flame shear layer for the weak flame near blow-off the presence of vortices are outside of the recirculation zone and they overlap with the heat release region of the flow. The reactants penetrate into the recirculation zone behind the bluff body in an asymmetric flame at the final stage of blow-off. At this stage the flame kernel survives only for a few milliseconds before it completely blows off. In contrast, in a robust and stable flame the recirculation zone consists of combustion products, with reactions taking place along the shear layers. It encompasses the recirculation zone and thus, the combustible mixture reacts before entering the recirculation zone in a strong flame. These observations in numerical simulation affirm the experimental observation cited in many research papers pertaining to blow-off dynamics.

4.2 Blow-off Through Reduction of Equivalence Ratio

The criterion to confirm this phenomenon is set by the experimental work conducted by Cetegen [3] and Lieuwen et al. [14]. They observed that when the flame is approaching the blow-off condition, the recirculation zone behind the bluff-body shrinks to the point that the flame intermittently appears to switch from symmetric to asymmetric type of vortex shedding mode. Although this stage acts as a marker towards flame blow-off, it has been suggested that the flame can survive indefinitely at

this stage [51, 52]. Therefore, careful observation was conducted during the simulation to make sure that the condition of the flame is deteriorating and that the recirculation zone is continually shrinking as the time progresses. If no change is observed in the flame, then the condition is deemed quasi-steady and the mixture equivalence ratio was decreased until the complete annihilation of the recirculation was observed. The sinusoidal vortex shedding effect became the dominant feature of the flow structure.

Figure 4.5 shows the contour of CO₂ gradient, which overlap with the flame front, at three different equivalence ratios. All these models employ the laminar flame finite rate model with the chemical kinetic model of Peters et al. [79]. The coarse mesh resolution is used for this investigation to facilitate the rapid assessment of the effects.

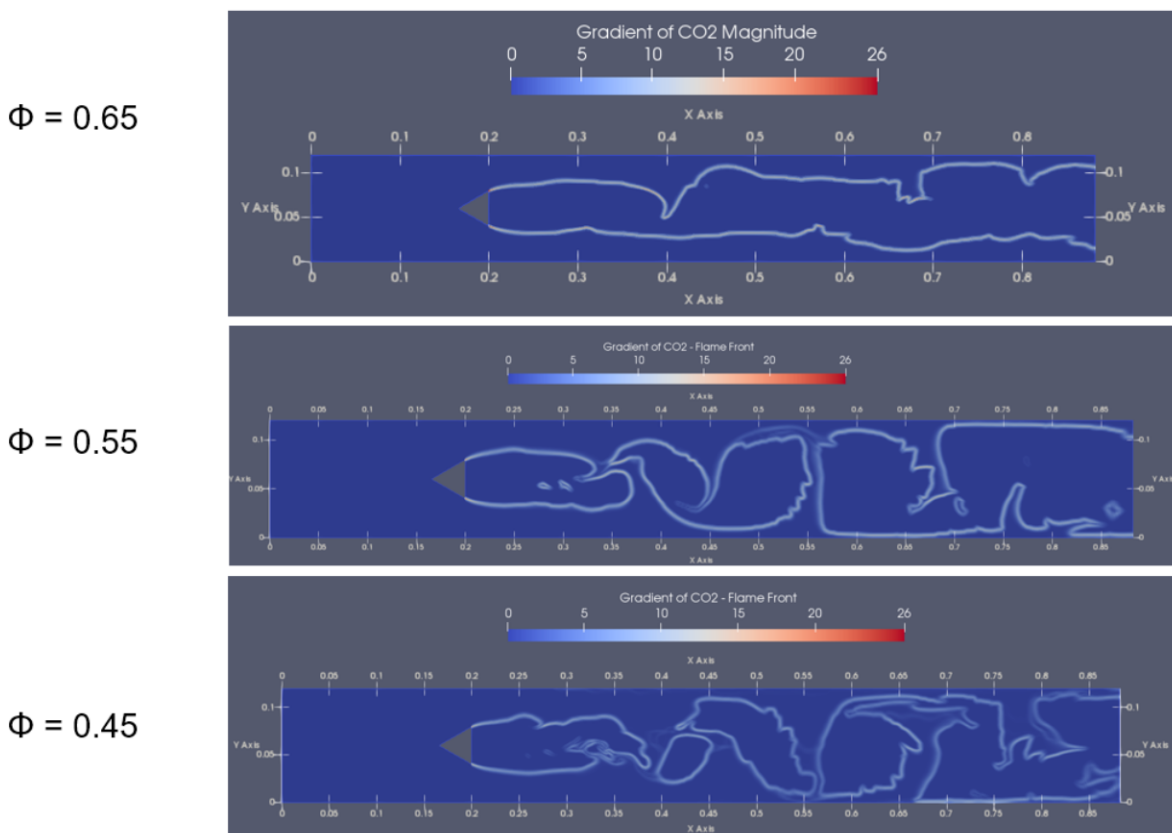


Figure 4.5: The effect of equivalence ratio variation on the flame structure

As shown, when the fuel becomes more diluted with air, the flame breaks up and becomes more unstable. At $\phi = 0.45$ the flame breaks up but it can survive indefinitely at this condition. The

alternate vortex shedding becomes stronger and the effect of heat dilatation becomes weaker. The oscillation is also believed to be responsible for shortening and pushing the flame into the recirculation zone. This mechanism is believed to ultimately lead the flame to extinction. The flame is still strong enough to survive even at $\phi = 0.45$.

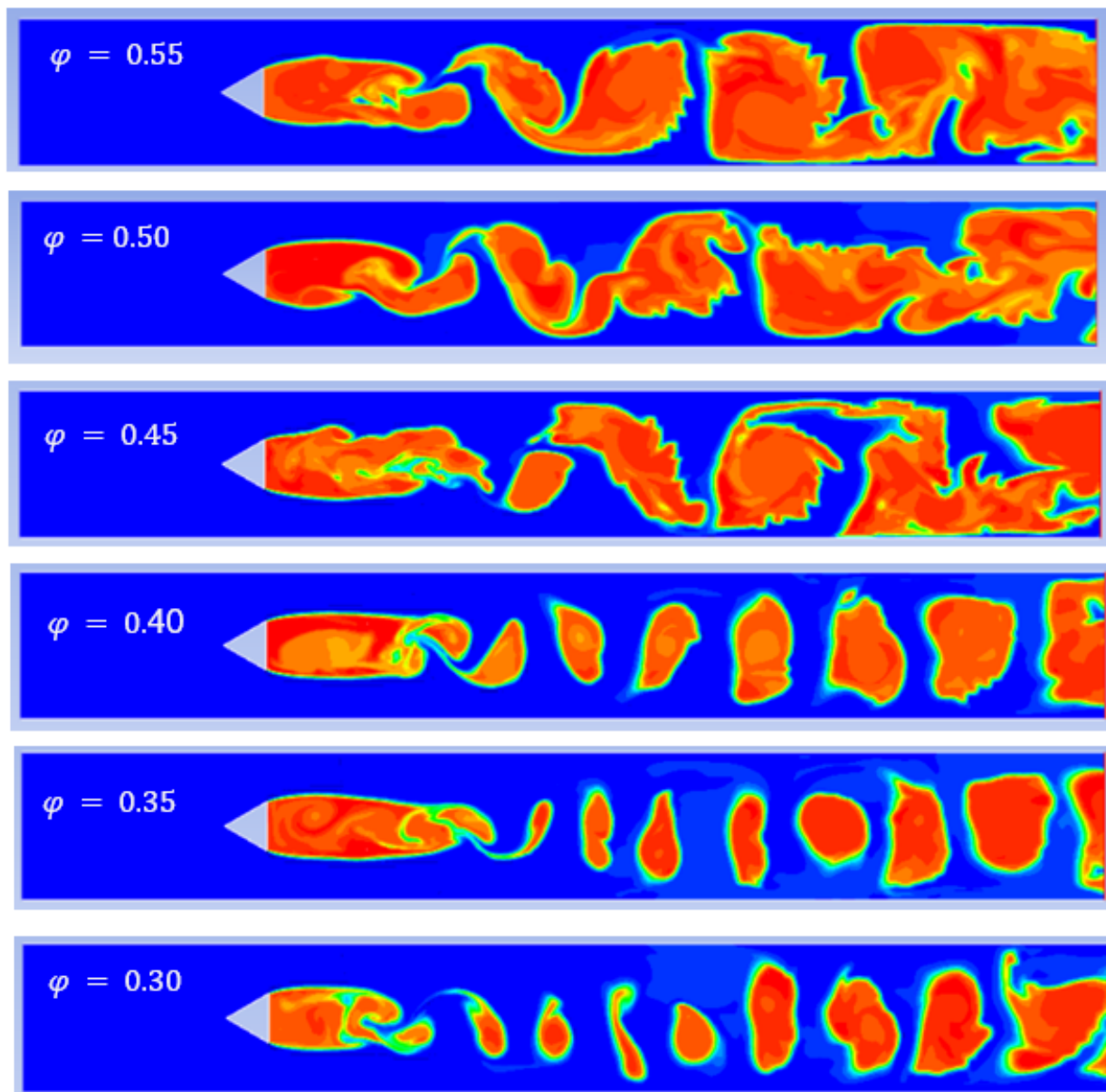


Figure 4.6: Determination of blow-off equivalence ratio. Temperature contours are shown in a descending order from $\phi=0.55$ to $\phi=0.30$. Due to flame behavior at $\phi = 0.30$, this is taken as the blow-off equivalence ratio

The process of decreasing the equivalence ratio is continued until the recirculation zone becomes shorter and narrower as shown in figure 4.6. Finally the flame blow-off occurs at $\phi=0.30$. It should be noted that the mesh resolution can affect the exact blow-off equivalence ratio but the observed trend is fully captured here.

For the purpose of this study, $\phi = 0.30$ is taken as blow-off equivalence ratio. During the determination process, all the numerical setups and physical models are kept unchanged and the only variable was the fuel to air ratios. After finding the equivalence ratio where the blow-off occurs, the ratio of $\phi=0.32$ was selected as a near blow-off equivalence ratio. The effect of ITI on the flame dynamics is then investigated at this condition.

4.3 Verifying 2D and 3D Behavior At Near Blow-off

In this section we will establish the justification of implementing 2D simulation instead of the normal 3D simulation to investigate the blow-off of the bluff-body stabilized flame. According to previous work [16, 69], the main difference between 2D and 3D LES results for both non-reacting and reacting flows are in the downstream region of the computational domain where the flame is attached to the bluff body. For the 2-dimensional simulation, vortex islands appear further downstream due to vortex stretching effect not properly captured in the flow dynamics of 2D simulation compared to 3D simulation. In the 3D simulation the vortex breakdown appears further upstream and closer to bluff-body. These prior observation are confirmed in this work.

According to Yang et al. [16], a 2D treatment can usually obtain good agreement with experimental measurements in the near field. To achieve reliable predictions in the far field, however, a 3D analysis is essential. In other words, the flame exhibits a quasi-2D structure near the bluff body, but develops 3D structures in the downstream region. The near field flame evolution is influenced mainly by the quasi 2D separated shear layers, while in the far field the flame is dominated by the large 3D vortical structures.

For the reacting cases, the 2D and 3D simulations yield acceptable results that are quite close to experimental results, especially near the bluff body. The vortex stretching effect is responsible for vortex breakdown and for this reason the appearance of vortex islands is more toward the upstream of the flow region for the 3D case than in the 2D case.

The flame can be represented either by steep gradient of the temperature across the flame front or by gradient of CO₂ concentration across the flow region. The flame is anchored by a sheet-like structure stemming from the upper and lower edges of the flame stabilizer. The flame shear layer is situated outside of the recirculation zone causing a significant density gradient across its very small thickness.

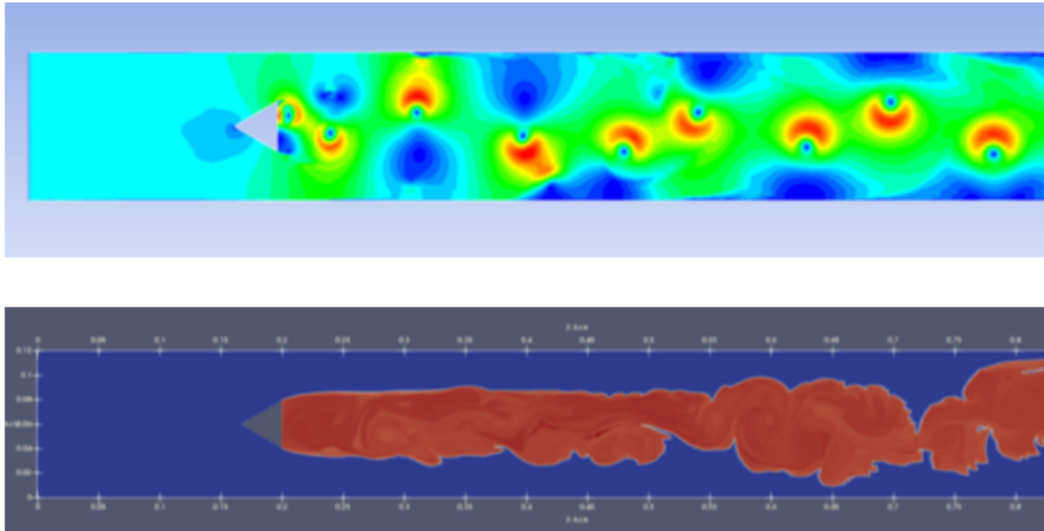


Figure 4.7: The comparison of non-reacting (top) and reacting flow (bottom) in terms of vortex shedding effect. The absence of the shedding in the reacting case improves 2D approximation of the 3D flow.

This generates a baroclinic torque which damp the rotational effect of the vortex shedding. This damping will suppress the sinusoidal instability that is very strong in the non-reacting flow. By damping the vortex stretching that is the root cause of vortex shedding, a more symmetrical flame structure appears. To a great extent it is independent of the impact of 3D fluid dynamics. In other words, the baroclinic torque generated by the reacting flow causes a mode change in the type of flow

from a 3D flow dynamics to more of a 2D flow dynamics. This shift of behavior is in agreement with experimental result and justifies our use of 2D LES to capture the main features of the stabilized flame, Fig. 4.7.

The prediction of the recirculation zone length (the location of the inflection point in the time-averaged axial velocity along the centerline) and the magnitude of the normalized axial velocity in both 2D and 3D reacting flow are also in good agreement with experimental data, Fig. 4.8. The time-averaged axial velocity in this figure also shows that a strong flow reversal is present immediately behind the bluff-body flame holder which helps with flame survival at the near blow-off conditions.

Some differences are noticed between 2D and 3D numerical results for the axial x-velocity profile along the centerline. Adding the third dimension in the simulation changes the grid arrangement and exposes the flow to additional boundary conditions on both ends of the span-wise direction.

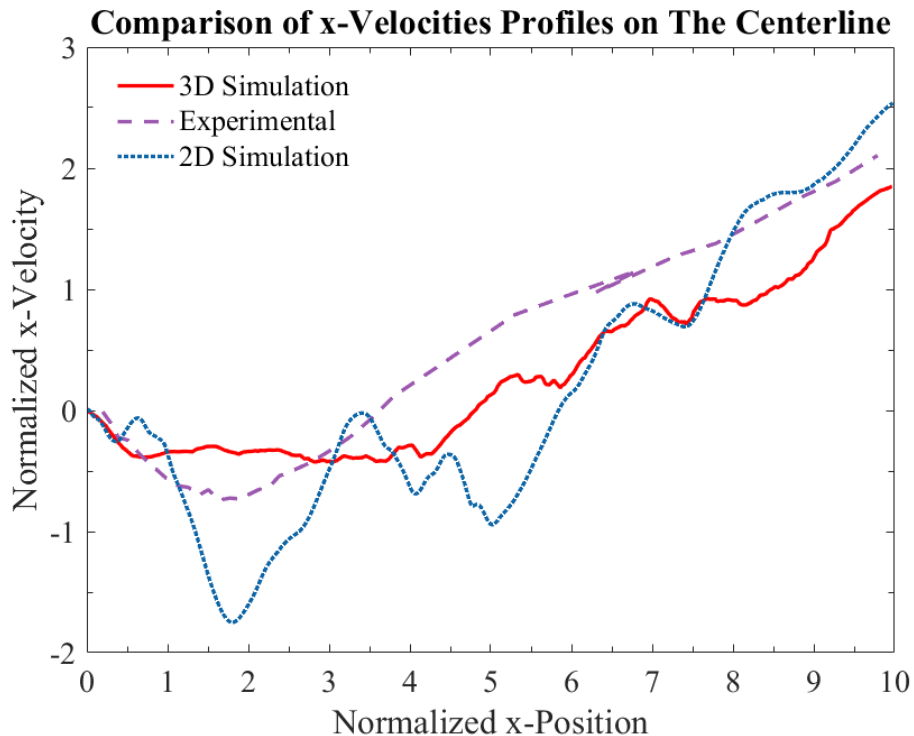


Figure 4.8: Comparison of axial velocity between 2D, 3D, and experimental results. The x-positions are normalized by the length of the bluff body and the velocities are normalized by incoming flow velocity

As mentioned the transition to sinusoidal movement of the flame at the downstream region was also captured in 2D simulation. The planar behavior of the reacting flow, especially near the flame holder, is more evident due to the damping of vortex stretching by heat dilatation. The vortex stretching is the main fluid dynamical feature in the span-wise direction that gives any turbulent flow its 3-dimensional property. Because this stretching is suppressed in the reacting flow, the dynamics becomes a predominantly 2-dimensional flow. This justifies the 2D approach whose benefit is to save significant computational time in parametric and exploratory studies as done in this work. This is especially useful when detailed chemical kinetic models and LES approaches are used. These more computationally involved models are needed in order to capture the highly blow-off transient lean flame.

The temperature contour at $\phi = 0.30$ based on the 3D tetrahedron grids is shown in figures 4.9, 4.10, and 4.11. It can be seen from these figures that in the 3D case, the tail of the reacting flow narrows down in width while the sinusoidal flow becomes more dominant in the downstream of the flow. This behavior is the necessary condition for the initiation of the blow-off process. A similar pattern was observed in the 2D simulation. It was observed that by further decreasing the equivalence ratio or by allowing for a longer flow time, the flame will blow-off. This presumption is confirmed by several experimental studies regarding blow-off phenomena [14, 15, 55]. As expected, the local extinction of the flame shear layer appears at the downstream of flame shear layer and the vortex shedding effect becomes more dominant in that region. Also, the recirculation width decreases at the end. These results are similar to the observation in the 2D case. It was observed from 2D simulation that continuation of flame operating at this condition will lead to complete blow-out of the flame. The difference with this 3D case is that it appears that a longer flow duration will be needed.

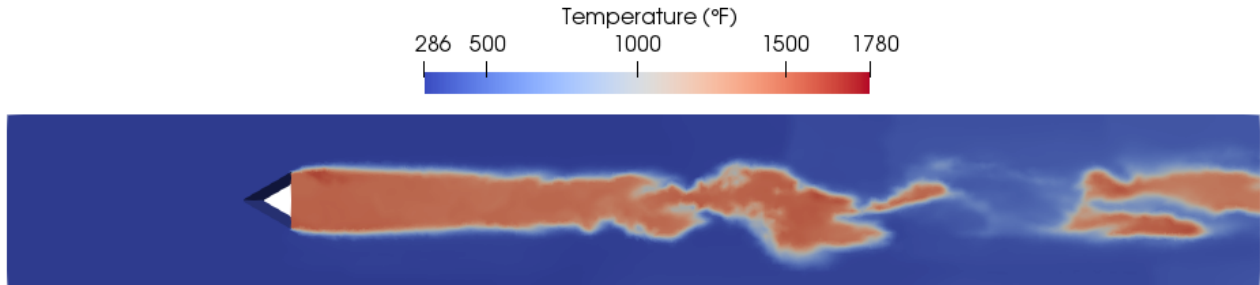


Figure 4.9: The instantaneous temperature contour of the bluff-body stabilize flame operating near blow-off condition. This is based on 3D simulation using tetrahedron grids with LES and detailed chemistry models at $\phi = 0.30$.

Figures 4.9 and 4.10 show the same instances. The isometric view of the latter figure helps with better visualization of the vortex stretching and the subsequent sinusoidal movement of the flame.

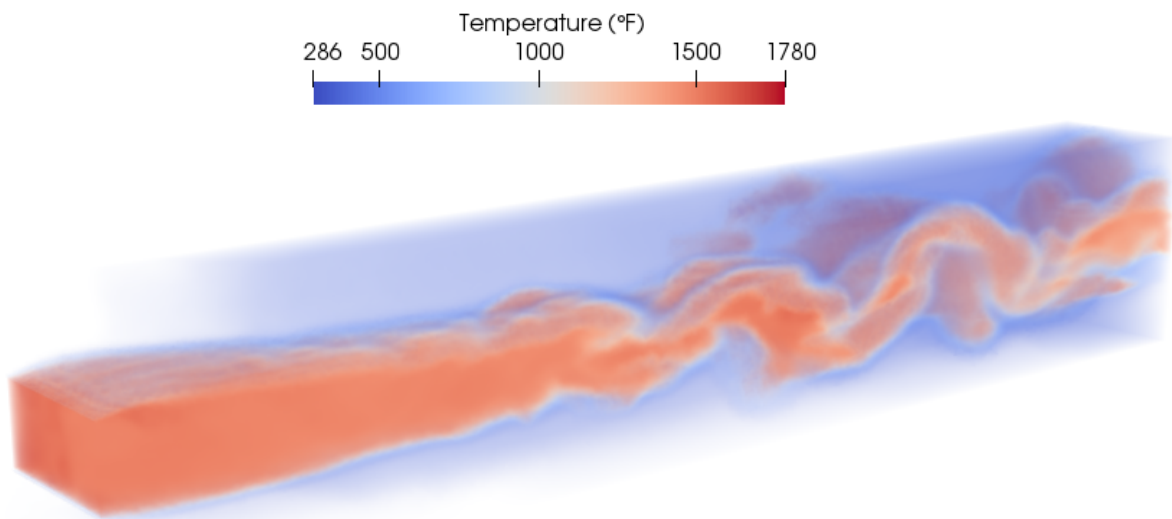


Figure 4.10: Same contour as figure 4.9 showing the result in isometric view. The vortex shedding downstream of the flow is more visible.

Since the span-wise direction of the 3D simulation is important to understand the effect of the vortex stretching on the flame a top view of the computational domain is needed. Figure 4.11 serves this purpose. From this view, it can be seen that flame shear layer extinguishes at different locations in the span-wise direction. The islands of the reacted zone is also visible from this view.

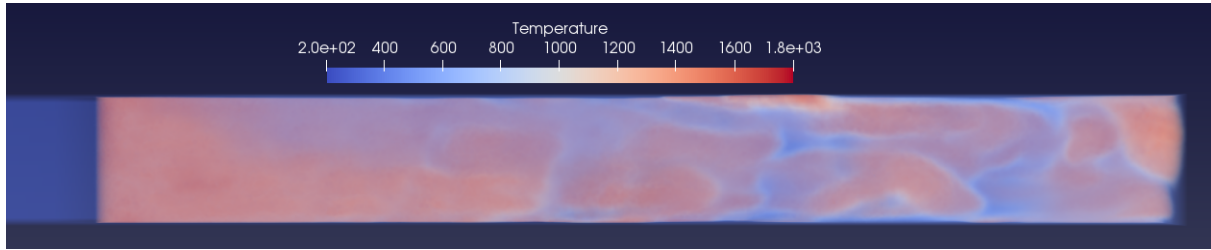


Figure 4.11: Top view of the 3D domain showing the consistency of the flame near bluff-body stabilizer in span-wise direction while showing variation in the flame extinguished region further downstream.

The 3D temperature contour demonstrates the variations of flame shear layer extinction locations in span-wise direction. This variation, however, is more toward the downstream of the domain. This means that although the flame is weak, the impact of vortex stretching is less realized near the bluff-body where it is anchored. The 3D simulation as it is illustrated in this image shows that the flame shear layer is more consistent in span-wise direction in the upstream of recirculation zone close to the bluff-body even at near blow-off condition. This confirms the initial hypothesis that a 2-dimensional domain is sufficient for the investigation of the bluff-body stabilized flame near its blow-off condition. This is so because the dynamics of blow-off only occurs when the flame is completely detached from its anchored location. The results from the 3D simulation affirm that the impact of 3D vortex stretching is insignificant in this region at near blow-off equivalence ratios. The 2D LES invoked at the beginning is therefore a reasonable tool to probe blow-off and inlet turbulence interactions.

Chapter 5

Effect of Inlet Turbulence Intensity On The Flame At Near Blow-off Equivalence Ratio

The considered boundary conditions is the inlet turbulence intensity condition. This is defined as:

$$ITI = \frac{\sqrt{\frac{1}{3}(u'^2 + v'^2 + w'^2)}}{U_{mean}} \quad (5.1)$$

where u' , v' , and w' are the fluctuating part of velocity component around the mean value in x, y, and z coordinates, respectively. In ANSYS Fluent, the inlet turbulence intensity for LES is generated by two different methods: the vortex method and the spectral synthesizer method [83]. In the vortex method, a perturbation is added to the mean velocity profile. This perturbation is a 2D fluctuating vorticity field that is Lagrangian in the plane normal to streamwise direction. To compensate for the streamwise velocity fluctuation, ANSYS uses another method called the simplified linear kinematic model. The spectral synthesizer is an alternative method to generate a randomly fluctuating inlet velocity profile. This is based on the random flow generation technique proposed by Kraichnan [92] and later modified by Smirnov et al. [93]. In this method, by synthesizing a divergence-free velocity vector field from summation of Fourier harmonics, the fluctuating velocity field can be computed. This is the method selected in this research to generate the random inlet velocity field

about the given mean velocity. Figure 5.1 shows the comparison of inlet velocity profiles at two different ITI levels; 1.7% and 27.5%.

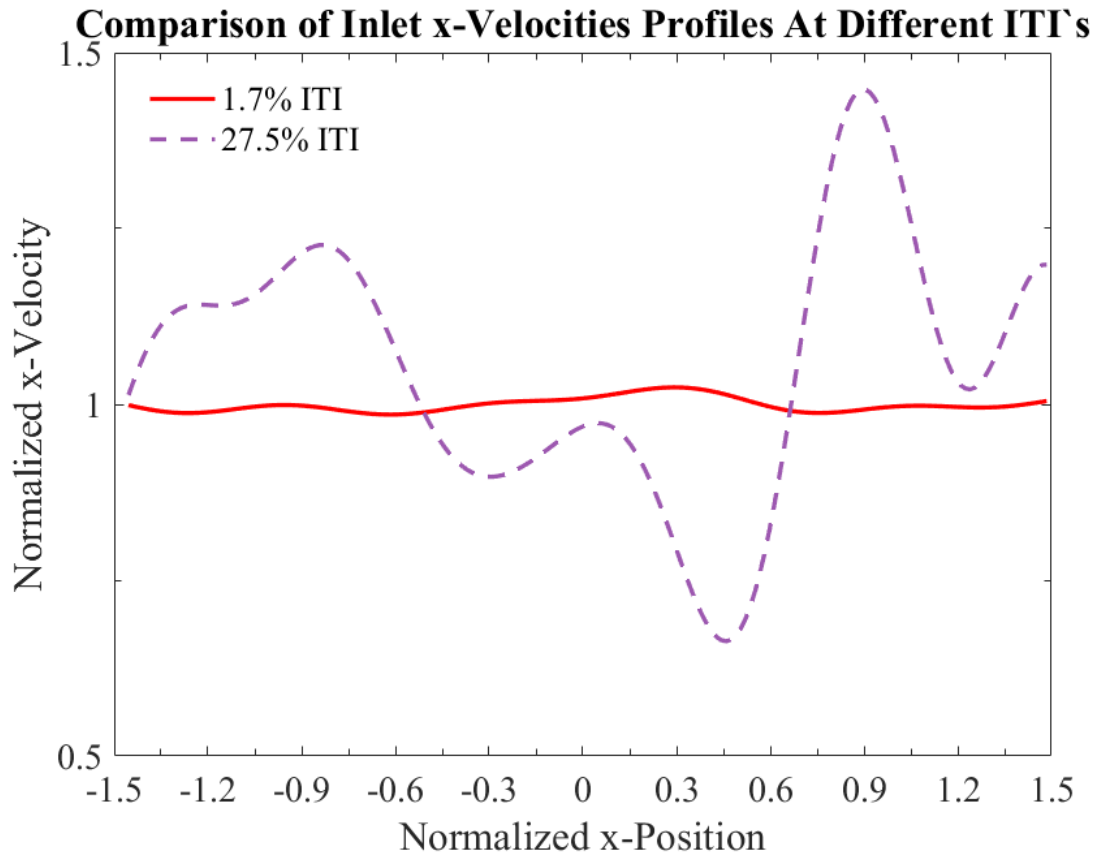


Figure 5.1: Comparison of instantaneous inlet velocity profiles for ITI=1.7%, red line, and ITI=27.5%, broken line. In both cases the mean velocity is set at 17.6 m/s

The impact of ITI is investigated for a reacting flow. But the effect can be first examined in the non-reacting case. Also, when the velocity contours are generated in the non-reacting case the impact of elevated ITI can be visibly noticed in the related contours 5.2. There are more perturbations in the inlet section of the computational domain. The maximum axial velocity is also 2 m/s higher in the case with higher ITI although in both cases the mean velocities are equal. Thus, if a flow field is affected by the interaction of vortical structure as in the flame, we can expect more effects of ITI.

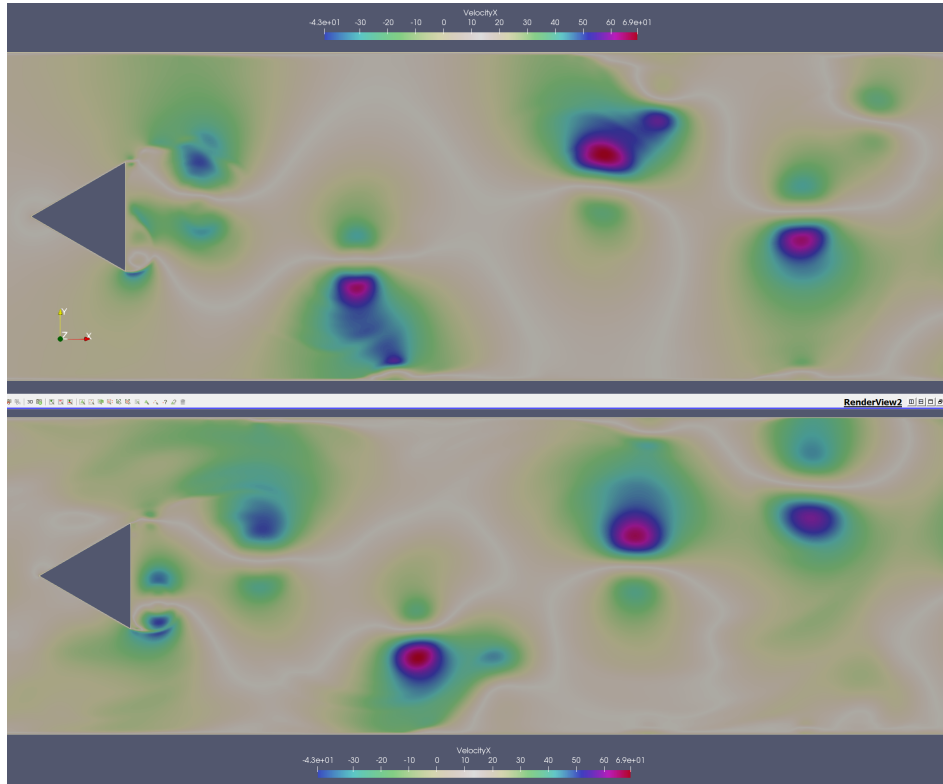


Figure 5.2: Comparison of instantaneous velocity contours for ITI=1.7%, top, ITI=27.5%, bottom, for non reacting cases. The vortex shedding phenomena are produced in both cases while the turbulent behavior is more dominant in higher ITI case as shown by the more intense vortices especially behind the bluff-body region.

In the following sections the effect of ITI on a flame is first investigated for a strong flame and then for flame near blow-off condition.

5.1 The Effect of Inlet Turbulence Intensity On A Strong Flame

The effect of ITI on flame structure is investigated with intensities of 0% to 10% in increments of 5%. In these cases, the coarse mesh is used when $\phi = 0.65$. All the numerical and physical models as well as operating and boundary conditions are identical except for ITI. Therefore, the differences seen are only caused by variation of the turbulence intensity at the inlet. The purpose of this investigation is to observe the effect that ITI will have on the flame structure.

In figure 5.3, the temperature contours are compared. The flame becomes more unstable as the

ITI is increased. This behavior is expected. The flame brush becomes wider and alternate vortex shedding leaves stronger traces in the flow field as ITI increases. This can be considered to be the leading cause of the blow out. A healthy flame depends on a stabilized zone where hot products of combustion heat up freshly entrained fuel-air mixture and cause them to burn, sustaining the flame. The increased turbulence leads irregular displacement of the flame fronts and distortion of heat transfer that supports combustion.

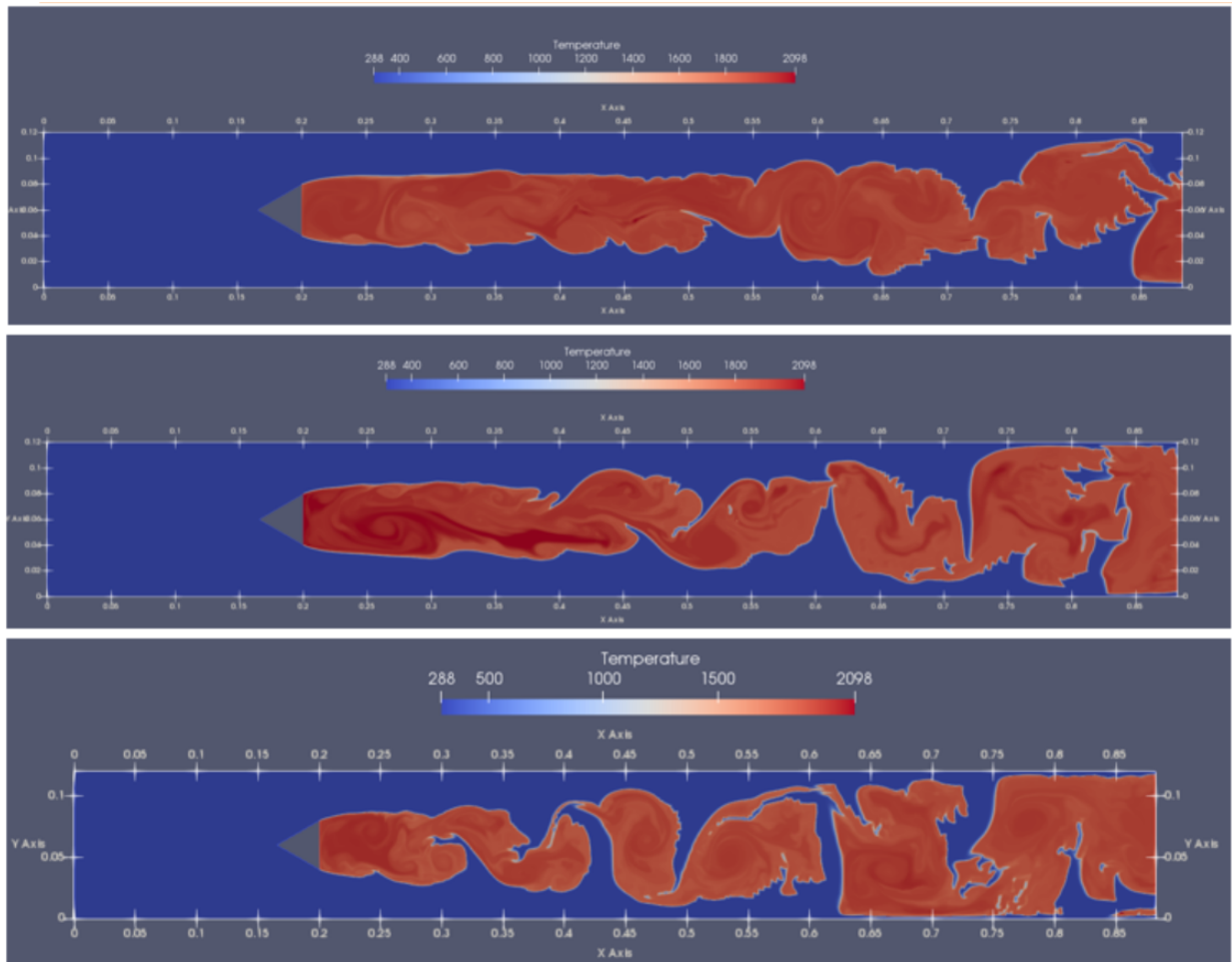


Figure 5.3: Effect of ITI on instantaneous temperature contour, top: ITI=0%, middle: ITI=5%, bottom: ITI=10%. The propane-air flame is at $\phi = 0.65$ and initial temperature of 288K operating at atmospheric pressure.

Figure 5.4 shows the flow field from the x-axis velocity perspective. It can be seen that the recirculation zone is shortened by increasing the ITI. The flame will be entrained into this zone.

This effect is considered to be the main reason for flow extinction [55]. But for a strong flame, this penetration will not cause a total extinction and the flame will persist in this condition with stronger vortex shedding effect downstream of the bluff-body as this figure demonstrates.

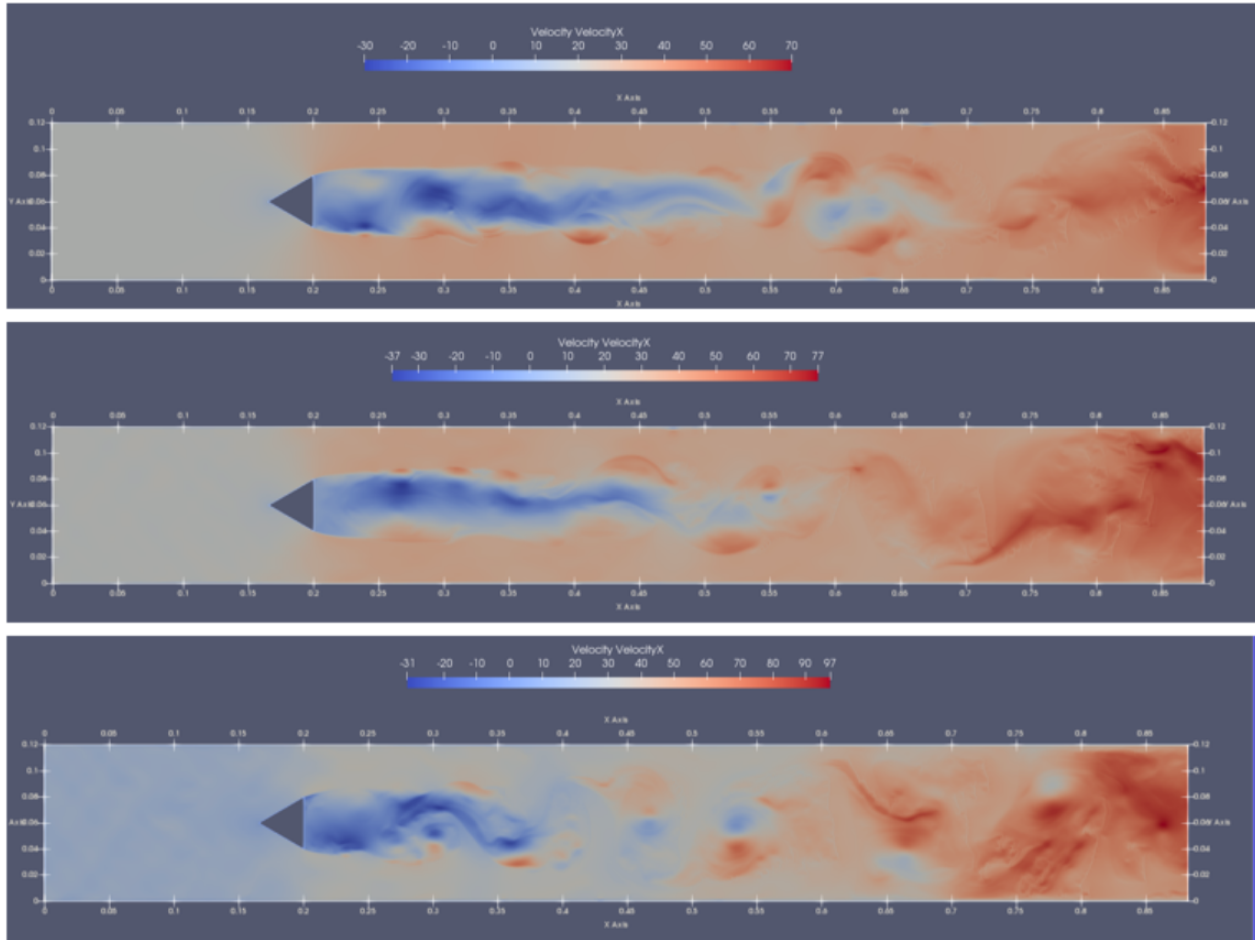


Figure 5.4: Effect of ITI on instantaneous velocity contour, top: ITI=0%, middle: ITI=5%, bottom: ITI=10%. The propane-air flame is at $\phi = 0.65$ and initial temperature of 288K operating at atmospheric pressure.

The turbulence effect can also be seen through vorticity. Figure 5.5 shows the comparison between vorticity magnitudes. More regions with stronger eddies are observed in the flow fields with higher ITI. The turbulence intensity at the inlet increases the overall turbulence level due to high Reynolds number flow. In a channel flow, the high turbulence at the inlet could decay as the flow progresses downstream. But the bluff-body and the stabilized flame cause the turbulence to manifest even further downstream. As seen here for the strong flame at $\phi = 0.65$, the turbulence is not yet linked

to blow-off.

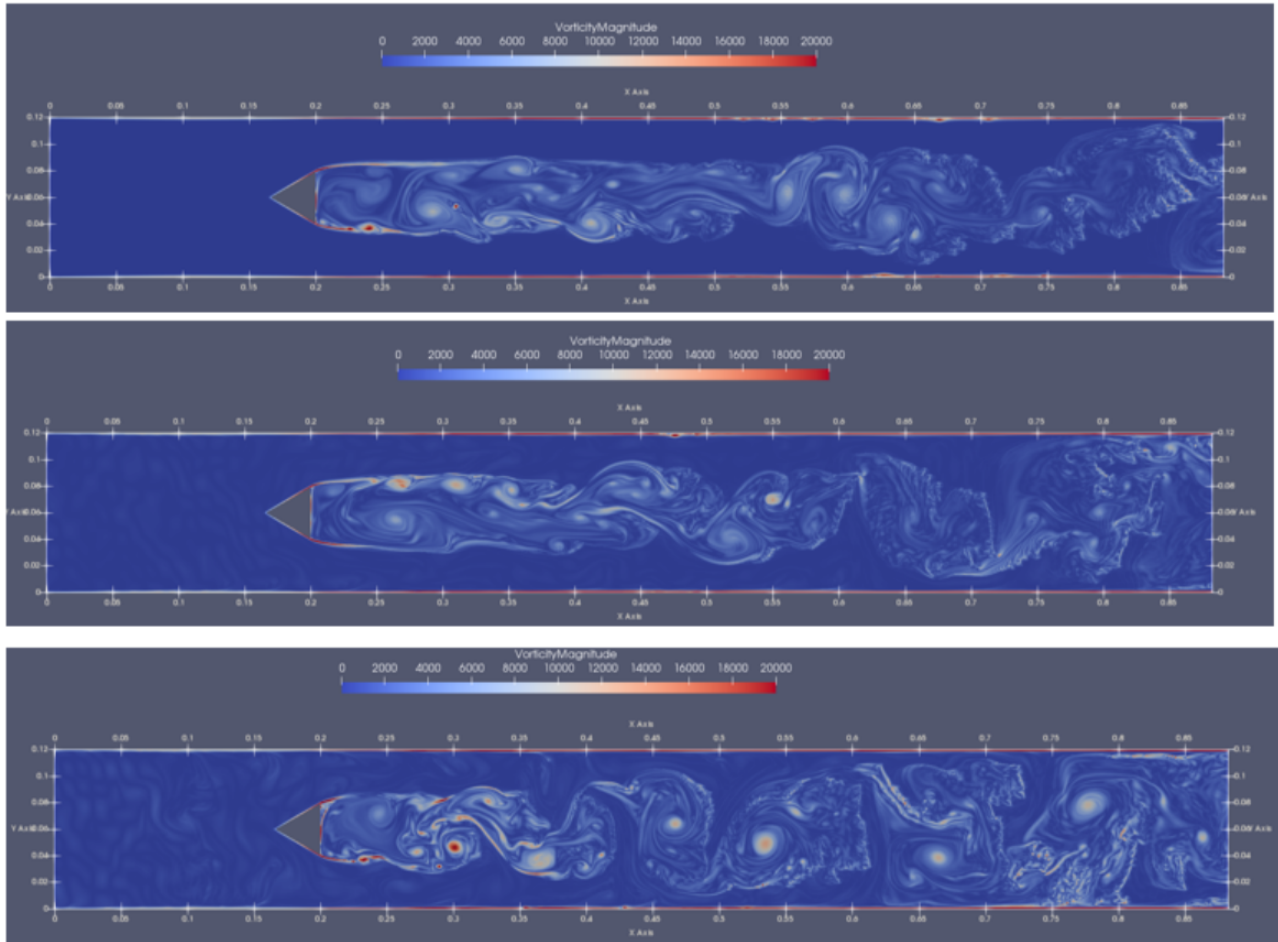


Figure 5.5: Effect of ITI on instantaneous vorticity contour at $\phi = 0.65$, top: ITI=0%, middle: ITI=5%, bottom: ITI=10%. The propane-air flame is at $\phi = 0.65$ and initial temperature of 288K operating at atmospheric pressure.

5.2 The Effect of ITI On Near Blow-off Flame

The effect of ITI on flame structure is investigated with inlet turbulent intensities of 0, 5, 10, and 15% at the near blow-off equivalence ratio of $\phi = 0.32$. The numerical methods, physical models, and all operating and boundary conditions except the ITI, are identical in these simulations. Therefore, the differences seen in the resulting contours and profiles, are solely due to the variation in ITI.

The effect of changing ITI can be visualized by measuring the sub-grid scale (sgs) turbulent viscosity

at the inlet. An example of the is figure 5.6. We observe that the amplitude of the sgs turbulent viscosity increases as the ITI is increased. The effect is also felt further downstream. This is to be expected given the functional definition of the turbulent viscosity.

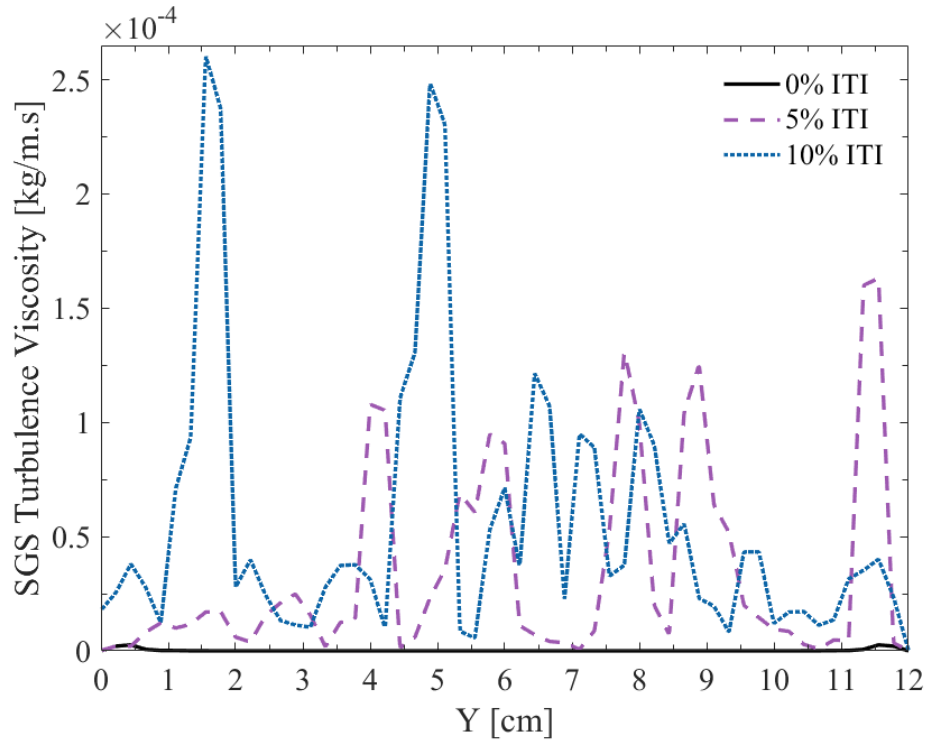


Figure 5.6: Effect of ITI on inlet sgs turbulent viscosity at different locations from the inlet. This is an instantaneous result, hence the variations in location of the peaks.

The effect of ITI on the flame structure can be also shown in terms of temperature distribution. An example of this visualization is Fig. 5.7 . It can be seen that the recirculation zone is shortened by increasing the ITI. In the absence of significant turbulence, the recirculation is mostly determined by the bluff-body effect on the flow field. With increasing degrees of turbulent, turbulent eddies from the inlet interact with the mixing layer and disrupt the recirculation flow. The entrainment of combustible mixtures into the recirculating flame also effects the total heat release in a manner that can affect blow-off.

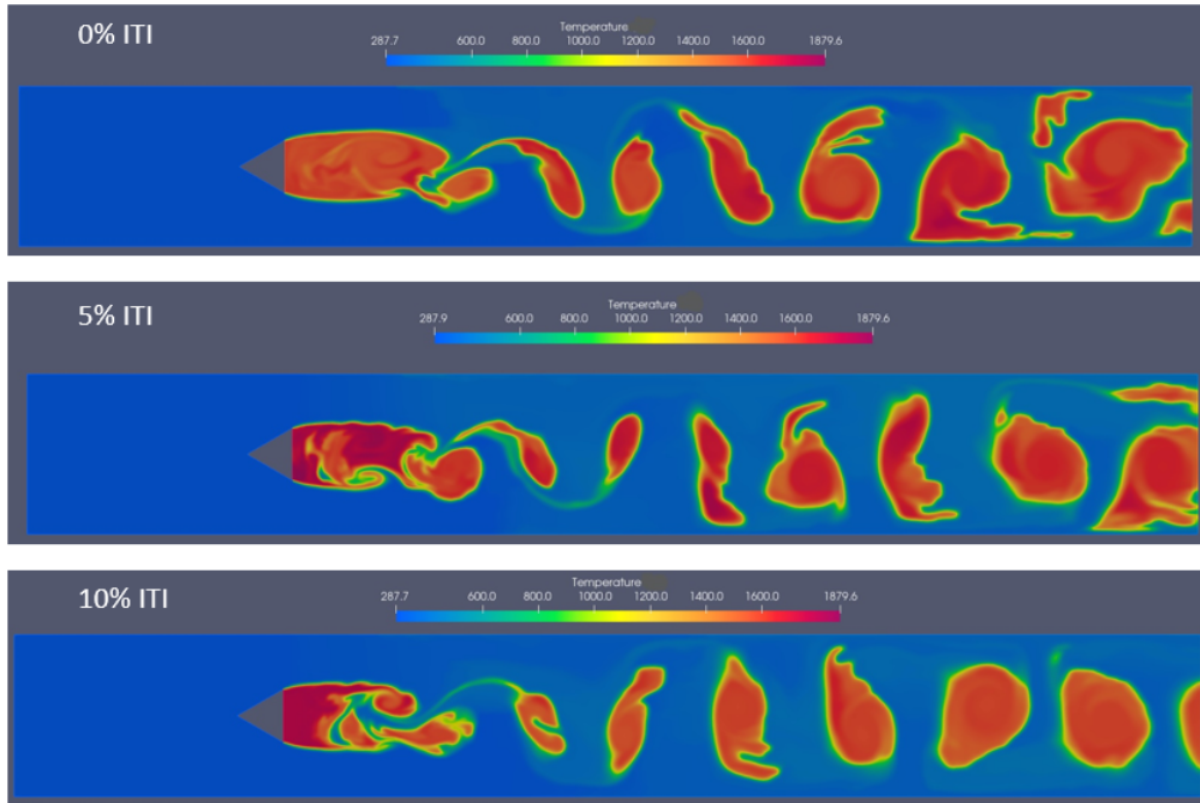


Figure 5.7: Effect of ITI on recirculation zone as seen in temperature contours. Increased ITI shortens the recirculation zone. This affects the heat release and strength of the flame.

A key result from this study is the non-linear trend of turbulence effect on blow-off. The effect of increasing ITI on the lean flame is not always toward the deterioration of the flame. It is observed that while the ITI of 5% causes blow-off, further increasing ITI to 10% preserves a healthy flame. This is mostly because of greater heat release arising from greater and balanced entrainment of combustible mixtures into the flame zone just behind the bluff-body.

We generally expect that increasing ITI should lead to blow-off. But this intuition fails to consider the additional heat release that results from enhanced entrainment into flame. This enhancement of the burning process is not to be expected over wider range of ITI. We therefore see that this balanced stabilization is again lost as the ITI is further increased to 15%. In another word, as ITI is increased from 5%, where the flame is extinguished, to 10%, the flame survives. This is initially not expected since the increasing of ITI should increase the effect of alternate vortex shedding which

is the main cause of flame blow-off. Indeed, by increasing the ITI to 15% the flame recirculation shrinks and eventually blows off. Therefore, for the case of ITI=10% there should be a mechanism which causes an optimal balance between turbulent disruption of the stabilized flame and chemical heat release dynamics, causing the flame stay lit at this condition. This phenomenon will be further discussed in the next section. But in essence, Fig. 5.8 demonstrates the non-linear trend of ITI causing flame blow-off at 5% and 15% while flame survives over a long period at ITI of 10%.

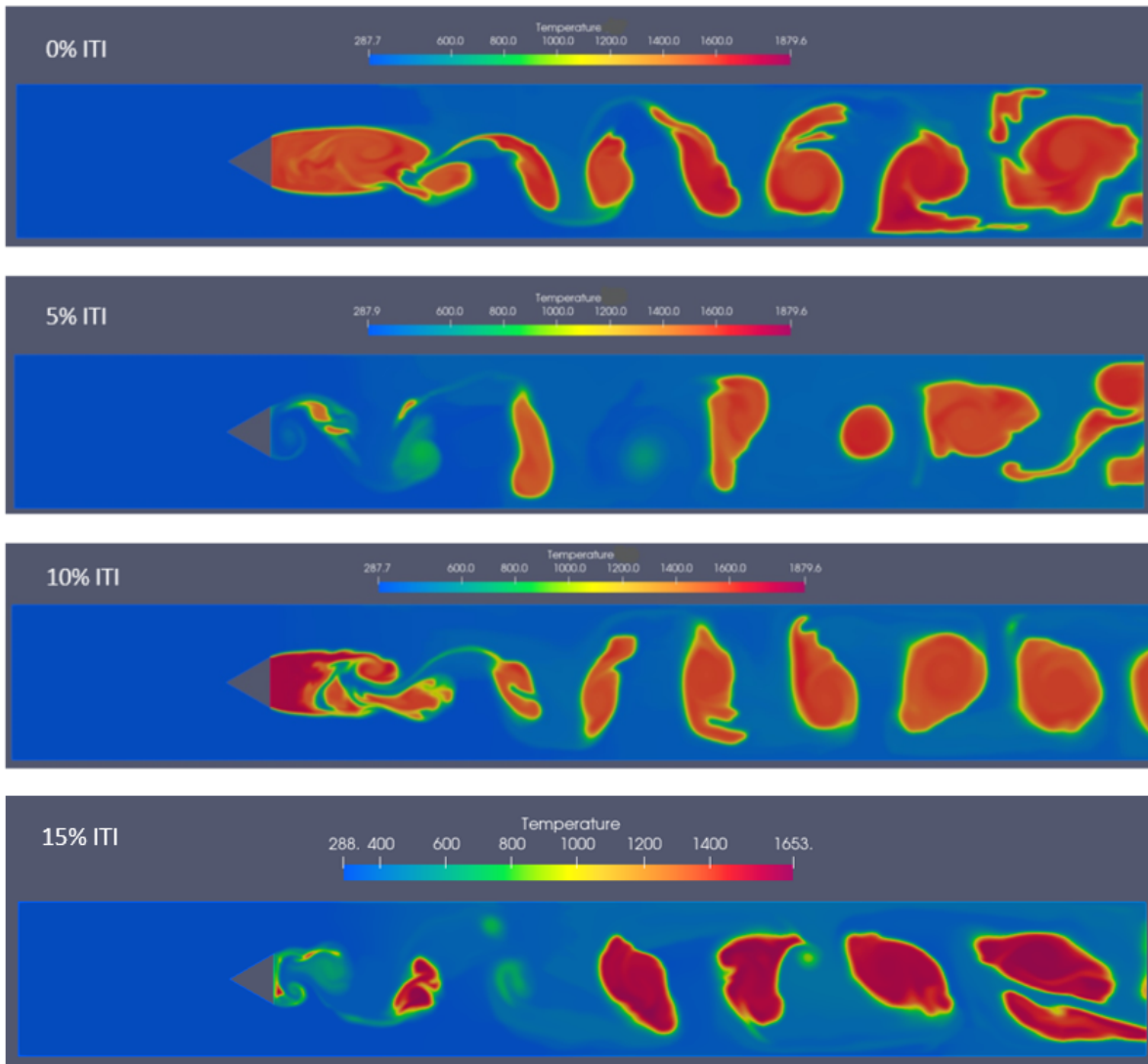


Figure 5.8: Blow-off caused by varying the ITI - temperature contours. flame extinguishes for ITI of 5% but survives at 10%

5.2.1 Effects of ITI On A Lean Flame Using 2D LES And 1-step chemistry vs. Detailed Chemistry

The above results on the effect of ITI on a near blow-off flame are obtained using an elaborate chemical kinetic scheme. This is a skeletal kinetic model with 43 species and 188 reactions. To understand the impact of chemical kinetics in blow-off process prediction of the numerical simulation we have conducted two types of simulations in 2D with the same mesh quality, operating and boundary conditions, as well as the same numerical models. The only difference between these two cases is the chemical kinetics, one is a global chemistry model and the other is a detailed(skeletal) chemistry model. For the global chemistry, after establishing the flame at an equivalence ratio of 0.65, the fuel-to-ratio is gradually decreased to the already established near blow-off equivalence ratio of 0.32. The flame is allowed to run at this condition in order to observe the dynamical differences related to the differences in chemical kinetics with respect to varying inlet turbulence intensity levels.

It is initially deemed that this computationally costly scheme is necessary for the prediction of kinetically sensitive processes such as flame blow-off. But there is no formal investigation justify the use of the more elaborate chemical scheme over the use of a global reaction model. We, therefore, contrast these two combustion chemistry approaches here. We do so by considering the effect of ITI on near blow-off flame using a one-step chemical kinetic model. If this model were to be found predictive enough it would significantly reduce computational cost for analysis of stabilized flame blow-off.

As was shown earlier, detailed chemistry is capable of capturing non-linear relation between ITI and flame blow-off behavior similar to the results obtained from previous experimental results obtained by Cetegen et al. [3, 17]. However, when a similar parametric study was conducted with global chemistry which neglect the crucial elementary reactions, the non-linearity effect of ITI on the flame blow-off is not fully observed. Our numerical results shows that by increasing ITI, the flame still

goes into blow-off and as ITI is increased the flow time needed for blow-off.

Our data shows that the blow-off time with 5%, 10%, and 15% are 1.31s, 1.34s, and 0.85s, respectively. As a result the global chemistry is not capable of fully capturing the non-linearity effect and at 10% it only extends the blow-off time relative to the blow-off time for the detailed chemistry at 5% ITI.

Therefore, with the detailed chemistry model, the non-linearity is well captured as the flame blows-off 660ms after ignition with 5% and does not show any signs of blow-off at ITI of 10% even 80ms after the blow-off occurs (with global chemistry at 10% ITI the flame extinguished 34ms after flame extinguished at 5% ITI). The comparison of results obtained from these two chemical kinetics at near blow-off condition is illustrated in figure 5.9.

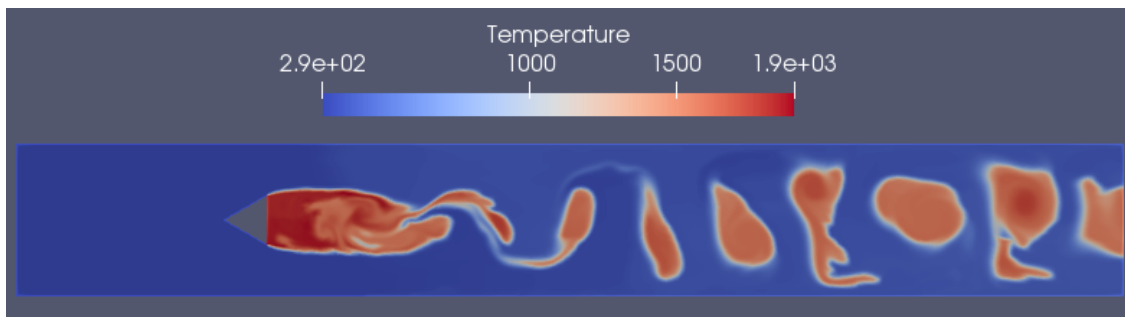


Figure 5.9: Flame with detailed chemistry survives with ITI=10% even 80ms after the blow-off time with 5%. With global chemistry with 10% ITI the flame blew off 34ms later than the blow-off with 5% ITI.

To ensure that the non-linearity result is completely captured with detailed chemistry we continue our numerical work by increasing the incoming turbulence intensity to 15%. It was observed that the flame blows off again at this condition only after 720ms. Therefore, with detailed chemistry the results and the non-linearity trend can well be captured as this non-linearity behavior was observed in the experimental research conducted by Cetegen et al. [3].

The numerical analysis also shows another difference between the quality of the results obtained from these two chemical kinetics which underscore the role of detailed chemistry. Let us consider

the case of ITI of 5%. Figure 5.10 shows the temperature contours obtained with global and detailed chemistry at different times. The results of detailed model show that flame blow-off is evident at about 660ms. In contrast, we see that the global chemistry model shows a healthy flame operational at 900ms. We could wrongly conclude on the basis of this simplified modeling that the flame does not blow off. This would be a hasty conclusion as it is confirmed that flame eventually goes into extinction at 1.34s for the global chemistry simulation. We can, therefore, say that the use of the detailed chemistry leads to a faster response of the flame that in turns determines the fate of the flame and the sensitivity analysis of flame with response to variation of inlet turbulence intensity.

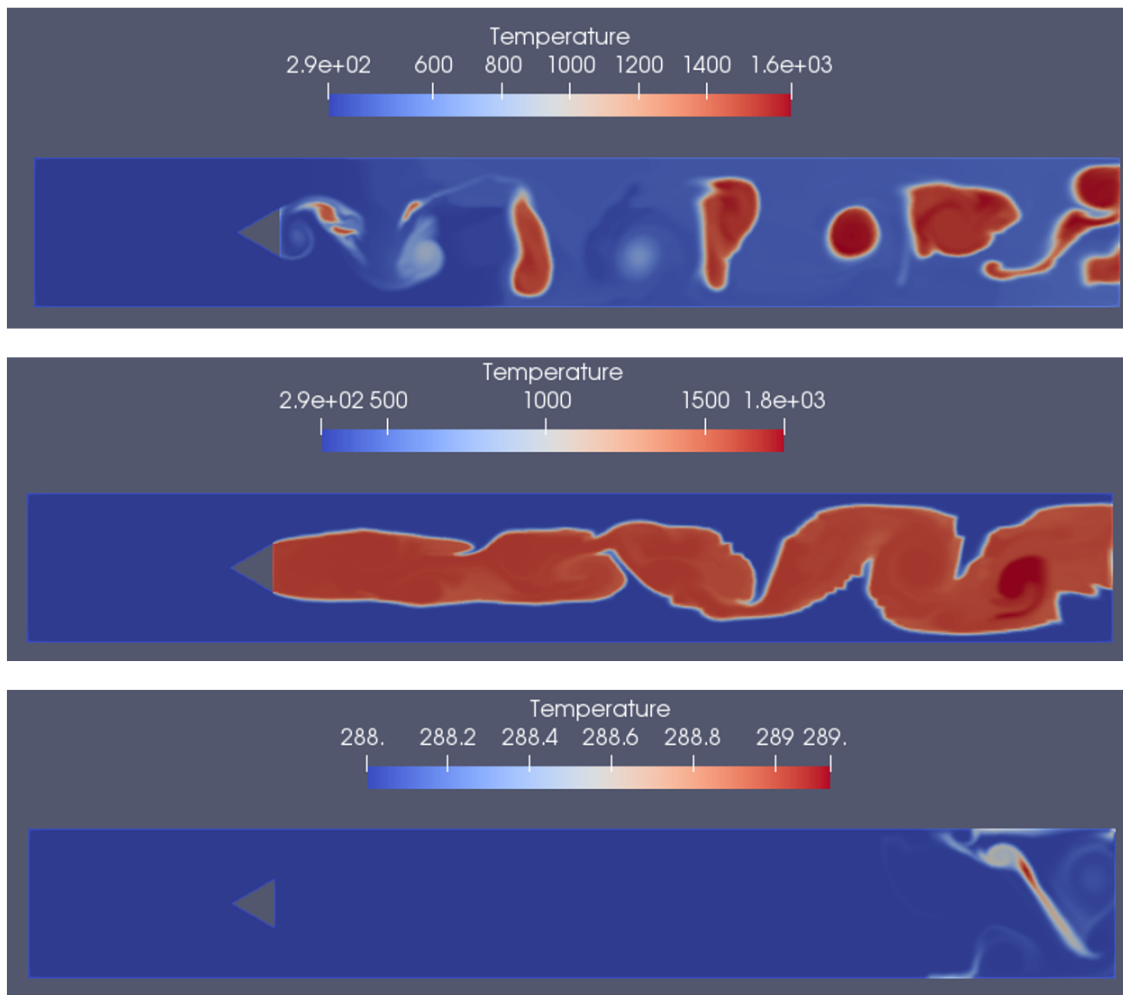


Figure 5.10: Chemical kinetic impact analysis on flame blow-off prediction. Top:detailed chemistry at t=660ms of flow time, middle:no signs of blow-off at t=900ms of flow time with one-step chemistry, bottom:one-step chemistry at t=1.36s of flow time

Therefore, two observations from our numerical simulation need further analysis and explanation. First, the fact that the flame does eventually blow off for the global chemistry case at 10% ITI and second, the difference in time for blow-off between detailed and global chemical kinetics.

The global chemistry failure to capture the non-linearity behavior can be explained as follow. With global chemistry the effect of mixing and entrainment of products into the recirculation zone, which can cause flame stability at certain conditions, is not accounted for due to the absence of elementary reactions which generates radicals that can help sustaining the flame. In other words, our results prove that blow-off in 1-step chemistry is purely a turbulence event and the chemical kinetics has minimal effect in this prediction. The thermochemical effect of flame temperature is controlled by equilibrium thermodynamics, not chemical kinetics.

With detailed chemistry, on the other hand, when the ITI is increased from 5% to 10% although the perturbation of the incoming mixture increases as it was shown earlier causing more sinusoidal flapping of the flame which in turns increase the local flame shear layer stretch causing local flame extinction at the same time it enhances mixing of the products and reactants causing preheating of the reactants. The increasing temperature of reactants and the distribution of hydroxyl in the reaction zone at certain inlet turbulence intensity can lead to a sustainable flame as demonstrated in the results with detailed chemistry at 10% ITI. At the same time the preheating of the reactants can help overcome the activation energy needed to trigger the elementary reaction related to the release of hydroxyl.

Figure 5.11 shows the profile of hydroxyl concentration behind the bluff-body with different level of inlet turbulence intensities.

As it can be seen the level of OH concentration is an order of magnitudes higher with 10% ITI than 5% and 15%. The higher level of OH is associated with flame sustainability as OH is a highly active radical that participates in chain initiation and chain branching reactions causing ignition and propagation of the flame. The high level of OH concentration with 10% can be justified by a balance

between mixing and preheating of the reactants. This can initiate the elementary reactions with relatively low activation energy. This leads to the generation of active radicals such as hydroxyl. The formation of OH produced positive feedback to the combustion process and generates more initiating radicals.

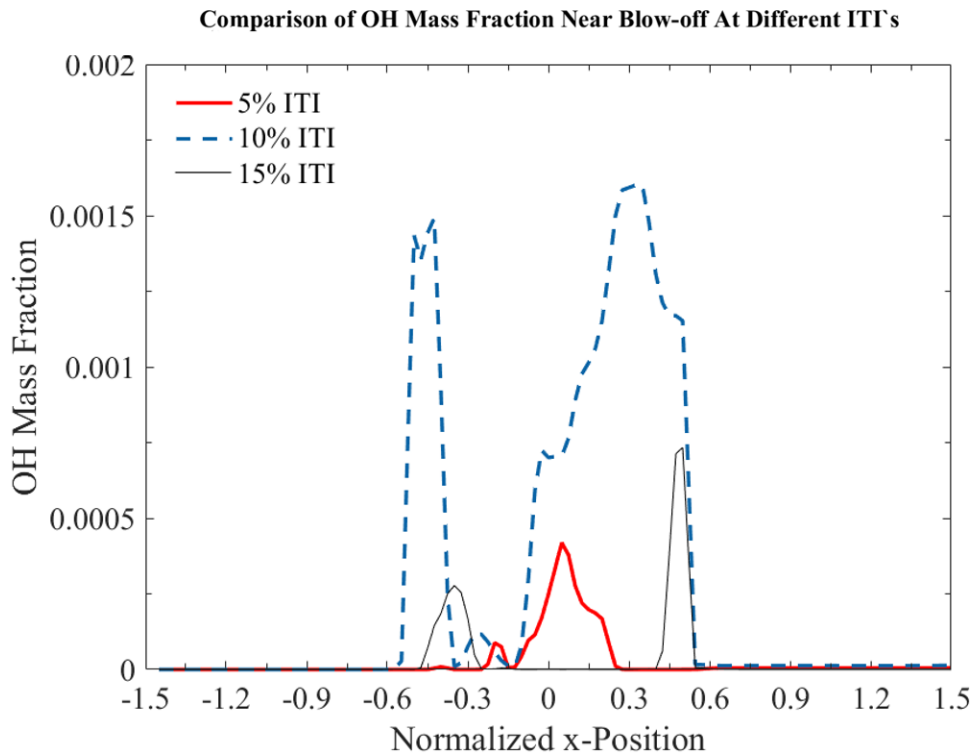


Figure 5.11: At ITI=10% more heat release is evident behind the bluff-body by higher concentration of hydroxyl (OH) compared to ITI = 5% and 15%

The balance between the effect of preheating of the reactants and the asymmetrical vortex shedding is again lost at higher ITI with the effect of asymmetrical vortex shedding becomes more dominant causing disappearance of active radicals in the recirculation zone and eventual flame blow-off. These elementary reactions are not accounted for in global chemical model and therefore no radicals such as OH produced to sustain the flame at 10% ITI causing the flame dynamics to be dominated by turbulence.

Regarding the differences in blow-off time prediction, the detailed chemistry is able to track the

real behavior of the flame better than the global chemistry. Elementary reactions and the mixing of radicals contribute to the flame when increased turbulence changes the mixing and promotes heat loss through gradients. The detailed chemistry reacts first through radicals and elementary reactions. The global chemistry, on the other hand, is slower to react since it does not invoke the elementary reactions with lower activation energy. The eventual blow-off of the global chemistry case is purely thermochemicals given the high temperature at the flame front. The global reactions simply act as a switch to transition the flame from unburned to burned states. Increased turbulence mostly promotes mixing of unburned mixtures with flame products but when distortions of the flame finally lead to excessive heat loss, the flame does take the effect elementary reactions into account and it blows off. Thus, it is not possible to accurately predict the effect of ITI on a bluff-body flame based on global chemistry models.

5.3 Implication of ITI Effect On Blow-off

We need to consider the broader implications of our results on the effect of ITI on near blow-off stabilized flames. Depending on the length of inlet section, the effect of inlet turbulence intensity can be felt differently on the flame. This is due to damping by the viscosity of the flow which lessens the vortex intensity of incoming mixture. Although the effect of initial sgs turbulence viscosity can be damped out before entering the combustor segment, there will be residual turbulence that is strong enough to change the structure of a lean flame. This turbulence field upstream and downstream of the combustion is illustrated in Fig. 5.12.

By further increasing the ITI, smaller and narrower recirculation appears until the expected flame extinction occurs. This is not always the case. As the simulations have shown, we observed that at 5% ITI, blow-off occurs while at 10% the flame survives. We further increased the ITI to 15% and observed that the flame once more extinguishes. The reason for this phenomenon can be explained that at 10% ITI a sort of balance happens between more effective mixing where the entraining flow at the end of the recirculation zone becomes preheated before ignition and that causes higher

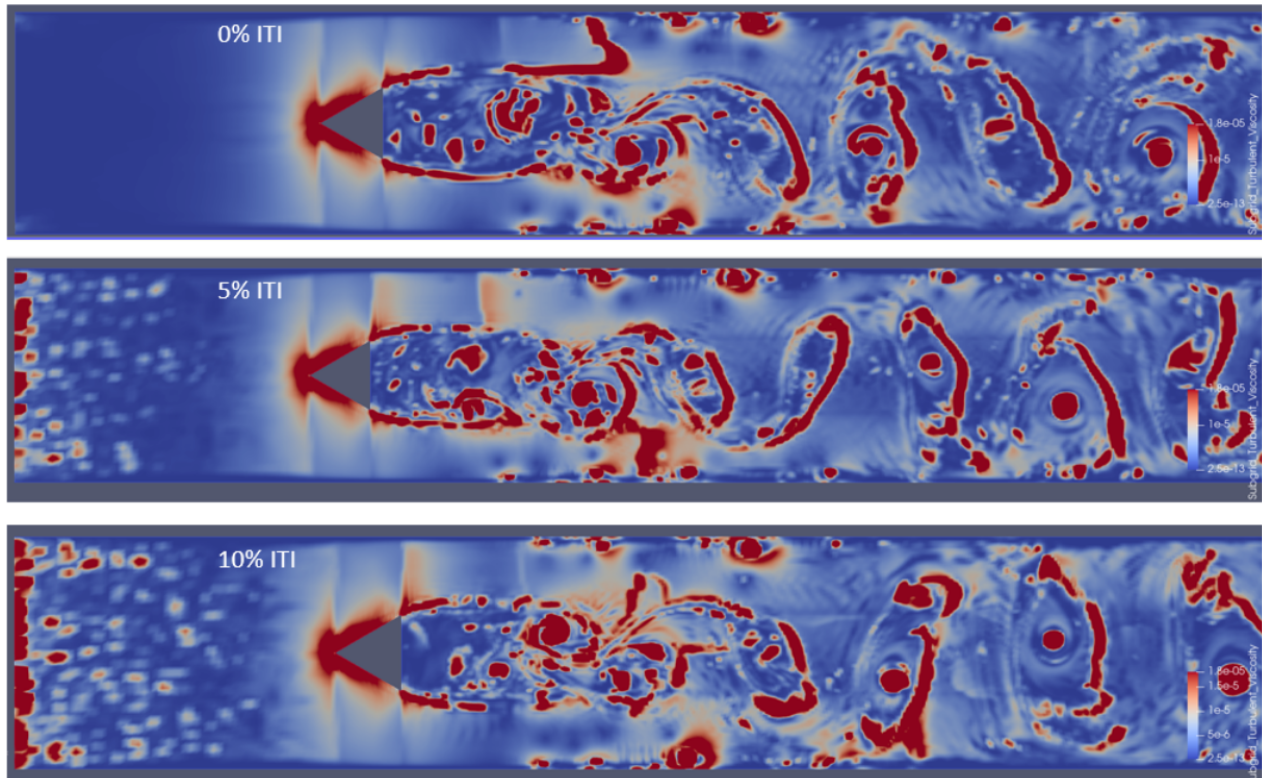


Figure 5.12: Effect of ITI on sgs turbulence viscosity in the flow field. Shown is the field of turbulent viscosity at 0%, 5%, and 10% from top to bottom.

flame temperature. This balance of preheating which leads to a stronger flame and the effect of vortex shedding become tuned at 10% ITI such that they prevent the flame blow-off. At 5% or 15%, however, the effect of vortex shedding dominates the effect of increased turbulence viscosity which leads to eventual flame blow-off. This phenomena can be observed by taking the flame temperature for these cases, see figure 5.13. The profile is taken along the 2D duct at 1 cm behind the bluff body. It is seen that increasing the ITI also increases the flame temperature that can be caused by stronger eddies downstream of the recirculation zone at the wake zone. But the highest temperature increases is for 10%, correlating with the healthier nature of the flame at 10%.

In order to validate our argument, we have generated a profile of vorticity magnitude in the recirculation region at 1 cm behind the bluff body. This is shown in figure 5.14. The dotted purple (5% ITI) shows higher values comparing to the other two profiles. This means that when the ITI is increased, the effect of increasing turbulent velocity is suppressed at certain level of ITI. In the

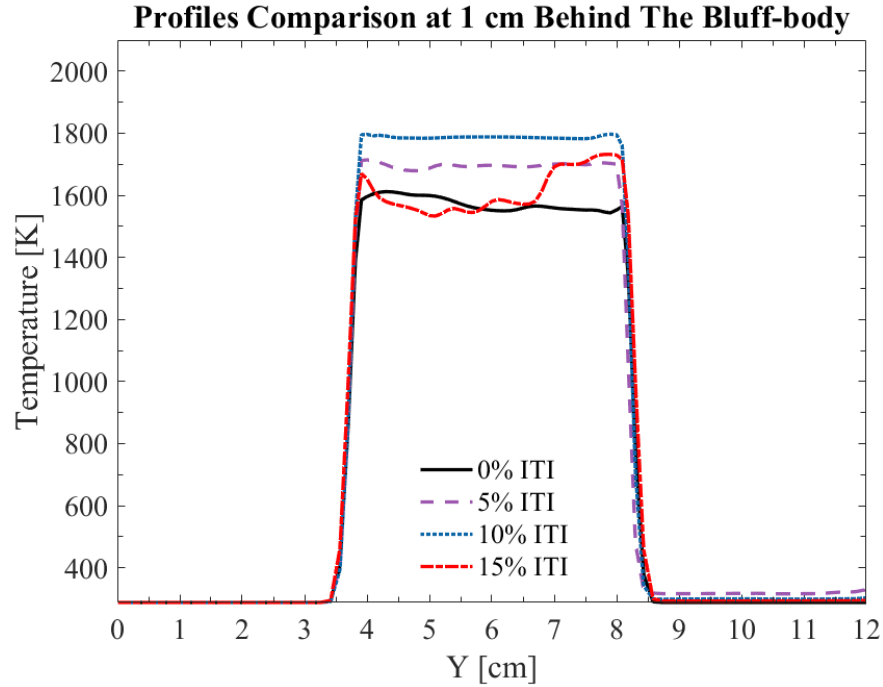


Figure 5.13: Effect of elevated ITI on the flame temperature. the profile is taken 1 cm behind the bluff body

same figure with the blue solid line (10% ITI) all fluctuations observed in the flow with 5% are absent when the ITI is increased. As explained, this can be related to pre-heat of the fuel-air mixture and the consequent higher flame temperature.

The results of this study have practical implications for the design of bluff-body stabilized flames and for computational analysis of combustion.

With respect to practical design of the bluff-body stabilized flames, the key findings of non-linear response to ITI is interesting. It means that inlet turbulence can be used at near blow-off to stabilize the flame. This expands the range of equivalence ratios that can be used to obtain low NOx emissions from flames while retaining flame stability. This is the direction of future combustion systems that seeks to meet more stringent NOx emission regulations.

Although we have established that higher ITI can rescue a near blow-off flame from extinction, we have not completely established the conditions and limits within which ITI enhances burning

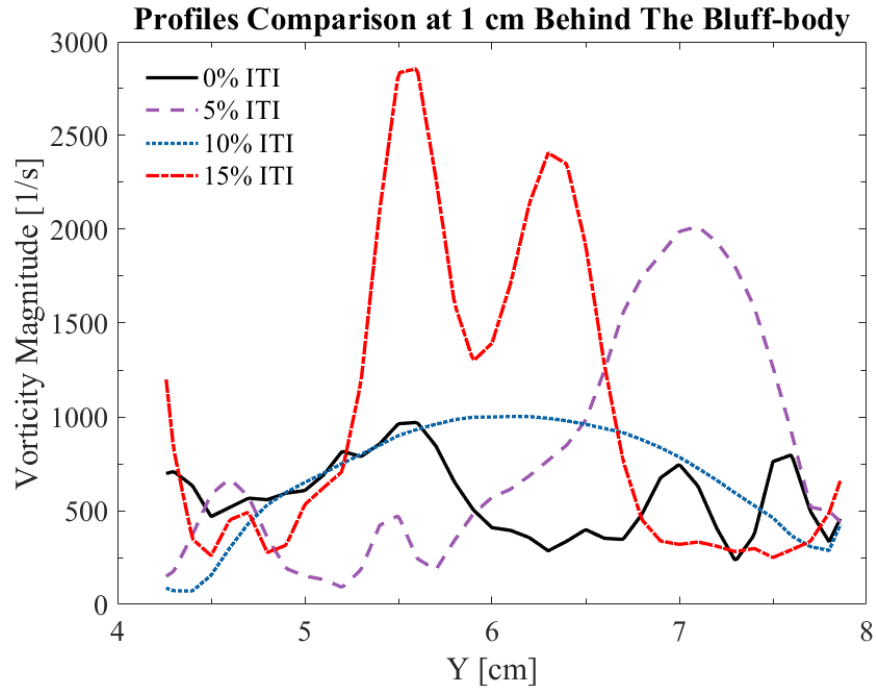


Figure 5.14: Vorticity magnitude 1 cm behind the bluff body at three different ITI's

and outside which a flame is blown out. This precision can best be established through combined computational study and experiments. The fuel type, unburnt flame temperature, pressure, flow velocity, and geometry of the bluff-body can affect the actual range of ITI over which a flame survives turbulent perturbations. What can be observed from this work is that turbulence, mixing, and the equivalence ratio affect the size of the recirculation zone and the strength of the flame.

With respect to implication of these ITI influences for computational analysis, some limits are imposed on the simplifications that can be applied to the 3D turbulent reacting flow. While the assumption of 2D behavior is reasonable, at critical conditions that depend on the balance of competing affects, some details may be lost in 2D compared to 3D simulations.

With respect to the use of a simple one-step reaction model, the critical phenomenon of blow-off shows the inability of this model to capture the onset of blow-off. The heat release that is controlled by equilibrium thermodynamic can ultimately establish that a flame will extinguish in most conditions. This one-step chemistry cannot, however, capture kinetics of blow-off. The

reaction rate may also be turned to appear mixing controlled, thus falsely predicting flame survival.

These results were based on the assumption that the blow-off equivalence ratio of 0.30 is physically reasonable. In reality, this critical ratio depends on computational methods, mesh, and models. Experimental blow-off equivalence ratio of the flame with 0% ITI may be higher than this value of 0.32. However, the trends established can be expected to hold for experimental flames with higher blow-off equivalence ratios. This is so because the trends depend on the balance of general flame features such as entrainment, recirculation, heat release rate, and total heat release confirmed by experimental results pertained to the study of non-linearity effect of ITI on the stabilized flames. With these limits in mind, the current study points to further computational studies of bluff-body flame response to ITI.

Conclusion and outlook

The main purpose of this research was to investigate the effect of boundary conditions, namely inlet turbulence intensity, on a near blow-off premixed turbulent flame stabilized by a triangular bluff body. Experimental data to validate the results pertinent to boundary condition effects are rare. Nonetheless, it was necessary to justify the choice of methods and models for this study. Therefore, a unique methodology was developed for this investigation as follows:

- The set of models and solution methods were validated against experimental result by conducting a numerical analysis with the same boundary and operating conditions at which the experiment was conducted. This is done in 3D computational domain. The Volvo Flygmotor experimental data were used as validation target. The choice of methods and models included the analysis of mesh sensitivity.
- Since the work involved parametric studies, computational cost needed to be minimized choosing 2D LES over 3D LES. The use of 2D LES needed to be justified by comparatively establishing the dominant 2D nature of the flow.
- The Volvo Flygmotor experiment was successfully validated and the combination of models and methods were used to further study the effects of inlet turbulent intensity on a near blow-off flame.

- The blow-off equivalence ratio was established by starting from the validation equivalence ratio of 0.65 and decreasing gradually until blow-off was attained. The equivalence ratio of 0.30 was found and the equivalence ratio of 0.32 was taken as the near blow-off equivalence ratio. The sensitivity of the near blow-off equivalence ratio to ITI and choice of combustion chemistry model was then investigated.

Two main types of conclusions were reached. One type relates to the simplification of the complex reacting flow problem for cost effective computational analysis. The other type relates to the sensitivity of near blow-off flame to ITI.

With respect to the acceptable simplification of the bluff-body stabilized flame, the following conclusions have been established:

- Because of the structure of the bluff-body stabilized flame, a 2D simplification can capture the key dynamics without loss of accuracy, compared to 3D. This is specially true for a strong flame such as the validation case. The reason for this is that the channel flow and recirculation is predominantly 2D and that the 2D LES formulations is robust enough to track vortical structure.
- With respect to the choice of a combustion chemistry model, a on-step global model can capture the dynamics of a strong flame such as that at $\phi=0.65$. At the leaner near blow-off condition, however, this one-step model predicts a stable flame than the more realistic case of detailed chemical kinetics. The simple one step reaction model cannot therefore be relied on deciding the sensitivity of flames at near blow-off conditions. The reason for the failure of the global chemistry model is its lack of radicals and multi-step reactions that can capture the effect of turbulence on the mixing layer.
- With respect to the sensitivity of the near blow-off flame to ITI, a key finding is that increasing ITI initially leads to blow-off. But at a higher ITI, the balance of entrainment and turbulence modification of the recirculation zone can lead to a stronger flame that resists blow-off. At

yet higher ITI, the flame blows off as expected. The reason for this non-linear behavior is the possibility of creating zones of larger pockets of combustible mixtures pre-heated to higher temperatures and releasing more heat. More intense turbulence can disrupt this balance and still lose stability. The observed non-linear response of the near blow-off flame is in agreement with experimental observation by Cetegen, [3, 17].

This computational confirmation of this behavior motivates further research to accurately establish the conditions for these different responses. The demonstrations of the strength of 2D LES and the limits of the one-step chemistry model can further guide intensive parametric studies toward cost-effective simulations of bluff-body stabilized flames.

Bibliography

- [1] E. I. Administration. “World energy outlook 2018”. In: (). URL: <https://www.eia.gov/>.
- [2] A. Sjunnesson, C. Nelson, and E. Max. “LDA measurements of velocities and turbulence in a bluff-body stabilized flame”. In: *Volvo Aero Technical Report S-46181* (1991).
- [3] B. Chowdhury and B. Cetegen. “Experimental study of the effects of free stream turbulence on characteristics and flame structure of bluff-body stabilized conical lean premixed flames”. In: *Combustion and Flame* 178 (2017), pp. 311–328.
- [4] E. Zukoski. “Flame stabilization on bluff bodies at low and intermediate Reynolds numbers”. PhD thesis. 1954.
- [5] E. Zukoski and F. Marble. “The Role of Wake Transition in the Process of Flame Stabilization in the Bluff Bodies”. In: *Researches and Reviews, Butterworth Scientific Publishers, London* (1955), pp. 167–180.
- [6] E. Zukoski and F. Marble. “Experiments Concerning the Mechanism of Flame Blowoff from Bluff Bodies”. In: *Gas Dynamic Symposium on Aerothermochemistry, Northwestern University* (1956), pp. 205–210.
- [7] S. Fujii and K. Eguchi. “A comparison of cold and reacting flows around a bluff-body flame stabilizer”. In: *Journal of Fluid Engineering* 103 (1981), pp. 328–334.
- [8] S. Sanquer. “Experimental Study of a Bluff Body Wake, in Presence of Combustion, in Fully Developed Turbulent Channel Flow. Turbulence Scales and Critical Analysis of Transport and Combustion Models”. PhD thesis. 1998.

- [9] B. Kiel, K. Garwick, and J. Gord. "A detailed investigation of bluff body stabilized flames". In: *AIAA 2007-0168* (2007).
- [10] A. Chaparro and B. Cetegen. "Blowoff characteristics of bluff-body stabilized conical premixed flames under upstream velocity modulation". In: *Combustion and Flame* 144 (2006), pp. 318–335.
- [11] R. Blanchard and A. Wickersham. "Simulating Bluff-Body Flameholders: On the Use of Proper Orthogonal Decomposition for Combustion Dynamics Validation". In: *Journal of Engineering for Gas Turbines and Power* 136 (2014).
- [12] L. Hua-Guang, M. Dong-Jun, and H. Ying. "Large Eddy Simulation of Combustion Dynamics of Bluff Body Stabilized Flame". In: *AIAA 2011-783* (2011).
- [13] J. Cambala. "Large Structure in the far wakes of 2-dimensional bluff bodies". PhD thesis. 1984.
- [14] T. Lieuwen and S. Shanbhogue. "Dynamics of bluff body flames near Blowoff". In: *AIAA* 169 (2007).
- [15] S. Shanbhogue, S. Husain, and T. Lieuwen. "Lean blow-off of bluff-body stabilized flames: scaling and dynamics". In: *Progress in Energy and Combustion Science* 35 (2009), pp. 98–120.
- [16] H. Li, H. Sung, and V. Yang. "A Large-Eddy-Simulation Study of Combustion Dynamics of Bluff-Body Stabilized Flames". In: *Combustion Science and Technology* 188 (2016), pp. 92–952.
- [17] B. Chowdhury and B. Cetegen. "Effects of free stream flow turbulence on blow off characteristics of bluff-body stabilized premixed flames". In: *Combustion and Flame* 190 (2018), pp. 302–316.
- [18] R. Erickson and M. Soteriou. "The influence of reactant temperature on the dynamics of bluff body stabilized premixed flame". In: *Combustion and flame* 158 (2011), pp. 2441–2457.
- [19] I. Porumbel and S. Menon. "Large Eddy Simulation of Bluff Body Stabilized Premixed Flame". In: *AIAA-44th* 152 (2006).

- [20] C. Nottin, R. Knikker, and D. Veynante. “Large Eddy Simulations of an Acoustically Excited Turbulent Premixed Flame”. In: *Proceedings of The Combustion Institute* 28 (2000), pp. 67–73.
- [21] C. Fureby. “A computational study of combustion instabilities due to vortex shedding”. In: *Proceedings of the Combustion Institute* 28 (2000), pp. 783–791.
- [22] E. Hodzic, M. Jangi, and X. Bai. “Large eddy simulation of bluff body flames close to blow-off using an Eulerian stochastic field method”. In: *Combustion and Flame* 181 (2017), pp. 1–15.
- [23] A. Prasad and A. Williamson. “The instability of the shear layer separating from a bluff body”. In: *Journal of Fluid Mechanics* 333 (1997), pp. 375–402.
- [24] P. Cocks, M. Soteriou, and V. Sankaran. “Impact of numerics on the predictive capabilities of reacting flow LES”. In: *Combustion and flame* 162 (2015), pp. 3394–3411.
- [25] B. Emerson, J. O’Connor, and T. Lieuwen. “Density ratio effects on reacting bluff-body flow field characteristics”. In: *Journal of Fluid Mechanics* 706 (2012), pp. 209–250.
- [26] T. Poinso and D. Veynante. *Theoretical and Numerical Combustion*. Third ed. CNRS, 2011. ISBN: 2746639904.
- [27] R. Ryden, L. Eriksson, and S. Olovsson. “Large eddy simulation of bluff body stabilised turbulent premixed flames”. In: *ASME International Gas Turbine and Aeroengine Congress and Exposition* Cincinnati, OH (1993), May.
- [28] C. Fureby and S. Moiled. “Large Eddy Simulation of Reacting Flows Applied to Bluff Body Stabilized Flames”. In: *AIAA paper* 3.12 (1995).
- [29] C. Fureby. “A Comparison of Flamelet LES Models for Premixed Turbulent Combustion”. In: *AIAA paper* (2006).
- [30] E. Baudoin, X. Bai, and C. Fureby. “Comparison of LES Models Applied to a Bluff Body Stabilized Flame”. In: *AIAA paper* 2009-1178 (2009).
- [31] P. Wang and X. Bai. “Large Eddy Simulation of Turbulent Premixed Flames Using Level-set G-equation”. In: *Proceedings of the Combustion Institute* 30 (2005), pp. 583–591.

- [32] U. Engdar and P. Nilsson. “Investigation of turbulence models applied to premixed combustion using level-set flamelet library approach”. In: *ASME TurboExpo* Atlanta, GA (2003), June.
- [33] U. Engdar, P. Nilsson, and J. Klingmann. “Investigation of turbulence models applied to premixed combustion using level-set flamelet library approach”. In: *J. Eng. Gas Turbines Power* 126 (2004), pp. 701–707.
- [34] F. Ghirelli. “Turbulent premixed flame model based on a recent dispersion model”. In: *Computational Fluids* 44 (2011), pp. 369–376.
- [35] A. Lipatnikov and J. Chomiak. “Dependence of heat release on the progress variable in premixed turbulent combustion”. In: *Proceedings of Combustion Institute* 28 (2000), pp. 227–234.
- [36] A. Lipatnikov and J. Chomiak. “Developing premixed turbulent flames: Part I. Self-similar regime of flame propagation”. In: *Combustion Science and Technology* 162 (2001), pp. 85–112.
- [37] A. Lipatnikov and J. Chomiak. “A simple model of unsteady turbulent flame propagation”. In: *SAE Trans J Eng* 106 (1997), p. 2441.
- [38] A. Lipatnikov and J. Chomiak. “Transient and geometrical effects in expanding turbulent flames”. In: *Combustion Science and technology* 154 (2000), p. 75.
- [39] A. Lipatnikov and J. Chomiak. “Turbulent flame speed and thickness: phenomenology, evaluation, and application in multi-dimensional simulations.” In: *Progress in Energy and Combustion Science* 28 (2002), pp. 1–74.
- [40] V. Zimont and A. Lipatnikov. “A numerical model of premixed turbulent combustion”. In: *Chemical Physics* 14 (1995), pp. 993–1025.
- [41] W. Jones, A. Marquis, and F. Wang. “Large eddy simulation of a premixed propane turbulent bluff body flame using the Eulerian stochastic field method”. In: *Fuel* 140 (2015), pp. 514–525.

- [42] C. Lee and R. Cant. “CFD Investigation of hydrodynamic and acoustic instabilities of bluff-body stabilized turbulent premixed flames”. In: *ASME Turbo Expo Germany* (2014), June.
- [43] V. Moreau. “A self-similar premixed turbulent flame model”. In: *Applied Mathematical Modelling* 33 (2009), pp. 835–851.
- [44] N. Park and S. Ko. “Large eddy simulation of turbulent premixed combustion flow around bluff body”. In: *J. of Mechanical Science Technology* 25 (2011), pp. 2227–2235.
- [45] N. Salvador, M. de Mendonca, and W. da Costa Dourado. “Large eddy simulation of bluff body stabilized turbulent premixed flame”. In: *Journal of Aerospace Technology and Management* 5 (2013), pp. 181–196.
- [46] G. Tabor and H. Weller. “Large eddy simulation of premixed turbulent combustion using Xi flame surface wrinkling model”. In: *Flow, Turbulence and Combustion* 72 (2004), pp. 1–28.
- [47] H. Weller. “The development of a new flame area combustion model using conditional averaging”. In: *Proceedings of the European Conference on Computational Fluid Dynamics Thermo-Fluids Section Report TF9307* (1993), Imperial College of Science, Technology and Medicine.
- [48] L. Zhou, L. Hu, and F. Wang. “large-eddy simulation of turbulent combustion using different combustion models”. In: *Fuel* 87 (2008), pp. 3123–3131.
- [49] S. Chaudhuri and B. Cetegen. “Blowoff characteristics of bluff-body stabilized conical premixed flames with upstream spatial mixture gradients and velocity oscillations”. In: *Combustion and Flame* 153 (2008), pp. 616–633.
- [50] S. Chaudhuri and B. Cetegen. “Response dynamics of bluff-body stabilized conical premixed turbulent flames with spatial mixture gradients”. In: *Combustion and Flame* 156 (2009), pp. 706–720.
- [51] S. Nair and T. Lieuwen. “Near-Blowoff Dynamics of a Bluff-Body Stabilized Flame”. In: *Journal of Propulsion and Power* 23 (2) (2007), pp. 421–427.

- [52] S. Nair and T. Lieuwen. “Acoustic Detection of Blowout in Premixed Flames”. In: *Journal of Propulsion and Power* 21 (1) (2005), pp. 32–39.
- [53] S. Yamaguchi, N. Ohiwa, and T. Hasegawa. “Structure and blow-off mechanism of rod-stabilized premixed flame”. In: *Combustion Flame* 62 (1985), pp. 31–41.
- [54] J. Pan, M. Vangsness, and D. Ballal. “Large Eddy Simulation of a Bluff Body Stabilised Premixed Flame Using Flamelets”. In: *J. Eng. Gas Turb. Power* (1992), pp. 783–789.
- [55] S. Chaudhuri et al. “Blowoff dynamics of bluff body stabilized turbulent premixed flames”. In: *Combustion and flame* 157 (2010), pp. 790–802.
- [56] P. Mehta and M. Soteriou. “Combustion heat release effects on the dynamics of bluff body stabilized premixed reacting flows”. In: *AIAA Paper 2003-0835* 41 (2003).
- [57] P. Gokulakrishnan et al. “Influence of Turbulence-Chemistry Interaction in Blow-out Predictions of Bluff-Body Stabilized Flames”. In: *AIAA* 2009-1179 ().
- [58] *Detailed reaction mechanism for small hydrocarbons combustion: Release 0.5*. 2000. URL: <http://homepages.vub.ac.be/~akonnov/>.
- [59] Y. Afarin and S. Tabejamaat. “The effect of fuel inlet turbulence intensity on H₂/CH₄ flame structure of MILD combustion using the LES method”. In: *Combustion Theory and Modeling* 17 (2013), pp. 383–410.
- [60] G. Tabor and M. Baba-Ahmadi. “Inlet conditions for large eddy simulation: a review”. In: *Computers Fluids* 39, No.4 (2010), pp. 553–567.
- [61] B. Dally, A. Karpetsis, and R. Barlow. “Structure of turbulent non-premixed jet flames in a diluted hot coflow”. In: *Proc. Combust. Inst.* 29 (2002), pp. 1147–1154.
- [62] C.-X. Lin and R. Holder. “Reacting turbulent flow and thermal field in a channel with inclined bluff body flame holders”. In: *J. of Heat Transfer* 132 (2010).
- [63] B. Manickam, J. Franke, and F. Dinkelacker. “Large-eddy simulation of triangular-stabilized lean premixed turbulent flames: Quality and error assessment”. In: *Flow, Turbulence and Combustion* 88 (2012), pp. 563–596.

- [64] I. Celik, Z. Cehreli, and I. Yavuz. “Index of resolution quality for large eddy simulations”. In: *Journal of Fluids Engineering* 127 (2005), pp. 949–958.
- [65] I. Celik, M. Klein, and J. Janicka. “A test of validation of turbulent premixed models for high pressure Bunsen flames”. In: *Proceedings of FEDSM 2006, ASME Joint U.S. European Fluids Engineering Summer Meeting* Miami, FL (2006), July.
- [66] M. Klein. “An attempt to assess the quality of large eddy simulations in the context of implicit filtering”. In: *Flow, Turbulence and Combustion* 75 (2005), pp. 131–147.
- [67] A. Sjunnesson and R. Henriksson. “CARS measurements and visualization of reacting flows in bluff body stabilized flame”. In: *AIAA* (1992).
- [68] N. Zettervall and K. Nordin-Bates. “Large Eddy Simulation of a premixed bluffbody stabilized flame using global and skeletal reaction mechanisms”. In: *Combustion and Flame* 179 (2017) 1-22 ()
- [69] E. Giacomazzi, V. Battaglia, and C. Bruno. “The coupling of turbulence and chemistry in a premixed bluff-body flame as studied by LES”. In: *Combustion and Flame* 138 (4 2004).
- [70] M. Ebaid and K. Al-Khishali. “Measurements of the laminar burning velocity for propane: Air mixtures”. In: *Advances in Mechanical Engineering* 8 (6) (2016), pp. 1–17.
- [71] R. Borghi and M. Destriau. “Combustion and Flames:chemical and physical principles”. In: *Éditions TECHNIP* (1998).
- [72] M. Terracol, P. Sagaut, and C. Basdevant. “A multilevel algorithm for large-eddy simulation of turbulent compressible flows”. In: *Journal of Computational Physics* 167.2 (2001), pp. 439–474.
- [73] U. Piomelli. “Large-eddy simulation: achievements and challenges”. In: *Progress in Aerospace Sciences* 35.4 (1999), pp. 335–362.
- [74] A. Favre. “Turbulence: Space-time statistical properties and behavior in supersonic flows”. In: *The Physics of fluids* 26.10 (1983), pp. 2851–2863.
- [75] F. Nicoud. “Subgrid-scale stress modelling based on the square of the velocity gradient tensor”. In: *Flow, turbulence and Combustion* 62.3 (1999), pp. 183–200.

- [76] F. Nicoud and T. Poinso. “Wall-adapting local eddy-viscosity models for simulations in complex geometries”. In: *Numerical Methods for Fluid Dynamics VI* (1998), pp. 293–299.
- [77] *Ansys Fluent Theory Guide, edition 19.1.*
- [78] A. Montorfano, F. Piscaglia, and A. Onorati. “Wall-adapting subgrid-scale models to apply to large eddy simulation of internal combustion engines”. In: *International Journal of Computer Mathematics* 91 (2014), pp. 62–70.
- [79] N. Peters and B. Akih-kumgeh. “Comparative Analysis of Chemical Kinetic Models Using the Alternate Species Elimination Approach”. In: *Journal of Engineering for Gas Turbines and Power* 137 (2015).
- [80] *Chemical-kinetic mechanisms for combustion applications, Mechanical and Aerospace Engineering (Combustion Research), UCSD.* URL: <https://web.eng.ucsd.edu/mae/groups/combustion/mechanism.html>.
- [81] G. Smith et al. *GRI-Mech 3.0.* URL: http://www.me.berkeley.edu/gri_mech.
- [82] H. Wu and M. Ihme. “MVP Workshop Contribution: Modeling of Volvo Bluff Body Flame Experiment”. In: *55th AIAA 2017* (), pp. 9–13.
- [83] *Ansys Fluent User Guide, edition 18.2.*
- [84] S. M. Salim and K. C. Ong. “Performance of RANS, URANS and LES in the prediction of airflow and pollutant dispersion”. In: *IAENG Transactions on Engineering Technologies* (2013), pp. 263–274.
- [85] *Star CCM+ Documentations.*
- [86] *NASA polynomials or Heat capacity, enthalpy, and entropy.* URL: http://combustion.berkeley.edu/gri-mech/data/nasa_plnm.html.
- [87] J. Kim and S. Pope. “Effects of combined dimension reduction and tabulation on the simulations of a turbulent premixed flame using a large-eddy simulation/probability density function method”. In: *Combustion Theory Model* 18(3) (2014), pp. 388–413.
- [88] S. Cannon, F. Champagne, and A. Gleze. In: *Exp. Fluids* 14 (6) (1990), pp. 447–450.
- [89] J. Longwell, ed. 4. Combustion Institution. 1953, pp. 90–97.

- [90] F. Williams. "Flame stabilization in premixed turbulent gases". In: *Applied Mechanics Surveys* Spartan Books, Washington (1966), pp. 86–91.
- [91] B. Emerson et al. "Density ratio effects on reacting bluff body flow field characteristics". In: *Journal of Fluid Mechanics* 76 (2012), pp. 219–250.
- [92] R. Kraichnan. "Diffusion by a random velocity field". In: *Physics of Fluids* 11 (1970), pp. 21–31.
- [93] R. Smirnov, S. Shi, and I. Celik. "Random Flow Generation Technique for Large Eddy Simulations and particle-Dynamics Modeling". In: *Journal of Fluids Engineering* 123 (2001), pp. 359–371.

Vita

Amir Ali Montakhab received his B.Sc. in Mechanical Engineering from the Iran University of Science and Technology in 2002. He graduated with honor for his thesis entitled *Numerical Investigation of Supersonic Flow Over a 2D Airfoil*. He joined the Mechanical and Aerospace Engineering Department of California State University of Northridge in 2006 with a focus on energy and computational flow dynamics. He was nominated as an honor student and recipient of Rocketdyne scholarship program. He received his Master of Science degree in Mechanical and Aerospace Engineering in December 2010. He joined United Technologies Corporation and was accepted into company Ph.D. sponsorship program when started the program in 2014 at Syracuse University.